

INFORMATION TO USERS

This manuscript has been reproduced from the microfilm master. UMI films the text directly from the original or copy submitted. Thus, some thesis and dissertation copies are in typewriter face, while others may be from any type of computer printer.

The quality of this reproduction is dependent upon the quality of the copy submitted. Broken or indistinct print, colored or poor quality illustrations and photographs, print bleedthrough, substandard margins, and improper alignment can adversely affect reproduction.

In the unlikely event that the author did not send UMI a complete manuscript and there are missing pages, these will be noted. Also, if unauthorized copyright material had to be removed, a note will indicate the deletion.

Oversize materials (e.g., maps, drawings, charts) are reproduced by sectioning the original, beginning at the upper left-hand corner and continuing from left to right in equal sections with small overlaps. Each original is also photographed in one exposure and is included in reduced form at the back of the book.

Photographs included in the original manuscript have been reproduced xerographically in this copy. Higher quality 6" x 9" black and white photographic prints are available for any photographs or illustrations appearing in this copy for an additional charge. Contact UMI directly to order.

UMI

A Bell & Howell Information Company
300 North Zeeb Road, Ann Arbor MI 48106-1346 USA
313/761-4700 800/521-0600

NOTE TO USERS

The original manuscript received by UMI contains pages with indistinct print. Pages were microfilmed as received.

This reproduction is the best copy available

UMI

UNIVERSITY OF ALBERTA

**DETERMINATION OF THE ORIGIN OF MIGRATING GASES IN THE HEAVY
OIL FIELDS OF ALBERTA AND SASKATCHEWAN USING CARBON ISOTOPE
ANALYSES**

BY

DEVON MICHAEL ROWE ©

A thesis submitted to the Faculty of Graduate Studies and Research in partial fulfillment
of the requirements for the degree of Master of Science

Department of Earth and Atmospheric Science

Edmonton, Alberta

Fall 1998



**National Library
of Canada**

**Acquisitions and
Bibliographic Services**

**395 Wellington Street
Ottawa ON K1A 0N4
Canada**

**Bibliothèque nationale
du Canada**

**Acquisitions et
services bibliographiques**

**395, rue Wellington
Ottawa ON K1A 0N4
Canada**

Your file Votre référence

Our file Notre référence

The author has granted a non-exclusive licence allowing the National Library of Canada to reproduce, loan, distribute or sell copies of this thesis in microform, paper or electronic formats.

The author retains ownership of the copyright in this thesis. Neither the thesis nor substantial extracts from it may be printed or otherwise reproduced without the author's permission.

L'auteur a accordé une licence non exclusive permettant à la Bibliothèque nationale du Canada de reproduire, prêter, distribuer ou vendre des copies de cette thèse sous la forme de microfiche/film, de reproduction sur papier ou sur format électronique.

L'auteur conserve la propriété du droit d'auteur qui protège cette thèse. Ni la thèse ni des extraits substantiels de celle-ci ne doivent être imprimés ou autrement reproduits sans son autorisation.

0-612-34410-X

“SCIENCE IS NOT A PRETTY THING. IT IS GENERALLY PRACTICED BY
THOSE WHO LACK A FLAIR FOR CONVERSATION.”

-Fran Lebowitz

ABSTRACT

Thousands of heavy oil wells in Western Canada have already reached or are approaching the end of their production lives, and require abandonment within the next decade. In the past, abandoned wells have been plagued by hydrocarbon gas migration around the wellbores, leading to soil and aquifer contamination. Efforts to arrest gas migration have been largely unsuccessful, due to a poor understanding of the origin of the gases.

Isotopic analyses of gases from the Lower Cretaceous Mannville and Colorado Groups show that there are two very different mechanisms responsible for gas generation in the heavy oil fields. The Mannville Group gases have $\delta^{13}\text{C}_{\text{C}_1} \approx -64$ ‰, $\delta^{13}\text{C}_{\text{C}_2} \approx -27$ ‰, $\delta^{13}\text{C}_{\text{C}_3} \approx -20$ ‰, $\delta^{13}\text{C}_{\text{nC}_4} \approx -22$ ‰ (PDB). The unique isotopic reversal between propane and butane is caused by extensive biodegradation. Colorado Group gases are significantly depleted in ^{13}C , with $\delta^{13}\text{C}_{\text{C}_1} \approx -55$ to -76 ‰, $\delta^{13}\text{C}_{\text{C}_2} \approx -63$ to -32 ‰, $\delta^{13}\text{C}_{\text{C}_3} \approx -42$ to -22 ‰, $\delta^{13}\text{C}_{\text{nC}_4} \approx -37$ to -23 ‰. These are extremely immature, incipient thermogenic gases.

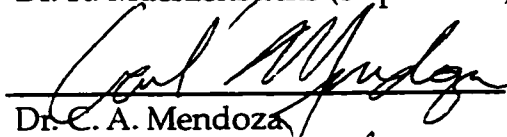
Isotopic ratios of migrating gases show that they are mostly sourced within the Colorado Group. Recognition of two distinctly different gas generation mechanisms has greatly aided the remediation of leaking wells.

UNIVERSITY OF ALBERTA
FACULTY OF GRADUATE STUDIES AND RESEARCH

The undersigned certify that they have read, and recommend to the Faculty of Graduate Studies and Research for acceptance, a thesis entitled Determination of the origin of migrating gases in the heavy oil fields of Alberta and Saskatchewan using carbon isotope analyses by Devon Michael Rowe in partial fulfillment of the requirements for the degree of Master of Science.



Dr. K. Muehlenbachs (Supervisor)



Dr. C. A. Mendoza



Dr. R. G. Bentsen

Date: September 25/98

ACKNOWLEDGMENTS

Funding for this study was provided by the Canadian Association of Petroleum Producers, Amoco Canada Petroleum Company Ltd., Chevron Canada Resources, Husky Oil Operations Ltd., Koch Exploration Canada Ltd., Murphy Oil Company Ltd., Norcen Energy Resources Limited, PanCanadian Petroleum Limited, Wascana Energy Inc., and additional laboratory analyses were performed by Maxxam Analytics Inc. In particular, Earl Jensen (Amoco Canada Petroleum Company Ltd.) and George Vilcsak (Maxxam Analytics Inc.) both spent a great deal of their time and energy in order to make this study a successful one. I would also like to thank the geologists, engineers, and field technologists from the various organizations listed above that have at one time or another contributed to this project. I benefitted from numerous conversations with Steve Talman on a variety of academic, and some not so academic topics.

This project would not have been successful without the supervision and help of Karlis Muehlenbachs. His dedication to this project, and the encouragement he provided was greatly appreciated, and made the entire experience a positive one.

Finally, thanks to mom, dad and Bryan for their encouragement along the way.

TABLE OF CONTENTS

CHAPTER	PAGE
1. INTRODUCTION	
1.1 Thesis Structure	1
1.2 Background	1
1.3 Previous Work	3
1.4 Objectives	4
1.5 Methods- Sampling and Instrumentation	4
1.6 Uncertainties	8
1.7 Summary	10
1.8 References	11
2. ORIGIN OF SHALLOW NATURAL GASES	
2.1 Introduction	12
2.2 Results and Discussion	13
2.3 Conclusions	19
2.4 References	22
3. IDENTIFICATION AND APPLICATION OF TRENDS IN THE $\delta^{13}\text{C}$ VALUES OF SHALLOW NATURAL GASES	
3.1 Introduction	23
3.2 Environmental Issue	25
3.3 Sampling and Measurement of Isotope Ratios	29
3.4 Results and Discussion	31

3.5.1 Gas Migration	37
3.6 Conclusions	40
3.7 References	41
4. ISOTOPIC ANOMALIES OF NATURAL GAS ASSOCIATED WITH HIGH TEMPERATURE STEAM INJECTIONS AT FORT KENT, ALBERTA	
4.1 Fort Kent Anomaly	43
4.2 Site Characterization	45
4.3 Results	45
4.4 Implications	52
4.5 Conclusions	54
4.6 References	55
5. CONCLUSIONS	
5.1 Conclusions	56
5.2 Future Work	57
APPENDICES	
A IAEA Calibration	59
B Mud-gas data	61
C Mannville Group production gas data	68
D Migration gas data	69
E Calculation of fractionation curves	74
F Index of abstracts	81

LIST OF TABLES

TABLE		PAGE
1.1	Standard deviations of $\delta^{13}\text{C}$ values	8
3.1	Carbon isotope compositions and estimated LOMs of Colorado Group gases	32
3.2	Carbon isotope and bulk gas compositions of $\text{C}_1\text{-C}_4$ and CO_2 gas components from the Lindbergh field, AB	36
4.1	Isotope ratios of migrating gases from wells at the Fort Kent Thermal Project	46
A.1	Measured $\delta^{13}\text{C}_{\text{C1}}$ values of NGS-3 standard gas	59
A.2	Variation in isotope ratios of gases sampled in Tedlar bags versus steel cylinders	60
B.1-B.20	Isotope ratios of mud-gas samples	61
C.1	Isotope ratios of Mannville formation gas samples	68
D.1	Isotope ratios of migrating gas samples	69

LIST OF FIGURES

FIGURE		PAGE
1.1	Schematic diagram of GC-C CF-IRMS system	5
1.2	Typical gas chromatogram for natural gas sample	6
1.3	Schematic diagram showing the travel path of drilling fluid (mud) through the drill pipe and annulus	8
2.1a	Mud-gas profile locations	12
2.1b	Example of an isotopic fingerprint from mud-gases	12
2.2	C_1/C_{2+} versus $\delta^{13}C_{C1}$ for Colorado and Mannville Group gases	13
2.3	$\delta^{13}C_{C3}$ versus $\delta^{13}C_{C2}$ for Colorado and Mannville Group gases	15
2.4	Application of isotopic fingerprint to determine source depth of migrating gas	17
3.1a	Stratigraphy of the WCSB Colorado and Mannville Groups	22
3.1b	Histogram of initial oil-in-place in the WCSB, by reservoir age	22
3.2	Schematic diagram of a 'leaking' heavy oil well	23
3.3	Carbon isotope composition of Colorado and Mannville Group gases	24
3.4	Difference in carbon isotope composition of Mannville Group and migrating gases	25
3.5	Location of mud-gas profiles	27
3.6a-c	Carbon isotope fingerprints from mud-gases	29

3.7	Comparison of the carbon isotope composition of unaltered Lower Cretaceous, altered Lower Cretaceous, and Upper Devonian natural gas	30
3.8	Maturity diagram of shallow Colorado Group mud-gases	31
3.9a	Chung plot of mud-gases from a single well	33
3.9b,c	Chung plots of Colorado gases from two wells	33
3.10a-c	Isotopic fingerprint used to estimate source depth of three migrating gases	37
3.10d	Isotopic composition of a 'Cummings' production gas	37
4.1	Map showing the location of the Fort Kent field	42
4.2	Plan view drawing of the Fort Kent Thermal Project	43
4.3	Carbon isotope ratios of migrating gases from the Fort Kent field	45
4.4	Comparison of $\delta^{13}\text{C}_{\text{C}_3}$ versus $\delta^{13}\text{C}_{\text{C}_2}$ between typical migrating gases and those from the Fort Kent field	47
4.5	Schematic diagram of an inclined well from the Fort Kent field	48
4.6	Plan view of Fort Kent site showing the correlation between thermal maturity of migrating gases and steam injection volumes	49
4.7	Variation in isotope ratios of C_1 - C_3 components due to mixing from two sources	51
D.1	Locations of gas samples that were analysed (from Appendices B, C, and D)	73

LIST OF APPENDICES

APPENDIX		PAGE
A	IAEA calibration of $\delta^{13}\text{C}$ values, instrumental uncertainty analyses	59
B	Isotope ratios of mud-gas samples	61
C	Isotope ratios and bulk compositions of Mannville Group gas samples	68
D	Isotope ratios and bulk compositions of migrating gas samples	69
E	Calculation of theoretical fractionation curves	74
F	Abstracts published pertaining to this thesis	81

CHAPTER ONE

INTRODUCTION

1.1 THESIS FORMAT

This thesis is written in ‘paper’ format. A brief introduction in Chapter 1 provides background information and the environmental motivation behind the project. Chapter 1 also discusses the methods and instrumentation used throughout this study, with a note on the standardization and uncertainty of reported measurements. The main ideas that have been developed are presented in two short papers that comprise Chapters 2 and 3. The first paper discusses possible generation mechanisms of shallow gases, and the second presents the environmental application of the isotopic fingerprinting technique. Chapter 4 deals specifically with data from one field located at Fort Kent, Alberta, where the heavy oil wells have been steamed. These data do not contribute to chapters 2 or 3, but they are nevertheless interesting and will be of use in further studies. The final chapter summarizes the results of the study, and provides some suggestions as to the directions of future research. Six attached appendices contain a large amount of data (Appendices A, B, C, and D) details of some relevant calculations used in chapters 2 and 3 (Appendix E), and a complete index of abstracts for papers that have been presented at major conferences (Appendix F).

1.2 BACKGROUND

Thousands of wells have been drilled in northeastern Alberta and adjacent Saskatchewan in order to develop the extensive heavy oil reservoirs. In as many as half of these wells, vertical migration of hydrocarbon gas from depth is a significant problem

(Erno and Schmitz, 1994). Gas migration is herein defined as vertical movement of gases from depth to the ground surface or to shallower horizons. The primary manifestations of gas migration are pressure build-up in well casings, contamination of surface soils, and dissolution into shallow aquifers.

Gas migration has been well documented (Saskatchewan Research Council, 1995) within the Lloydminster area of Alberta and Saskatchewan. The problem of gas migration, however, is not unique to the Lloydminster region, and it is expected that other heavy oil producing regions worldwide suffer from similar migration problems. There is a heightened awareness of gas migration in the Lloydminster area, due to the incredibly high number, and close spacing of abandoned heavy oil wells. Recent remediation efforts have been driven by:

1. industry and public concern regarding environmental damage to groundwater resources
2. government imposed 'zero tolerance' limits which require that wells are free of gas migration problems at the time of abandonment
3. a large number of wells nearing the end of their production lives, requiring abandonment within the next 10 years

Gas migration problems are largely due to a lack of understanding of actual migration pathways, and poor cementing techniques (during initial well installation and in remediation activities). The poorly consolidated shales overlying the heavy oil formations are intrinsically poor for achieving competent cement bonds. Well-specific remediation has tended to be extremely time consuming, costly and of limited success.

The primary threat posed by migrating gases is the potential contamination of potable surface aquifers. A directive issued by the Alberta Energy and Utilities Board (AEUB) called for migrating gases to be stopped by first identifying the source depth, and then initiating remediation efforts at the determined source depth (Wagenar, 1998). It is interesting to note that in accordance with the AEUB directive 'non-serious' gas migration problems, i.e. wells with surface casing vent flow rates less than 300m³/day, do not require addressing until the wells are abandoned. The Canadian Association of Petroleum Producers recognized, however, that traditional logging techniques (sound, cement bond) have not resulted in acceptable success rates in locating migrating gas source depths (Jensen, 1998). New techniques must therefore be developed and practiced in order to identify gas migration source depths in the Western Canadian Sedimentary Basin (WCSB). One such technique employs carbon isotope ratio analyses.

1.3 PREVIOUS WORK

Stable Carbon Isotope Gas Migration Research Program-Phase I (1995)

The Canadian Association of Petroleum Producers (CAPP) funded a two-year study of the isotope ratios of gases in the Mannville producing horizons in the Lloydminster area. The focus of that study was to determine the isotopic signatures of each of the production horizons, using both $\delta^{13}\text{C}$ and δD analyses. It was discovered that each of the Mannville formations had very similar carbon isotope ratios (Rich, 1995; Rich and Muehlenbachs, 1995), with $\delta^{13}\text{C}_{\text{methane}(C1)}$ values ranging from -60‰ to -70‰, $\delta^{13}\text{C}_{\text{ethane}(C2)}$ values from -30‰ to -25‰ and $\delta^{13}\text{C}_{\text{propane}(C3)}$ values from -18‰ to -25‰.

Analyses of migrating gases showed very different isotopic signatures from those of the Mannville gases. While the $\delta^{13}\text{C}_{C1}$ values were essentially the same, the

$\delta^{13}\text{C}_{\text{C2+(ethane, propane, butane)}}$ values were depleted in ^{13}C with respect to their Mannville counterparts. It was concluded that the majority of migrating gases were not produced in the Mannville formations from which the heavy oil wells produced, but rather the shallower Colorado Group shales. Rich suggested that a rare biological process such as ethanogenesis may account for the shallow gases, and realized that a more extensive study was necessary to investigate the shallow gas generation mechanisms.

1.4 OBJECTIVES

The objectives of this study (Phase II of the CAPP Carbon Isotope Gas Migration Research Program) are:

1. to devise an analytical method which can be used to identify the sources of migrating gases in the heavy oil regions of Alberta and Saskatchewan
2. to characterize the mechanism(s) that dominate natural gas generation in the Colorado and Mannville Groups
3. to expand the regional isotopic database to include fields outside of the Lloydminster area

1.5 METHODS- SAMPLING AND INSTRUMENTATION

Three types of samples were analysed in this study. The first was a set of approximately 40 samples from the producing heavy oil-associated Mannville and Colorado Group formations. These samples were collected from wells that did not have migration problems, and were used to broaden the regional extent of the 'background' database from Phase I. The second set comprised approximately 175 migrating gas samples from different wells throughout the heavy oil region. These gases were collected in 2L Tedlar®

bags or 500cc steel cylinders from surface casing vents and soils in wells troubled with gas migration. The most novel and important type of samples were mud-gases, obtained during the drilling of new heavy oil wells. Mud-gases were collected from the surface down to the targeted Mannville formation (~550m below surface for most wells) at 50m depth intervals for 23 new wells. Isotope ratios of mud-gases provided an isotopic depth profile, or 'fingerprint' for each of the wells sampled. The mud-gas sampling/analysis technique was developed specifically for this project with the help of G. Lorenz, G. Vilcsak and A. Muehlenbachs, and is described in more detail in Chapters 2 and 3. I personally sampled the first well, and the operators (according to my instructions) sampled the rest.

Measurement of isotope ratios

A gas chromatography-combustion continuous-flow interface was added to the existing isotope ratio mass spectrometer at the start of Phase II (August, 1996). The continuous-flow capabilities of the new system led to several analytical benefits, including:

1. the ability to measure $\delta^{13}\text{C}$ values of minute hydrocarbon components well below the detection limits of Phase I.
2. a decrease in sample analysis time from several hours, to approximately 30 minutes per sample.
3. higher precision in measured $\delta^{13}\text{C}$ values.

Figures 1.1 and 1.2 show a schematic diagram of the GC-C CF-IRMS system, and a typical gas chromatogram for a natural gas sample.

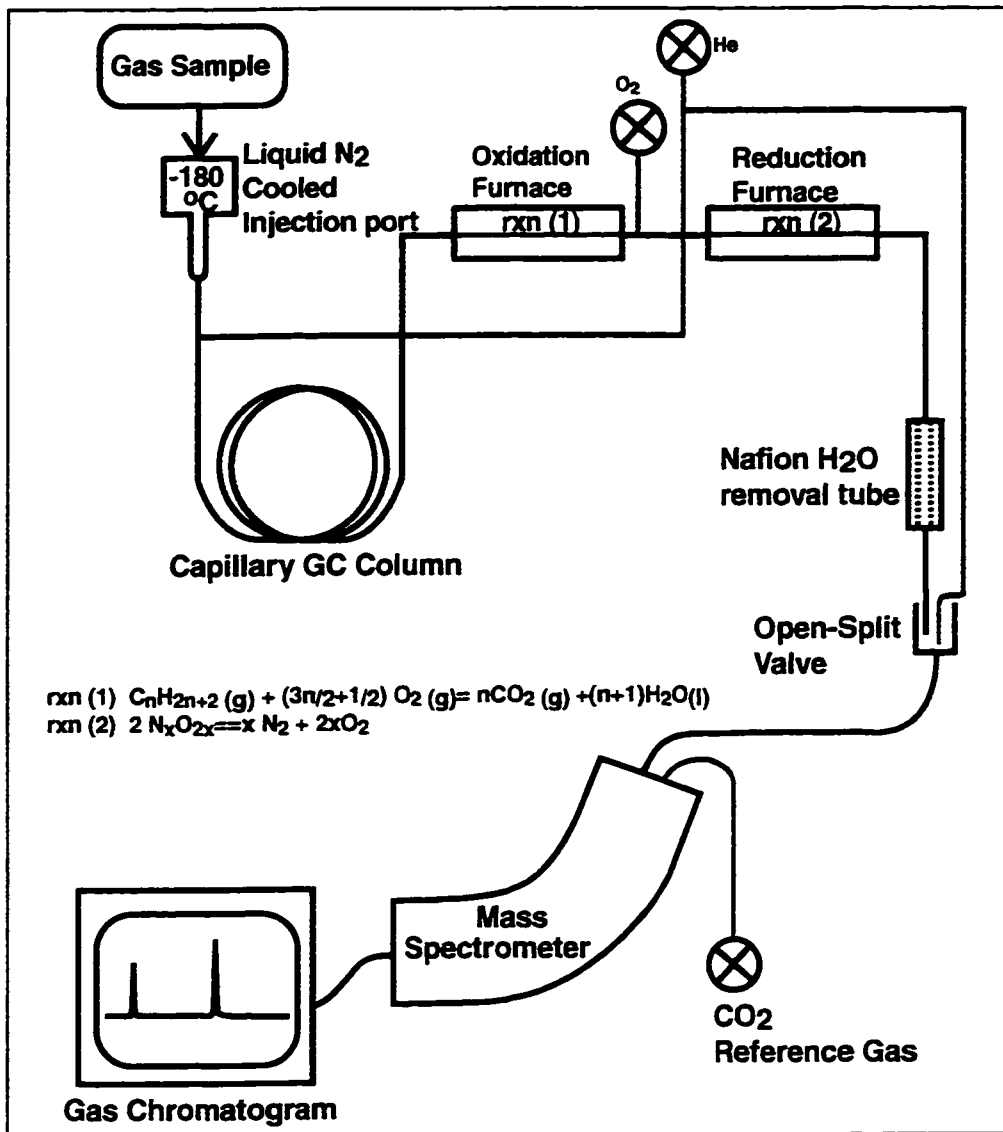


Figure 1.1 Schematic diagram of the Gas Chromatography-Combustion Continuous-Flow Isotope Ratio Mass Spectrometer (GC-C CF-IRMS).

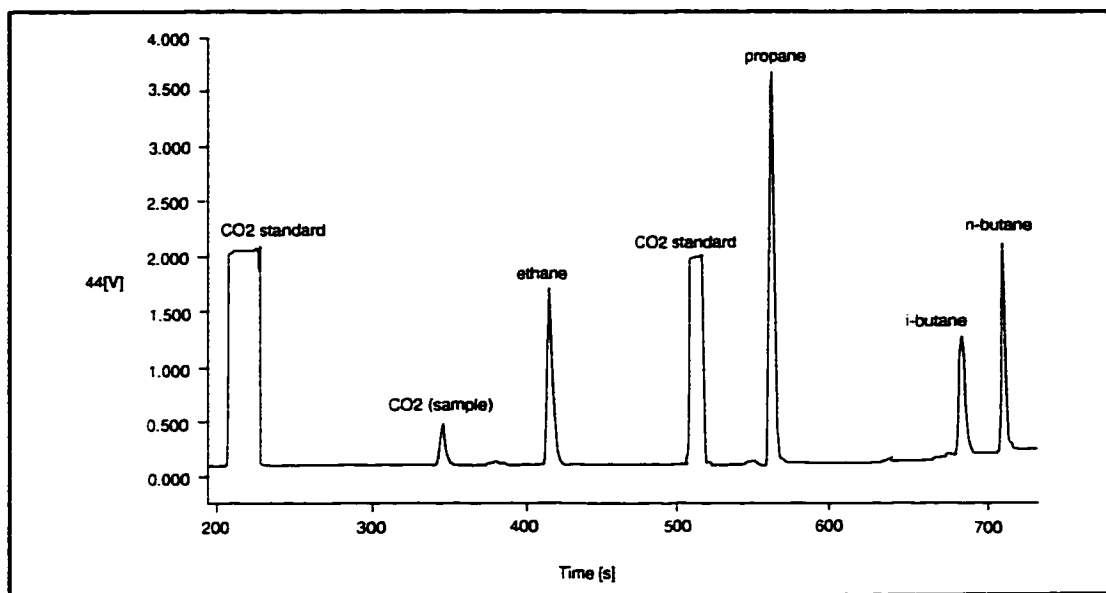


Figure 1.2 Sample gas chromatogram of a natural gas. Peaks are shown for C₂-C₄ hydrocarbons, carbon dioxide, and two standard reference injections.

Isotope ratios of hydrocarbon components were calculated by integrating the m/z 44, 45 and 46 ion currents of the CO₂ peaks resulting from on-line (continuous-flow) combustion of chromatographically separated compounds (Brand, 1996). Laboratory CO₂ pulses admitted directly into the mass spectrometer were used as reference. Isotopic analyses are reported using delta (δ) notation, representing the parts per thousand deviation from the isotopic composition of the PDB standard (CO₂(g) evolved from the acidification of the Peedee Belemnite formation). δ values are calculated using the following equation:

$$\delta^{13}\text{C}(\text{‰}) = \frac{(^{13}\text{C}/^{12}\text{C}_{\text{sample}} - ^{13}\text{C}/^{12}\text{C}_{\text{standard}})}{^{13}\text{C}/^{12}\text{C}_{\text{standard}}} \times 1000$$

A positive δ¹³C value (isotopically heavy, or enriched) indicates that the ¹³C/¹²C ratio in the sample is higher than in the PDB standard. In order to compare our δ¹³C values with the PDB standard, the working reference gas in the mass spectrometer was calibrated to

the VPDB (Vienna PDB) scale using the NBS-18 and NBS-19 standards. Analysis of the International Atomic Energy Agency (IAEA) NGS-3 gas standard produced $\delta^{13}\text{C}$ values that are within the accepted range of values on the VPDB scale (see Appendix A).

1.6 UNCERTAINTIES

Uncertainties in the reported $\delta^{13}\text{C}$ values are not indicated throughout the text. Instead, uncertainties that apply to the entire thesis are provided in table 1.1 (compound specific, for text and figures unless otherwise stated). Replicate analyses of a typical gas sample were used to determine the instrumental uncertainty of each $\delta^{13}\text{C}$ value (Appendix A contains the data).

	$\delta^{13}\text{C}_{\text{C1}}$	$\delta^{13}\text{C}_{\text{C2}}$	$\delta^{13}\text{C}_{\text{C3}}$	$\delta^{13}\text{C}_{\text{iC4}}$	$\delta^{13}\text{C}_{\text{nC4}}$
Standard Deviation (‰)	0.3	0.5	0.25	0.5	0.7

Table 1.1 Compound specific instrumental uncertainty in measured $\delta^{13}\text{C}$ values.

Chapters 2 and 3 discuss isotopic analyses of mud-gases sampled from various depths within the Colorado and Mannville Groups. In all cases, the depths are reported in metres (m) below the ground surface. It was assumed that the mud traveled through the annular space between the drill stem and the wellbore at a constant velocity, determined by the fluid injection rate (Q) and the diameters of the drill bit and stem (R , and r , respectively) (diameter of the drill collar was ignored, see figure 1.3), i.e.

Constant fluid injection rate (m^3/min), $Q_{in} = Q$

Assuming no fluid sinks or sources at depth, $Q_{in} = Q_{out} = Q$

Volume of fluid leaving annular space (m^3), $V_{ann} = V_{ann}$

= (Cross - sectional Area) · depth

= $A \cdot d$

from a given depth, the travel time, t (min) required for the mud at the sampling depth to reach the surface for collection is

$$t = \frac{V_{ann}}{Q} = \frac{\pi(R-r)^2 \cdot d}{Q} \text{ where } (R-r) \text{ is the annular width (space between}$$

the pipe and wellbore) .

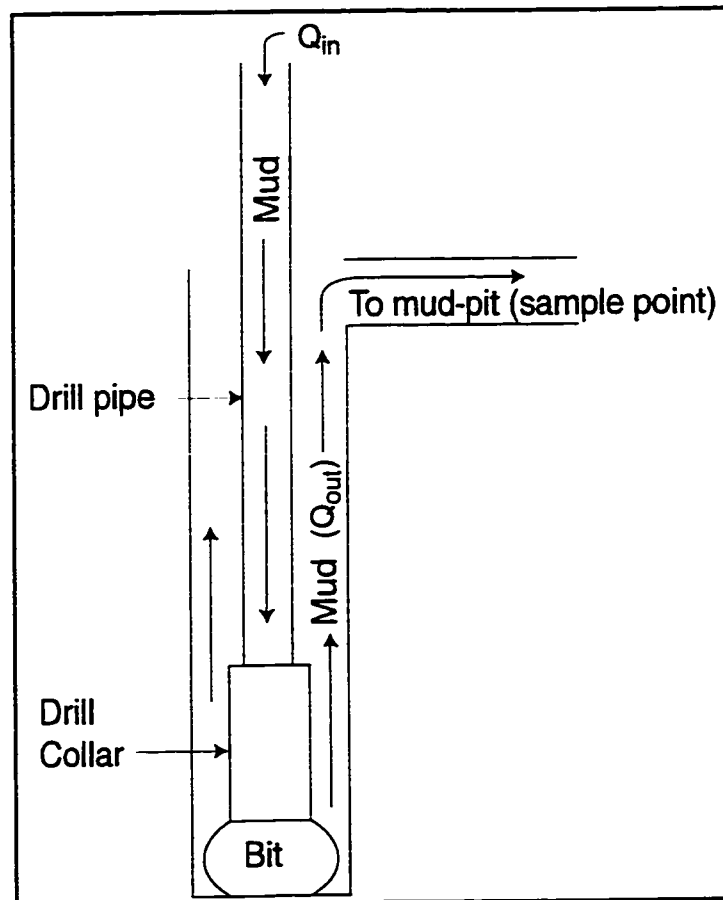


Figure 1.3 Schematic diagram showing the travel path of drilling fluid (mud) through the drill pipe and annulus.

Typical values for the above parameters used during drilling were $Q=1.4\text{m}^3/\text{min}$, $R=0.222\text{m}$, $r=0.111\text{m}$. Substituting these values in the equation for time (above) leads to travel times of approximately 1.4min (per 50m depth). If the uncertainty (due to timing errors) in obtaining mud samples is ± 10 seconds, then the corresponding sample depth will vary by $\pm 20\text{m}$. The strong correlation of the mud-gas data with stratigraphic picks from well-logs (accurate to $< \pm 5\text{m}$) suggests that our depth estimates are in fact more accurate than $\pm 20\text{m}$.

1.7 SUMMARY

The Lloydminster heavy oil region is infamous for its gas migration problems, with nearly half of its wells demonstrating measurable gas migration. Gas migration is not only a problem in the Lloydminster area, it occurs throughout the heavy oil region of Alberta and Saskatchewan. Previous isotopic studies have shown that most migrating gases are sourced in the Colorado Group shales, not the Mannville Group sands.

Remediation of wells plagued by migration has been unsuccessful because currently no method exists for accurately determining gas source depths within the Colorado Group. Isotopic analyses of mud-gases from various depths within the Colorado Group shales are a very useful tool for determining migrating gas source depths, and for investigating the gas type and maturity.

1.8 REFERENCES

- Brand, W. A. (1996) High precision isotope ratio monitoring techniques in mass spectrometry. *Jour. Mass. Spec.* **31**, 225-235
- Erno, B. and Schmitz, R. (1994) Measurements of soil gas migration around oil and gas wells in the Lloydminster area. Technical meeting of the Petroleum Society of the CIM, **94**, paper #73
- Jensen, E. (1998) The application of stable carbon isotopes to gas migration source detection. A submission by the Canadian Association of Petroleum Producers to the Alberta Energy and Utilities Board and Saskatchewan Energy and Mines.
- Rich, K. (1995) Determination of the source of migrating gas from oil and gas wells in the Lloydminster area using stable isotope analyses. M.Sc. Thesis, University of Alberta, 103 pp.
- Rich, K., Muehlenbachs, K., *Soc. Petrol. Eng.* **30265** (1995)
- Saskatchewan Research Council (1995) Migration of methane into groundwater from leaking production wells near Lloydminster. Canadian Association of Petroleum Producers, **1995-0001**, 48 p.
- Wagenar, R. (1998) Surface casing vent flow/gas migration requirements, Alberta Energy and Utilities Board Interim Directive

CHAPTER TWO

ORIGIN OF SHALLOW NATURAL GASES¹

2.1 INTRODUCTION

The evolution of petroleum occurrences in sedimentary basins worldwide can be better understood by distinguishing between products of biodegradation and thermal maturation processes. The integration of isotopic and geochemical data is an instructive tool in determining formation mechanisms, particularly when examining natural gas reservoirs (Fuex, 1977; Schoell, 1980). A recent study revealed that shallow gas deposits in the Michigan Basin shales are predominantly composed of biogenic methane formed *in-situ*, with small amounts of thermogenic ethane and propane that have migrated from deeper formations within the basin (Martini *et al.*, 1996). The origin of gas along the shallower margins of the Western Canadian Sedimentary Basin (WCSB) is remarkably different from the Michigan Basin. Along with *in-situ* biogenic methane, the shallow gases in the WCSB shales are derived by very low temperature, incipient thermogenesis. Gases from deeper within the basin are extensively microbially altered, and unlike the Michigan Basin, have not migrated vertically into shallower formations. Our discovery of measurable quantities of incipient thermal gas at shallow depths (less than 400m from surface) contradicts previous suggestions that bacterial activity alone may account for the existing Colorado gas reservoir (Rich, 1995; Rich and Muehlenbachs, 1995; Deroo *et al.*, 1977). Incipient thermogenic gas with near equilibrium isotopic composition derived at temperatures as low as 15°C is surprising, and questions our understanding of conventional petroleum generation mechanisms. Our findings provide new insight into the gas generation mechanisms of the

¹ A version of this chapter has been submitted for publication. D. Rowe and A. Muehlenbachs, *Nature* submission number R04703.

WCSB shales, and have led to the development of a very successful tool for efficient environmental remediation of leaking oil wells.

The WCSB Upper Cretaceous Colorado shale Group is a thermally immature set of marine deposits, ranging in organic content from about 4 to 12%wt (Leckie *et al.*, 1994). Gases contained within the shales are predominantly methane (CH₄), with varying amounts of ethane (C₂H₆), propane (C₃H₈), butane (C₄H₁₀) and carbon dioxide (CO₂). Detailed geochemical characterization of the Colorado Group is limited to regions where the reservoirs are economically viable; hence, there are few studies that have investigated the origin of hydrocarbon gases within these shallow horizons. Underlying the Colorado Group shales are the Lower Cretaceous Mannville sands which host one of the world's largest deposits of biodegraded heavy oil (remaining reserves greater than 20,000 x 10³ m³) and associated natural gas (McRory, 1982).

2.2 RESULTS AND DISCUSSION

We examined gases collected at 50 m depth intervals during the drilling of 21 oil wells located across the study area (figure 2.1).

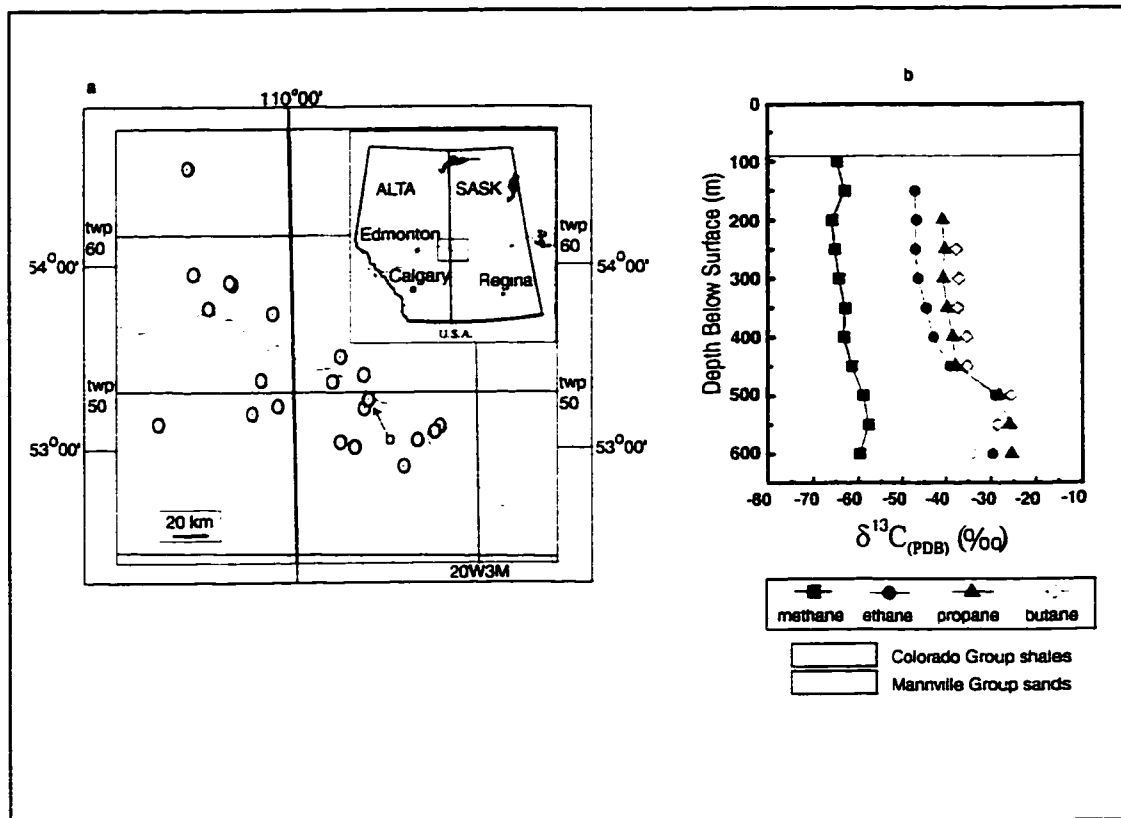


Figure 2.1 a) Study area in the Western Canadian Sedimentary Basin, Canada. The location of 21 sites are shown where shallow gases were collected. At each location, mud/water from 50 m intervals was collected in 1 L plastic bottles, leaving room in the bottles for gases to exsolve from the mud mixture. The ‘mud-gas’ that occupied the headspace in the bottles was analysed for bulk gas and carbon isotope composition. The $\delta^{13}C$ values of the hydrocarbons were determined using a Finnigan MAT 252 (Conflo II) continuous-flow isotope ratio mass spectrometer (Brand, 1996). **b)** Mud-gas isotopic depth profile or ‘fingerprint’ from a selected well (location marked in 1 a). The Colorado-Mannville geologic boundary coincides with a dramatic change ($\sim 10\text{‰}$) in isotopic compositions. At shallow depths, the $\delta^{13}C$ values increase with carbon chain length, a unique characteristic of thermally derived gases. Increased isotopic separations towards the ground surface (i.e. gentle ‘fanning out’ of data) show the effect of lower temperatures on isotope fractionations in thermally derived gases. $\delta^{13}C_{\text{methane}}$ is homogeneous throughout the profile.

The molecular compositions of the gases vary from roughly 95 to 99 vol.% methane, with C_{2+} components (ethane, propane, butane) accounting for up to 4 vol.%.

Colorado and Mannville Group gases are indistinguishable (except in a few cases) based on composition and $\delta^{13}C_{C1(\text{methane})}$ values (figure 2.2). $\delta^{13}C_{\text{methane}}$ values of -52 to

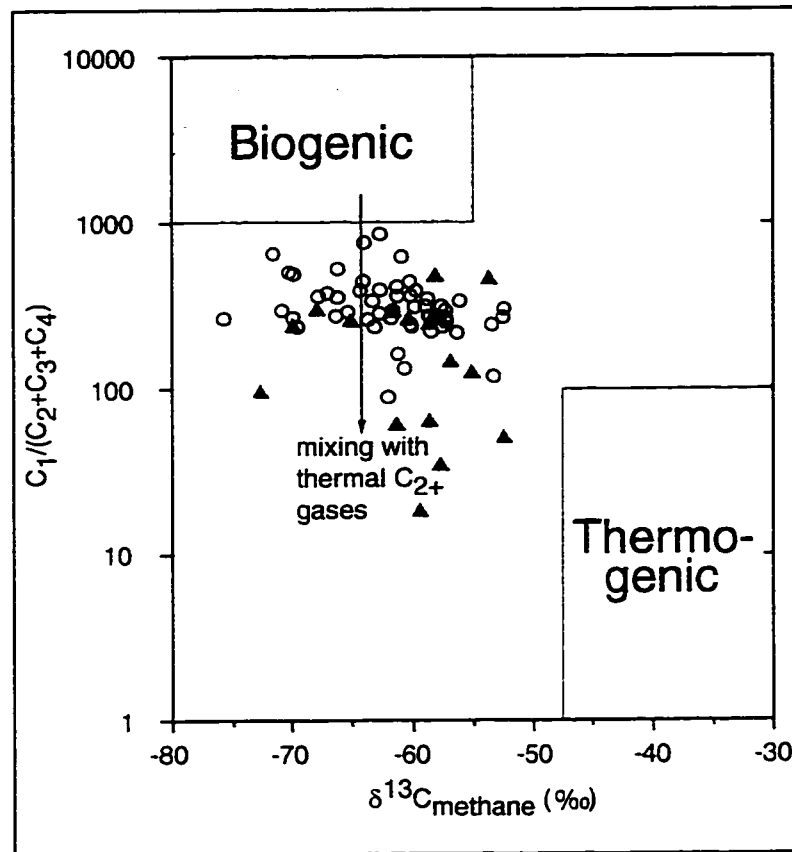


Figure 2.2 Plot showing (methane/ (ethane+propane+butane)) versus $\delta^{13}C$ (w.r.t. PDB) of methane for Colorado (circles) and Mannville (triangles) gases. Suggested biogenic and thermogenic fields have been included. Carbon isotope compositions indicate that both the Colorado and Mannville gases are composed of predominantly biogenic methane. The arrow shows the expected variation in composition due to mixing of biogenic methane with thermally derived C_{2+} gases (ethane +propane+butane).

-76 ‰ indicate a biogenic origin, with no regional or stratigraphic trends. The bulk composition ratios ($C_1/C_{2+} < 1000$) indicate that significant quantities of thermally derived C_{2+} components (especially in some of the deeper Mannville gases) have mixed with the biogenic methane in both the Colorado and Mannville Groups. Methane concentrations alone are often non-diagnostic of origin due to mixing from various sources (Coleman *et al.*, 1995). Carbon isotope ratios of the C_{2+} components in the Colorado and Mannville Group gases, however, display two very different isotopic signatures, and these data provide a more meaningful discriminant.

Isotopic depth profiles or ‘fingerprints’ from across the study area reveal a marked difference in the isotopic signature of gases contained within the Mannville and Colorado Groups (figure 2.1b). $\delta^{13}C$ values of C_2 indicate that the Colorado ($\delta^{13}C_2 = -39$ to -46 ‰) and Mannville Groups ($\delta^{13}C_2 = -28$ to -30 ‰) contain two very different types of gas. Isotopic fingerprints share three characteristics which suggest that the Colorado Group gases are thermogenic: 1) $\delta^{13}C$ values of shallow gases are more negative than gases at depth, 2) $\delta^{13}C$ values of shallow C_{2+} gases at a given depth increase with the number of carbon atoms, and 3) the isotopic separation between hydrocarbon components tends to increase at shallow depths.

Combining a theoretical ‘quasi-equilibrium’² thermal gas generation model with known source conditions in the WCSB allows us to explain these observed isotopic

² Hydrocarbon formation from organic matter is generally considered to be a kinetic process, however James (1983) suggests that the carbon isotope distribution in C_1 to C_4 gases may approach equilibrium distributions, hence the term ‘quasi-equilibrium’. Theoretical equilibrium fractionation factors for C_1 to C_4 gases have been calculated from gas partition functions. A discussion of these calculations with detailed references can be found in James (1983).

behaviours (James, 1983). Theoretical considerations require that the equilibrium isotopic ratios of hydrocarbon gases generated from a single source material vary with temperature. At a given temperature, calculated $\delta^{13}\text{C}$ values increase with increasing number of carbon atoms. Higher isotopic fractionation at low temperatures leads to more negative $\delta^{13}\text{C}$ values in general, but calculations show that the magnitude of this effect should decrease with increasing number of carbon atoms. Thus we also expect to see a gradual fanning, or spreading out of isotope data at lower temperatures (figure 2.1b).

A calculated $\text{C}_3\text{-C}_2$ fractionation line ($\delta^{13}\text{C}_{\text{propane}}$ versus $\delta^{13}\text{C}_{\text{ethane}}$) has been plotted for temperatures ranging between -10°C and 200°C , along with observed gas data (figure 2.3).

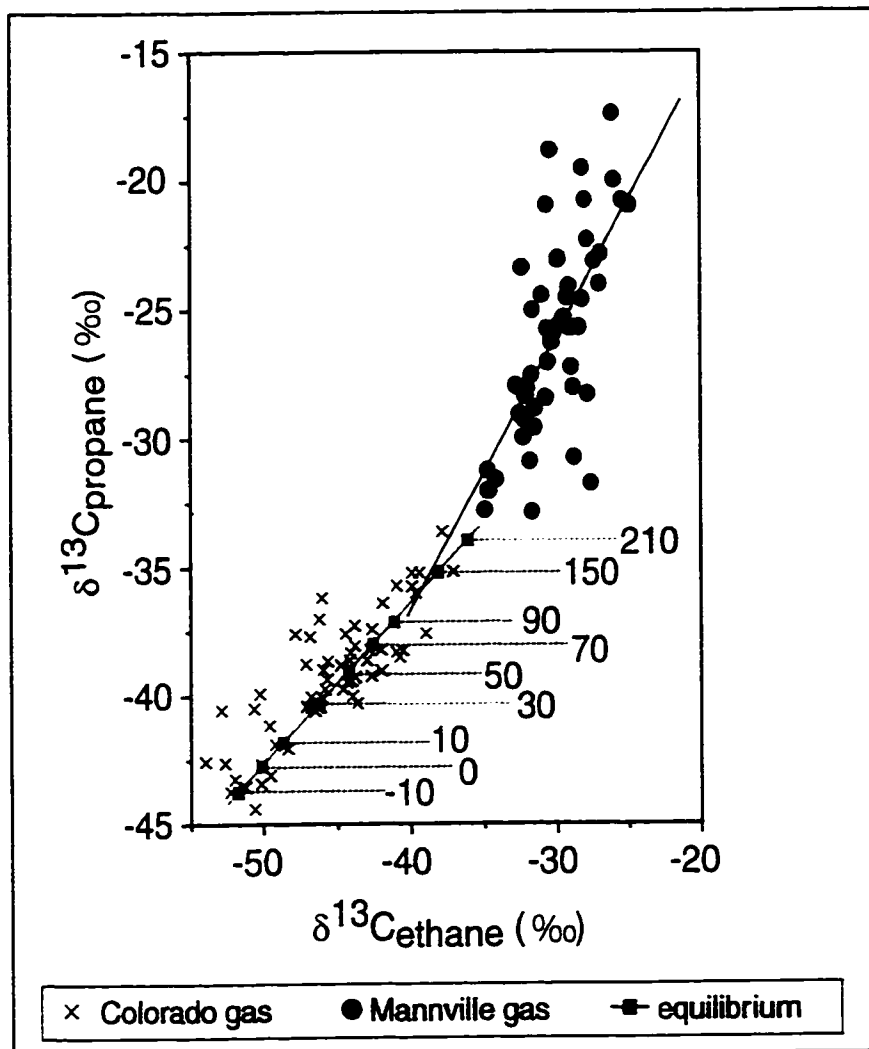


Figure 2.3 Isotope ratios of propane and ethane in WCSB gases. Colorado gas data show good agreement with theoretical propane/ethane fractionation, shown in red. Theoretical values have been calculated at several temperatures assuming 'quasi-equilibrium' thermal generation from a -30‰ organic source material. Biodegraded Mannville gases plot well away from the calculated fractionation line. A regression line of the Mannville data has been added ($y=1.20x-10.30$, $r^2=0.7$), intersecting the equilibrium fractionation line at approximately 180 °C. This corresponds to the (average) initial formation temperature and isotope ratios before biodegradation of these gases occurred.

The calculated fractionation line fits the Colorado, but not the Mannville Group data. The majority of Colorado samples indicate putative formation temperatures between 15°C and 65°C ($\pm 1\sigma$ deviation from mean temperature), although several samples lie considerably outside this range. Deviations in Colorado data are likely due to a combination of kinetic isotope effects that have been ignored in the 'quasi-equilibrium' treatment, and variations in source material composition for which we have not accounted (e.g. presence of localized coal beds (-25‰) versus the kerogen of the shales(-30‰)). The Mannville gases deviate significantly from the calculated fractionation line due to microbial alteration; this process preferentially cleaves ^{12}C - ^{12}C bonds and results in residual C_{2+} gases that become progressively enriched in ^{13}C (figures 2.1b, 2.3).

Contrary to the results found in the Michigan Basin, the C_{2+} components of the shallow shale gases in the WCSB could not have migrated from deeper formations. If the gases in the Mannville formations had migrated vertically into the Colorado shale Group, isotope ratios of C_{2+} in both Groups would be very similar. This is clearly not the case. Isotopic reversals between C_3 and C_4 components which are diagnostic of the Mannville gases (e.g. $\delta^{13}\text{C}_{\text{C}_4} < \delta^{13}\text{C}_{\text{C}_3}$, see figure 2.1b) do not occur in the Colorado shale gases.

2.3 CONCLUSIONS

The discovery of two gas reservoirs with distinctly different origins has important environmental applications. Thousands of heavy oil wells throughout the WCSB (and we expect other producing basins worldwide) are plagued by unwanted hydrocarbon gas emission from depth ('migrating gas') that leads to soil and aquifer contamination (Erno and Schmitz, 1994; Taylor, 1997). For the first time, the source depth of these gases can be accurately determined using isotopic fingerprints generated via routine analytical procedures. Past remediation strategies have often been based on the assumption that the

source of migrating gases was the Mannville production horizons. We have found that, in most cases, gases leaking around wellbores in the WCSB originate in the shallower Colorado shales. Therefore, remediation efforts to stop migrating gases can be focused on the Colorado shales, where the gases are actually sourced (figure 2.4).

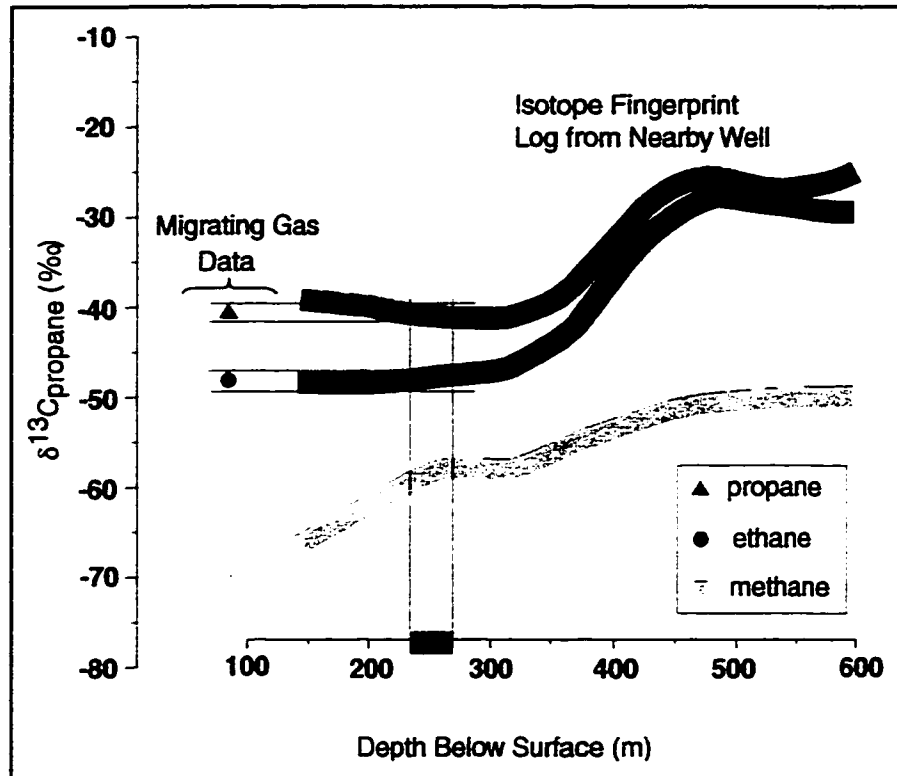


Figure 2.4 Isotope ratios of a migrating gas from a leaking well are compared to a fingerprint from a nearby well. By matching the isotopic separation of the ethane and propane components with the fingerprint ($\delta^{13}\text{C}_{\text{methane}}$ values are not diagnostic in determining gas sources), we can determine the source depth of the migrating gas, in this case approximately 250m. Accurate source depth determination has greatly increased remediation success in the WCSB.

Geochemical analyses continue to play an important role in assessing the origin of natural gas deposits. We have identified two distinct generation mechanisms that contribute to the gas deposits in the WCSB, and we are able to distinguish between the different types of gases using $\delta^{13}\text{C}$ values alone. The discovery of quasi-equilibrium thermogenic gas derived at temperatures below 70°C is surprising and suggests that we should reconsider the limits of thermal gas generation mechanisms. We have shown that gas generation mechanisms in two geologically similar environments can be very different, and hope that our findings will encourage geochemical studies of this type (and their applications) in other non-conventional gas deposits worldwide.

2.4 REFERENCES

- Brand, W. A. (1996) High precision isotope ratio monitoring techniques in mass spectrometry. *Jour. Mass. Spec.* **31**, 225-235
- Coleman, D.D., Liu, C., Hackley, K.C., Pelphey, S.R. *Environ. Geosci.* **2**, 95-103 (1995)
- Deroo, G., Powell, T. G., Tissot, B., and McCrossan, R. G. (1977) The origin and migration of petroleum in the Western Canadian Sedimentary Basin, Alberta: Geological Survey of Canada Bulletin 262
- Erno, B. and Schmitz, R. (1994) Measurements of soil gas migration around oil and gas wells in the Lloydminster area. Technical meeting of the Petroleum Society of the CIM, **94**, paper #73
- Fuex, A.N. (1977) The use of stable carbon isotopes in hydrocarbon exploration. *Jour. Geochem. Explor.* **7**, 155-188
- James, A. T. (1983) Correlation of natural gas by use of carbon isotopic distribution between hydrocarbon components. AAPG Bull., **67**, 1176-1191
- Leckie, D. A., Bhattacharya, J. P., Bloch, J., Gilboy, C. F., Norris, B. (1994) Cretaceous Colorado/Alberta Group of the Western Canadian Sedimentary Basin. In Geological Atlas of the Western Canadian Sedimentary Basin, G. D. Mossop and I. Shetsen (comps.), Canadian Society of Petroleum Geologists and Alberta Research Council, 335-352
- Martini, A., Budai, A., Walters, L., Schoell, M. (1996) Economic accumulations of biogenic methane, *Nature* **383**, 153-158
- McRory, R.E. (1982) Energy Heritage, Oil Sands and Heavy Oils of Alberta, 94
- Rich, K. (1995) Determination of the source of migrating gas from oil and gas wells in the Lloydminster area using stable isotope analyses. M.Sc. Thesis. University of Alberta
- Rich, K., Muehlenbachs, K., *Soc. Petrol. Eng.* **30265** (1995)
- Schoell, M. (1980) The hydrogen and carbon isotopic composition of methane from natural gases of various origins. *Geochim. Cosmochim. Acta.* **44**, 649-661
- Taylor, S.W., Sherwood-Lollar, B., Wasenaar, L., Hendry, M. J. (1997) Bacterial hydrocarbon production in a shallow bedrock aquifer and surficial till aquitards, CSPG-SEPM Abstracts, 276

CHAPTER THREE

IDENTIFICATION AND APPLICATION OF TRENDS IN THE $\delta^{13}\text{C}$ VALUES OF SHALLOW NATURAL GASES¹

3.1 INTRODUCTION

Thousands of wells have been drilled in northeastern Alberta and adjacent Saskatchewan in order to develop the heavy oil reservoirs of the Lower Cretaceous Mannville Group sands. In a large number of these wells, vertical migration of gas from previously unknown sources to the surface via well casings and surrounding soils represents a serious environmental problem. Mud samples from new wells being drilled in that area were collected at 50m intervals from the surface down to the completion depth, and the gases contained within the muds ('mud-gases') were analyzed for $^{13}\text{C}/^{12}\text{C}$ composition. Gases from the various Mannville Group sands do not show unique isotopic signatures; they are comprised of biogenic methane ($\delta^{13}\text{C}_{\text{C}_1} = -70\text{‰}$ to -60‰ (PDB)), with trace C_{2+} components that are residues from biodegradation processes. Gases from each of the overlying Upper Cretaceous Colorado Group shale units are, however, isotopically distinct. The $\delta^{13}\text{C}$ of methanes in the shales have values equivalent to those within the Mannville sands, but the $\delta^{13}\text{C}$ of the C_{2+} components are unambiguously different. Surprisingly, C_{2+} gases from the shallower Colorado shales are incipient thermal gases displaying equilibrium isotopic compositions. Based on the isotopic data, this may be the most immature suite of thermogenic gases ever reported ($\delta^{13}\text{C}_{\text{C}_2} \approx -63\text{‰}$ to -32‰ , $\delta^{13}\text{C}_{\text{C}_3} \approx -42\text{‰}$ to -22‰ , $\delta^{13}\text{C}_{\text{nC}_4} \approx -37\text{‰}$ to -23‰). Comparisons between the isotopic characteristics of the shallow gases and the migrating gases collected near surface reveal that most migrating gases are actually sourced in the Colorado Group shales, and not the Mannville sands in which the wells were completed.

¹ *A version of this chapter has been submitted for publication. Devon Rowe and Karlis Muehlenbachs, Journal of Organic Geochemistry.*

Carbon isotope fingerprints from mud-gases are used to identify specific source depths of migrating gases for the first time. The ability to estimate migrating gas source depth greatly aids in the remediation of 'leaking' wells within the Western Canadian Sedimentary Basin.

A variety of models exist proposing relationships between carbon isotope ratios of natural gases and the properties of their source materials (e.g. vitrinite reflectance, coal rank, isotopic composition) (Stahl and Carey, 1975; Chung *et al.*, 1988; Berner and Faber, 1996). These properties can be excellent indicators of the presence and/or type of petroleum deposits, and several researchers have proposed the use of carbon isotope ratios for the study of hydrocarbon pools (Chung *et al.*, 1988; Galimov, 1988; Clayton, 1991; Berner *et al.*, 1992). Many of the existing models cannot yet be utilized in the heavy oil region of the WCSB because very little isotopic data or source rock properties have been published. In this study, isotopic analyses of mud-gases collected from different depths at several locations provide a three-dimensional data set that is ideal for studying the isotopic characteristics of these shallow gases.

It is generally accepted that kinetic isotope effects control isotopic fractionation during natural gas formation. James (1983) proposed however, that the carbon isotope compositions of light hydrocarbons (C_1 to C_4) may approach equilibrium distributions, and he derived an accompanying set of fractionation curves for determining the maturity of gases based on these isotopic distributions ('maturity diagrams'). James' model has been successfully applied in a variety of geologic scenarios (James and Burns, 1984; James, 1990), which suggests that equilibrium isotopic compositions may widely exist in nature.

James' maturity diagrams are especially useful for comparing gases from different sources or when source properties are unknown, but derivation of his model requires a sophisticated knowledge of gas partition functions. Chung *et al.* (1988) introduced a simpler model for determining relative thermal maturity of gases, and for interpretation of natural gas origins. Laboratory heating experiments (Sackett, 1978;

Chung and Sackett, 1980) and natural examples from several basins (Chung *et al.* 1988) have also shown good agreement with this model. We have found that isotopic trends in shallow gases are best explained by combining the individual plotting techniques associated with James' and Chung *et al.*'s models.

3.2 ENVIRONMENTAL ISSUE

Enormous amounts of oil and natural gas are stored in the Lower Cretaceous Mannville Group sands and the overlying Upper Cretaceous Colorado Group shales of the Western Canadian Sedimentary Basin (WCSB) (figure 3.1).

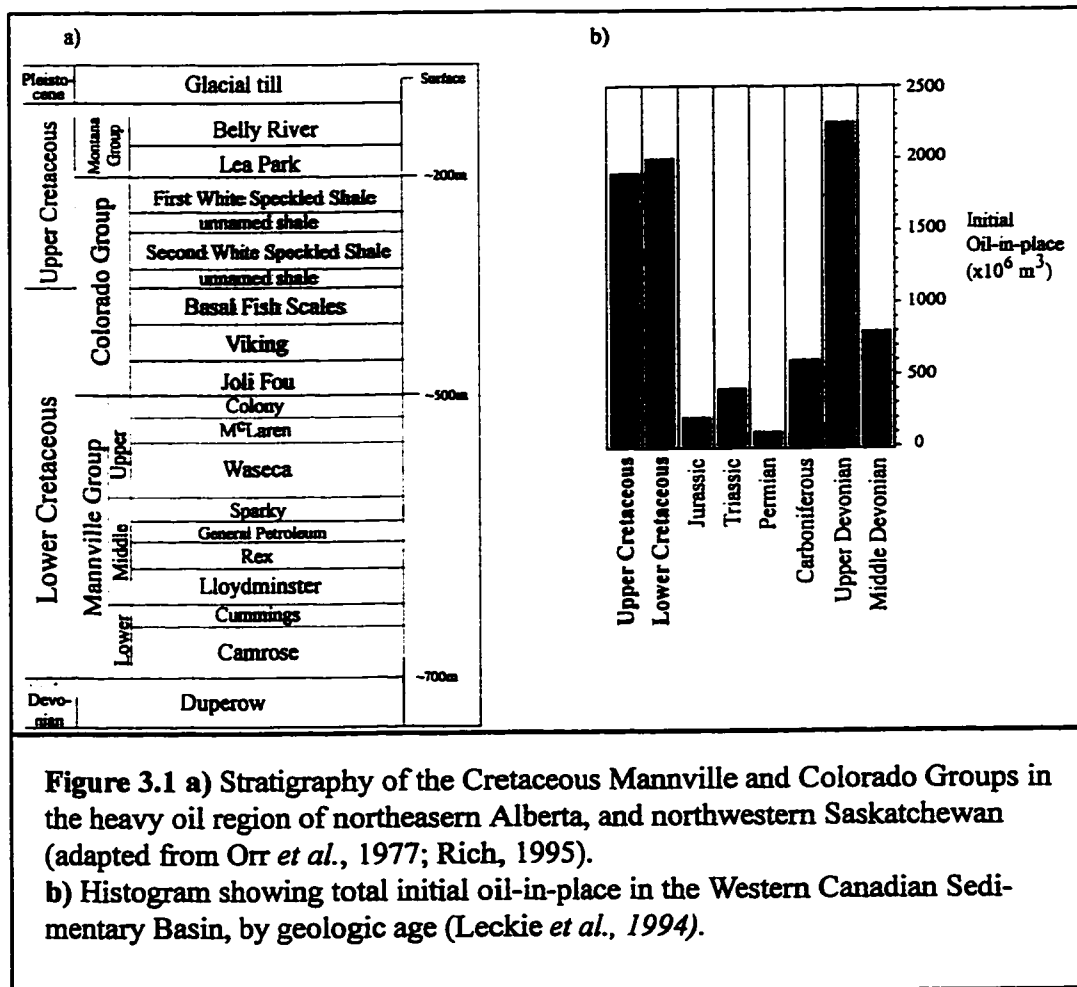


Figure 3.1 a) Stratigraphy of the Cretaceous Mannville and Colorado Groups in the heavy oil region of northeastern Alberta, and northwestern Saskatchewan (adapted from Orr *et al.*, 1977; Rich, 1995).

b) Histogram showing total initial oil-in-place in the Western Canadian Sedimentary Basin, by geologic age (Leckie *et al.*, 1994).

Several thousand wells are currently producing from the formations within these Groups, and remaining reserves are estimated to be among the largest in the world (McRory, 1982). Nearly half of the heavy oil wells in northeastern Alberta and adjacent areas of Saskatchewan are plagued by gas migration (Erno and Schmitz, 1994). Gases that migrate vertically from depth along the wellbores may contaminate shallow drinking water aquifers and destroy arable soils around wellheads, as well as contribute to the atmospheric methane concentration (figure 3.2).

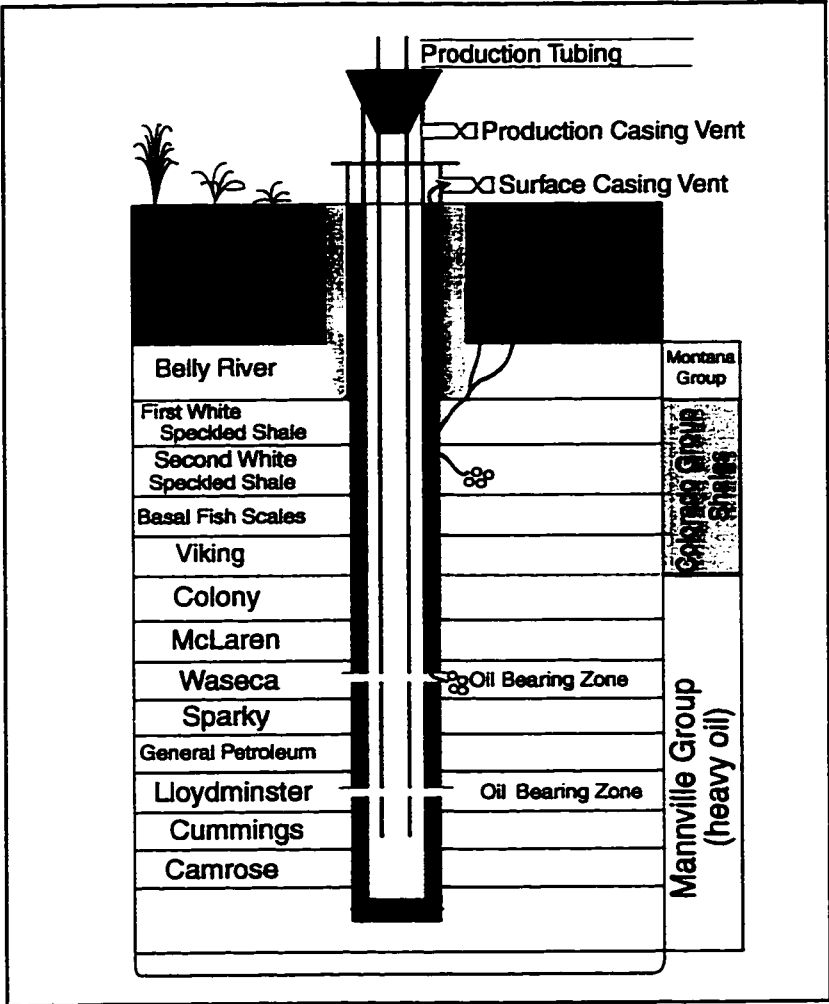


Figure 3.2 Schematic diagram of a typical heavy oil well, showing various gas migration pathways

Strict environmental regulations in Western Canada now require that gas migration in these 'leaking' wells be stopped at the source during well abandonments.

Initially, the origin of migrating gases was assumed to be the Mannville formations in which the majority of heavy oil wells are perforated. A study by Rich (1995) characterized the carbon isotope composition of the Mannville gases in the hopes of being able to identify gas migration sources based on their $\delta^{13}\text{C}$ values. Gases from each of the Mannville formations were found to be isotopically very similar ($\delta^{13}\text{C}_{\text{C}_1}$ from -57‰ to -68‰, $\delta^{13}\text{C}_{\text{C}_2}$ from -23‰ to -32‰, $\delta^{13}\text{C}_{\text{C}_3}$ from -17‰ to -25‰, $\delta^{13}\text{C}_{\text{C}_4}$ from -20‰ to -25‰, figure 3.3). The majority of migrating gases however, had distinctly

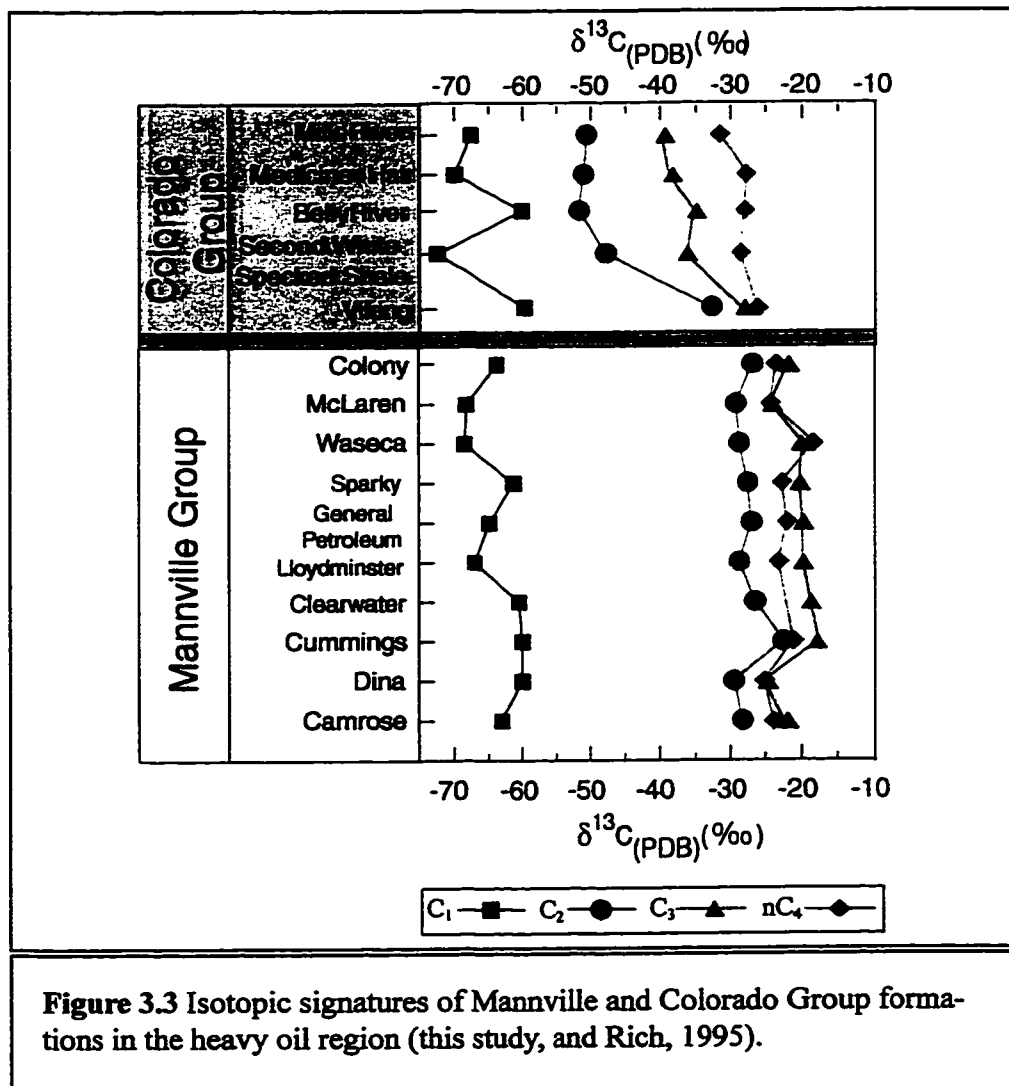
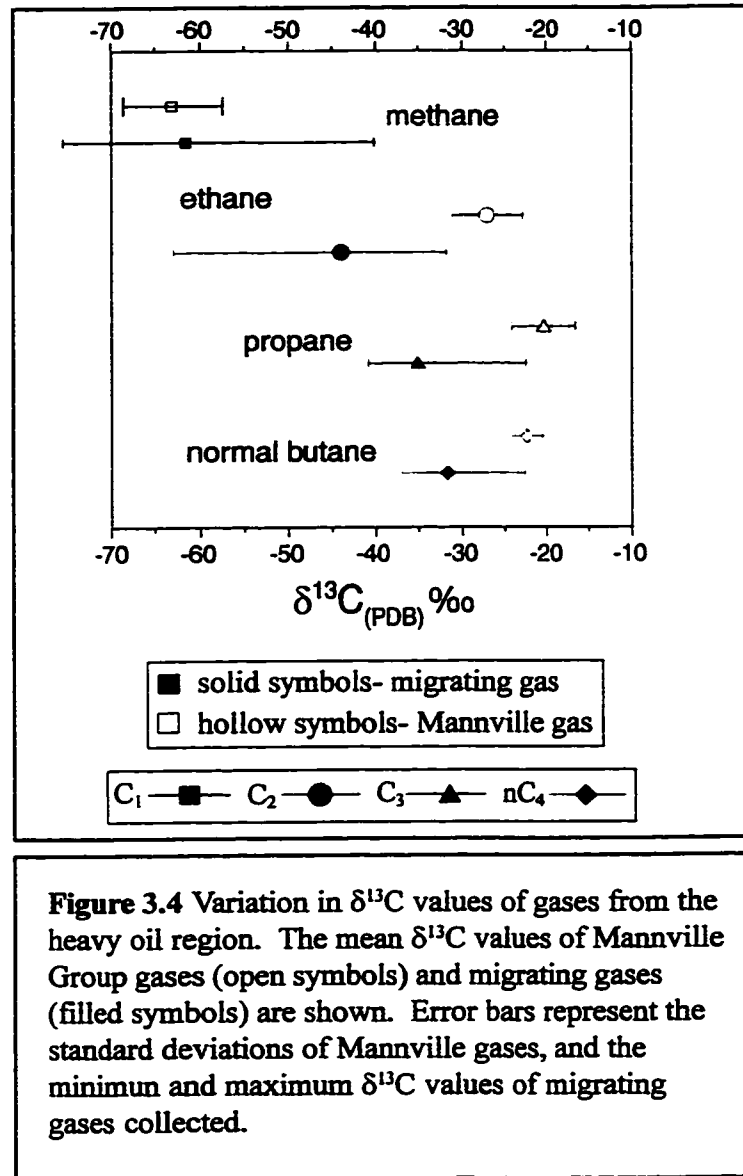


Figure 3.3 Isotopic signatures of Mannville and Colorado Group formations in the heavy oil region (this study, and Rich, 1995).

different isotopic ratios, characterized by unexpectedly light $\delta^{13}\text{C}_{\text{C}_2}$ (-63‰ to -31‰) and $\delta^{13}\text{C}_{\text{C}_3}$ values (-42‰ to -22‰) (figure 3.4). Contrary to previous assumptions, Rich



(1995) suggested that the source of these migrating gases was the overlying shallower Colorado Group shales, not the oil-bearing Mannville sands.

Due to the paucity of producing gas wells, isotope ratios of only a few Colorado Group gases have been previously studied. The method described herein utilizes gas

chromatography-combustion continuous-flow isotope ratio mass spectrometry (GC-C CF-IRMS) techniques to measure carbon isotope ratios of both Colorado and Mannville Group gases sampled during drilling activities.

3.3 SAMPLING AND MEASUREMENT OF ISOTOPE RATIOS

The study area consists of the 'heavy oil region' of Alberta and Saskatchewan, around the city of Lloydminster. Heavy oil wells are prolific in this area, and with a very high well density there is a heightened awareness of gas migration.

Mud samples from the Colorado and Mannville Groups were obtained during drilling of 21 new heavy oil wells (figure 3.5), and the carbon isotope ratios of the gases

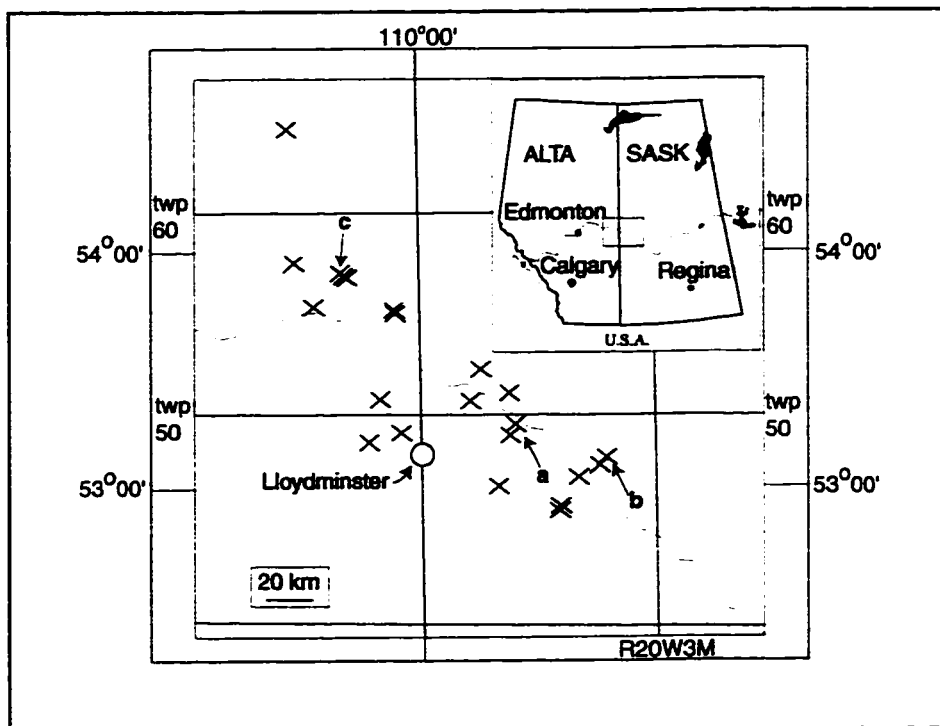


Figure 3.5 Locations of wells in the Western Canadian Sedimentary Basin where mud-gases were collected. Sampling concentrated on the heavy oil region, surrounding the city of Lloydminster.

contained within these muds ('mud-gases') were measured. Automated 'mud-loggers' are not common on shallow WCSB drilling rigs, so mud-gases were sampled by a more tedious manual procedure. Gases contained within the shale/rock matrix at depth were mixed with loosened material and drilling fluid (fresh water) as the bit penetrated the subsurface (wells were drilled overbalanced). This matrix/fluid mixture (mud) traveled up the annulus surrounding the drill stem at a constant velocity determined by the drilling fluid circulation rate. The time required for the mud to travel from the bit to the sampling point was a function of bit depth and circulation rate, allowing samples to be collected at known depth intervals. At each of the 21 wells, mud samples were collected from the surface down to the targeted Mannville formation at 50m depth intervals. Each sample was captured in a 1L plastic bottle before entering the 'shale-shaker', leaving a 3-5 cm headspace for the gases to occupy. Copper sulfate was added (to kill any bacteria) before sealing with tight fitting caps and electrical tape.

Carbon isotope ratios were obtained with a Finnigan-MAT 252 GC-C CF-IRMS system. The gas chromatograph was equipped with a PLOT fused silica capillary column (27.5m x 0.45mm, 0.32mm(I.D.), carrier gas: helium). Gases extracted directly from the headspace of the plastic bottles were injected into a liquid nitrogen cooled cryogenic trap. The cryogenic trap was then instantaneously heated to 180°C, and the gaseous sample was introduced onto the GC column. The column was held at 30°C for 7 minutes, ramped at 40°C/min to 80°C and held for 1 minute, ramped at 20°C/min to 200°C and held for 11 minutes.

Isotopic values were calculated by integrating the m/z 44, 45 and 46 ion currents of the CO₂ peaks resulting from on-line (continuous-flow) combustion of chromatographically separated compounds (Brand, 1996). Laboratory CO₂ pulses admitted directly into the mass spectrometer were used as reference. Carbon isotope compositions are reported as δ¹³C values in ppt (‰) with respect to the PDB standard. Reproducibility of the δ¹³C values was ±0.1 ‰ for methane, and ±0.2 ‰ for the C₂₊

components (ethane, propane and butane). The additional analytical uncertainty in the $\delta^{13}\text{C}_{\text{C}_{2+}}$ values is due to the extremely small concentrations of these components.

3.4 RESULTS AND DISCUSSION

Isotopic fingerprints from three wells are shown in figure 3.6a-c. In each of the

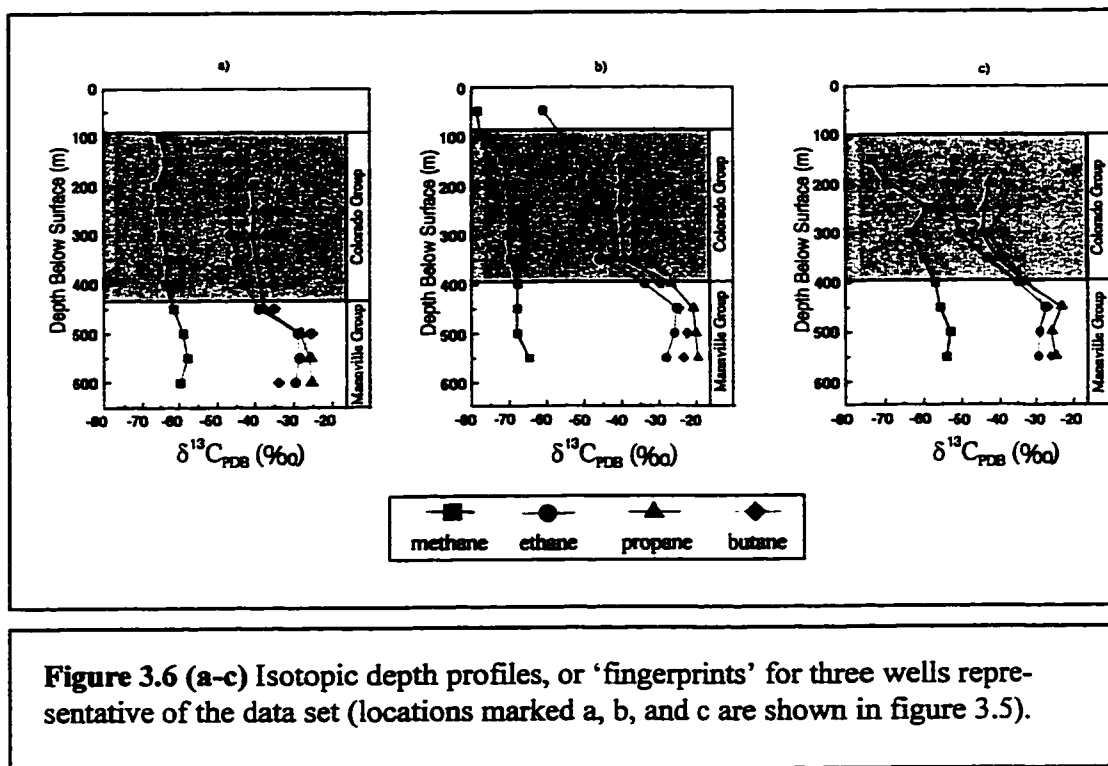


Figure 3.6 (a-c) Isotopic depth profiles, or ‘fingerprints’ for three wells representative of the data set (locations marked a, b, and c are shown in figure 3.5).

fingerprints, the Colorado/Mannville stratigraphic boundary is mirrored by a distinct change in isotopic signature. Mannville Group gases are significantly enriched in ^{13}C relative to the Colorado gases (in some cases by as much as 20‰), and can be easily identified from $\delta^{13}\text{C}_{\text{C}_{2+}}$ values alone. The isotopic partitioning between C_{2+} components (i.e. $\delta^{13}\text{C}_{\text{C}_3} - \delta^{13}\text{C}_{\text{C}_2}$ or $\delta^{13}\text{C}_{\text{nC}_4} - \delta^{13}\text{C}_{\text{C}_3}$) shows a definite depth trend. Isotopic separations gradually increase from $\sim 2\text{-}5$ ‰ at the Mannville/Colorado boundary, to differences of

10‰ or more in very shallow samples. These isotopic signatures reflect the different genetic histories of the Colorado and Mannville Group gas deposits.

The Mannville Group sands are a basin-wide hydrocarbon trap, accumulating oil and oil-associated gases sourced in underlying Jurassic, Mississippian and Devonian reservoirs (Leckie *et al.*, 1994). Gas chromatograms of Mannville oils in the Lloydminster area show that they have been extensively biodegraded during up-dip migration from deeper in the basin, resulting in the existing giant heavy oil deposits (Deroo *et al.*, 1977). Carbon isotope ratios of the gases associated with the heavy oils also show the effects of biodegradation (figure 3.7). Unaltered Lower Cretaceous gas

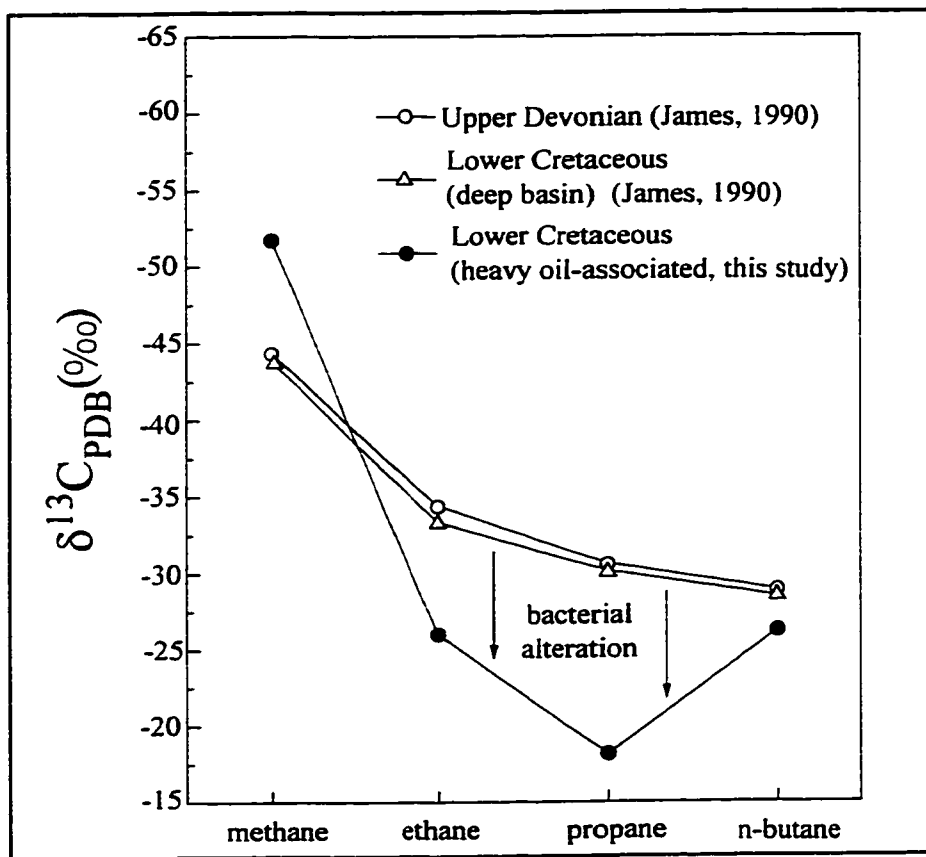


Figure 3.7 Isotopic composition of oil-associated Upper Devonian and Lower Cretaceous (Mannville Group) gases from the WCSB.

(from deeper in the basin) is isotopically almost identical to Upper Devonian gas, presumably because they share the same source. Lower Cretaceous Mannville gases associated with the heavy oils have migrated long distances, and bacterial oxidation has significantly altered their isotope ratios. Preferential cleavage of ^{12}C - ^{12}C bonds (over ^{13}C - ^{12}C bonds) during bacterial alteration of alkanes leads to residual gases that become enriched in ^{13}C (James and Burns, 1984). Bacterial alteration of Mannville gases has led to characteristic isotopic reversals between the $\delta^{13}\text{C}_{\text{C}_3}$ and $\delta^{13}\text{C}_{\text{C}_4}$ values (i.e. $\delta^{13}\text{C}_{\text{nC}_4} < \delta^{13}\text{C}_{\text{C}_3}$). Similar bacterial enrichment has been observed in the other fields (James, 1990). Mannville gases have mixed with large amounts of biogenic methane, which accounts for very negative $\delta^{13}\text{C}_{\text{C}_1}$ values (-70‰ to -60‰).

The Colorado Group is a self-sourced reservoir, containing unaltered incipient thermogenic gas. Unlike the Mannville Group, the isotope ratios of Colorado gases display the isotopic systematics expected for thermal gases, with methane being the isotopically lightest component, followed by ethane, propane, etc. The isotopic separation of the alkane components determines their maturities because the gases are thermogenic. Figure 3.8 is a 'maturity diagram' of the Colorado Group mud-gases.

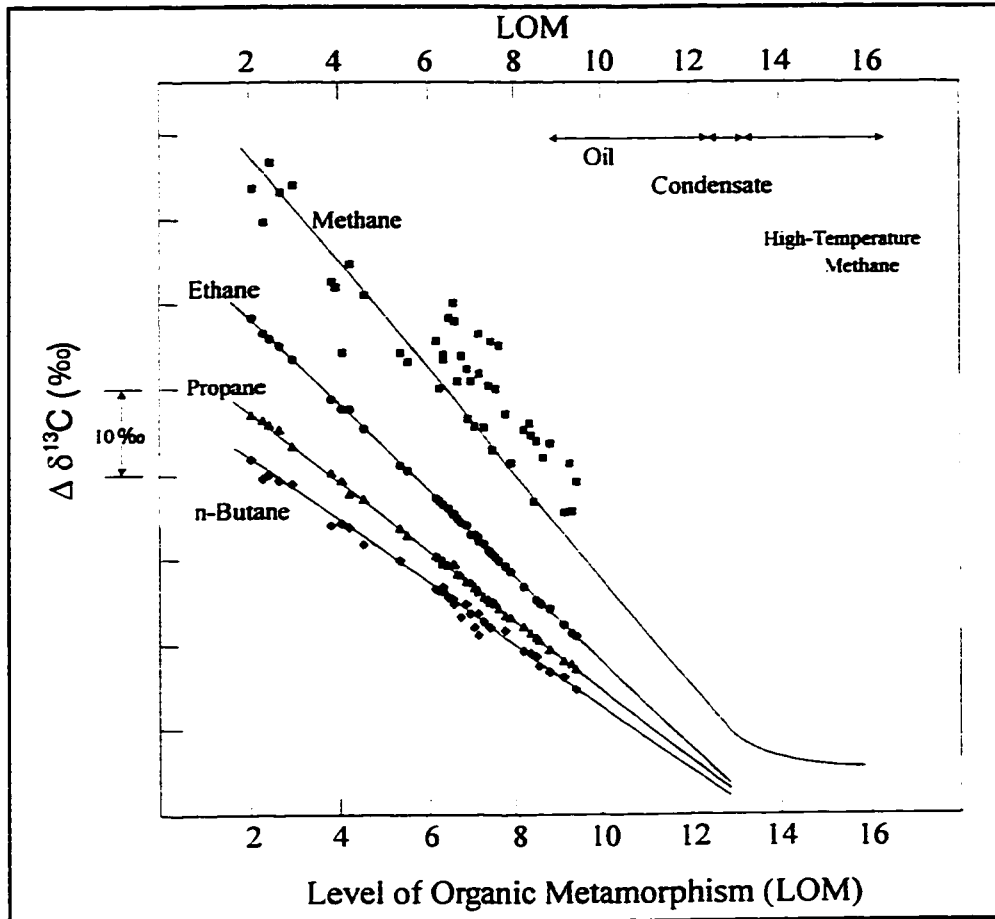


Figure 3.8 Colorado Group gases plotted on James' (1983) maturity diagram.

Following James (1983), carbon isotopic separations between gas components are plotted along the vertical axis using a sliding scale that is the difference (in ppt) between the $\delta^{13}\text{C}$ values of gas components. The best fit of the data is found by positioning the measured isotopic separations until they fit the calculated separations (lines), which then determines the gas' maturity in terms of the 'Level of Organic Metamorphism' (LOM, marked on the horizontal axis)(Hood *et al.*, 1975). The Colorado gas data fit the calculated curves extremely well, with measured data essentially defining the ethane, propane and butane curves. In most of the gases the methane values are considerably higher than the calculated lines predict. This is also due to mixing with isotopically light biogenic methane (James, 1983). The isotopic separations between Colorado gas components

indicate that the majority of these gases was generated at LOMs of 6-8, although several gases appear to be considerably less mature (LOMs ranging from ~2-5). These are some of the most immature gases ever reported (table 3.1).

Carbon Isotope Composition, $\delta^{13}\text{C}$ (‰)					
Methane	-69.2	-70.7	-65.2	-62.9	-62.5
Ethane	-54.0	-50.2	-49.6	-46.0	-42.6
Propane	-42.6	-39.9	-41.2	-39.0	-37.4
N-butane	-37.4	-35.6	-36.0	-37.1	-36.1
Estimated LOM	<2	~2	~4	7	8

Table 3.1 Carbon isotope compositions and estimated LOMs of several gases from the Cretaceous Colorado Group shales, Western Canadian Sedimentary Basin, Alberta.

It is evident that Colorado Group gases range considerably in their maturities. ‘Natural gas plots’ (Chung *et al.*, 1988) of mud-gases are useful for examining the maturity trends that exist within Colorado gases from individual wells. Plotting the $\delta^{13}\text{C}$ values of individual alkanes, versus the inverse number of carbon atoms (i.e. $\delta^{13}\text{C}_{\text{C}_3}$ versus $1/3$) should result in a straight line for unaltered gas components generated from the same source. The slopes of these lines reflect the relative gas maturities, and the y-intercepts provide an estimate of the isotopic composition of the source. Less mature gases tend to have larger isotopic separations, corresponding to steeper slopes on natural gas plots. Figure 3.9 contains natural gas plots for each of the isotopic fingerprints in

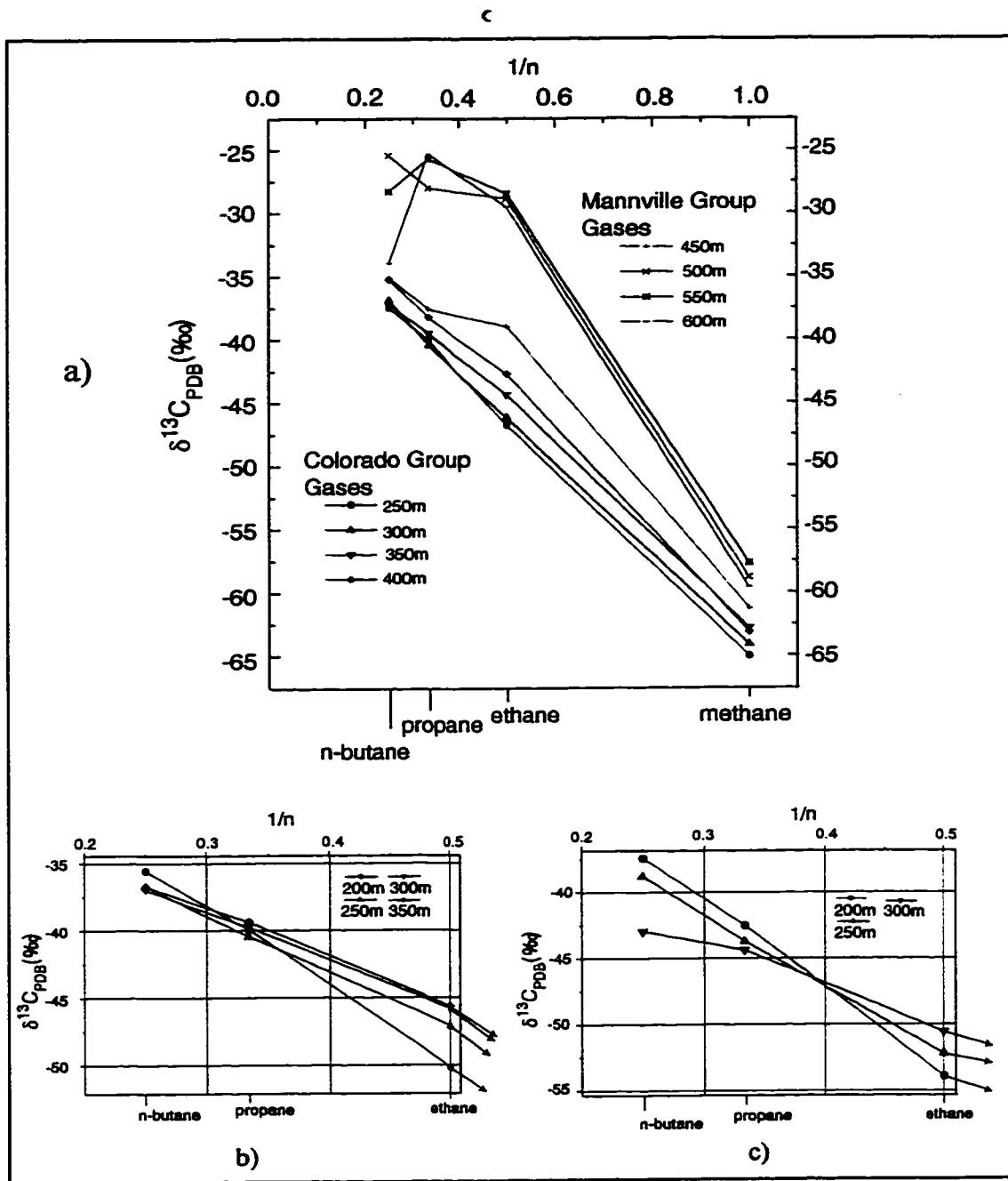


Figure 3.9 Isotopic data from figure 3.6 shown on 'natural gas plots' (after Chung *et al.*, 1988). Depths of Colorado Group gas samples are included. a) Mannville and Colorado Group gases from one well b,c) Close-up of Colorado Group gases from figures 3.6b and 3.6c (respectively).

figure 3.6. The isotope ratios of Colorado gases display linear relationships with their inverse carbon numbers, although agreement with the $\delta^{13}\text{C}_{\text{C}_1}$ values is probably coincidental since these methanes most likely are biogenic (following the logic of figure 8) rather than thermogenic. The Mannville Group gases display a variety of non-linear slopes due to the effects of bacterial alteration. In figures 3.9b and 3.9c only the Colorado gases are shown, to highlight the trends within this Group. Slopes of $\delta^{13}\text{C}_{\text{C}_{2+}}$ versus $1/n$ decrease with depth indicating (as one might expect) that Colorado gas maturities increase with depth. Two different source compositions are predicted from the y-intercepts. Gases from deeper than 200m appear to be generated from a -30‰ marine source (consistent with type-II kerogen), but gases from 200m or shallower (9 b.c) indicate an isotopically enriched -20‰ terrigenous source material.

3.5 ENVIRONMENTAL APPLICATIONS

The following example illustrates the application of isotopic fingerprints of mud-gases to the remediation of leaking oil wells.

3.5.1 GAS MIGRATION

Gas migration is primarily manifested as surface casing vent (SCV) flow, and/or soil gas bubbles around wellbores (figure 3.2). The SCV functions as a bleed-off valve, allowing built-up gases to vent directly into the atmosphere. SCV flow rates range from 0.01 m³/day to 200 m³/day (Schmitz *et al.*, 1993; Erno and Schmitz, 1994). Although gas migration through soils tends to occur at much lower rates (0.01 m³/day) than SCV flows, soil gases can often be observed bubbling through ponded water around wellbores. The gas migrating through soil frequently kills or stunts vegetation growth within a radius of

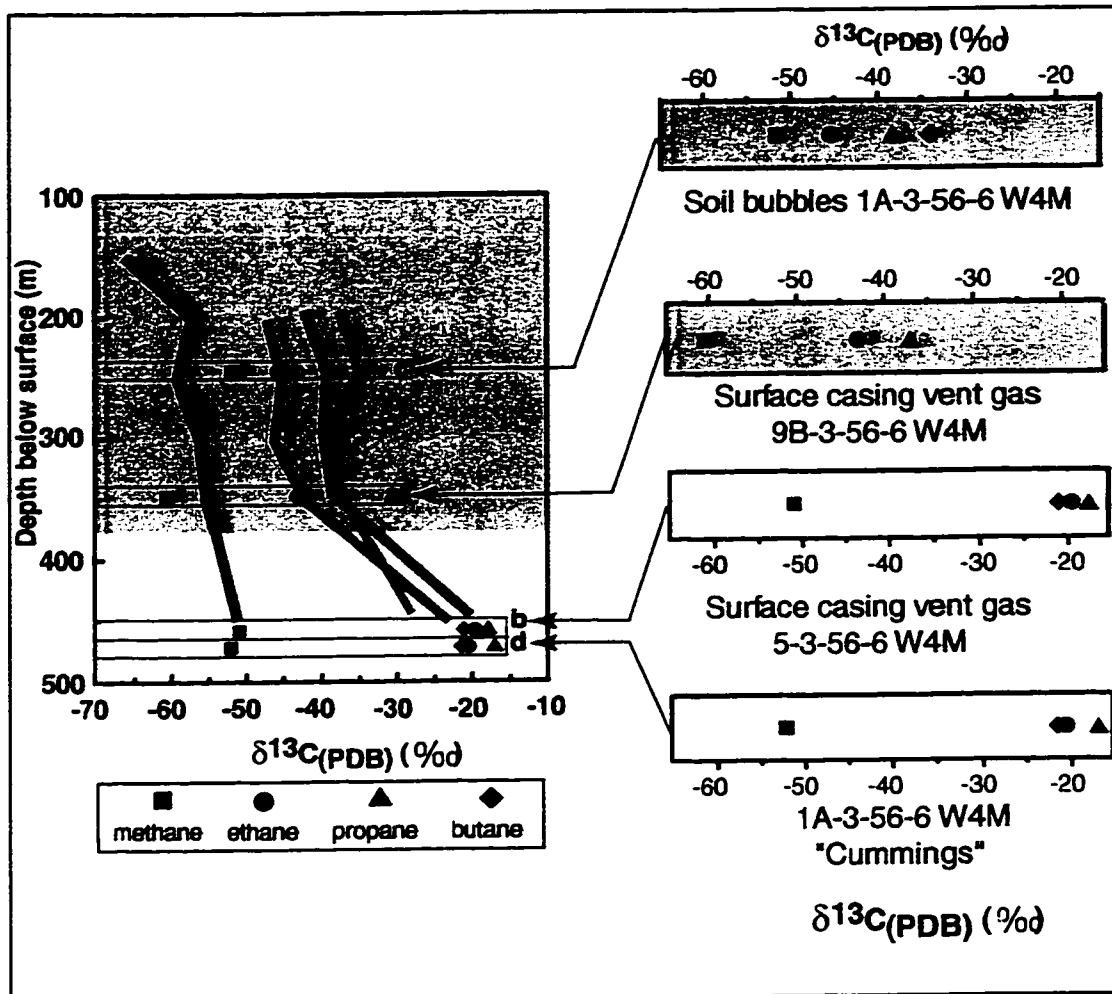


Figure 3.10 Isotope ratios of three migrating gases (a-c) superimposed over an isotopic fingerprint used to determine their individual source depths (Lindbergh field, Alberta). The Colorado and Mannville Groups have been shaded to indicate the boundary.

several meters surrounding the well (Rich, 1995). Isotopic analyses of hundreds of gases have shown that most migrating gases are sourced in the Colorado Group formations, not in the heavy oil pools of the Mannville sands. By matching the isotope ratios of migrating gases with isotopic fingerprints from the same field, accurate estimates of source depths can be made.

The isotope ratios of SCV gas from two wells, and soil gas from a third well, all from the same field are shown in figure 3.10a-c, and table 3.2.

	a) SCV		b) SCV		c) Soil gas		d) Production gas	
	$\delta^{13}\text{C}$	%vol	$\delta^{13}\text{C}$	%vol	$\delta^{13}\text{C}$	%vol	$\delta^{13}\text{C}$	%vol
Methane	-60.5	97.27	-50.9	96.72	-51.6	55.92	-52.0	99.50
Ethane	-43.0	0.33	-19.6	0.22	-45.4	0.20	-20.4	0.20
Propane	-37.3	0.02	-18.0	0.02	-38.6	0.01	-17.0	0.07
n-Butane	--	--	-21.0	0.02	-34.6	0.01	-21.3	0.03
Carbon Dioxide	--	--	--	0.15	-37.7	6.73	--	0.10
Source Depth	~350m		>450m		~245m		N/A	

Table 3.2 Carbon isotope and gas compositions of C_1 - C_4 and CO_2 gases from the Lindbergh field, AB. Isotope ratios of C_1 - C_4 components are used to estimate the source depths (figure 3.10). In (c), CO_2 derived from the oxidation of methane is mixed with migrating gas, resulting in high concentration and very negative $\delta^{13}\text{C}$ value.

Each data set has been superimposed over an isotopic fingerprint from that field. The best fit of each data set is found by sliding the data vertically until the isotope ratios of the C_{2+} components best match the underlying isotopic fingerprint. This allows the source depths to be extrapolated from the vertical axis. In gases a and c, remediation efforts must be targeted in the shallower Colorado shales (at ~350m and ~245m, respectively), rather than re-cementing the wells in the Mannville Group, the nominal producing depth of the well. The majority of migrating gases are sourced in the Colorado Group, but occasionally (e.g. figure 3.10b) the source horizon lies in the deeper Mannville Group. In this case, the migrating gas sampled at surface is very similar to the typical production gas from that field (gas sample d).

3.6 CONCLUSIONS

Isotopic fingerprints of mud-gases have shown that gases within the WCSB Colorado Group shales and Mannville Group sands have evolved by two different mechanisms. Surprisingly, it is the deeper Mannville Group gases that are extensively biodegraded, whereas the shallow gases in the Colorado Group have remained unaltered. The Colorado Group contains immature incipient thermal gases, displaying near equilibrium isotopic compositions. When combined with isotopic fingerprints of mud-gases, $\delta^{13}\text{C}$ values of Colorado gases provide an accurate estimate of source depth. The ability to determine source depths of shallow gases is particularly useful for the remediation of numerous leaking heavy-oil wells in the WCSB.

3.7 REFERENCES

- Berner, U., Faber, E. and Stahl, W. (1992) Mathematical simulation of carbon isotopic fractionation between huminitic coals and related methane. *Chem. Geol.* **94**, 315-319
- Berner, U. and Faber, E. (1996) Empirical carbon isotope/maturity relationships for gases from algal kerogens and terrigenous organic matter, based on dry, open-system pyrolysis. *Org. Geochem.* **24**, 947-955
- Brand, W. A. (1996) High precision isotope ratio monitoring techniques in mass spectrometry. *Jour. Mass. Spec.* **31**, 225-235
- Clayton, C. (1991) Carbon isotope fractionation during natural gas generation from kerogen. *Mar. Petrol. Geol.* **8**, 232-240
- Chung H. M., Gormly J. R. and Squires R. M. (1988) Origin of gaseous hydrocarbons in subsurface environments: Theoretical considerations of carbon isotope distributions. *Chem. Geol.* **71**, 97-103
- Chung, H. M. and Sackett, W. M. (1980) Carbon isotope effects during pyrolytic formation of early methane from carbonaceous materials. In: A. G. Douglas and J. R. Maxwell (Editors), *Advances in Organic Geochemistry*, 705-710
- Deroo, G., Powell, T. G., Tissot, B., and McCrossan, R. G. (1977) The origin and migration of petroleum in the Western Canadian Sedimentary Basin, Alberta: Geological Survey of Canada Bulletin 262
- Erno, B. and Schmitz, R. (1994) Measurements of soil gas migration around oil and gas wells in the Lloydminster area. Technical meeting of the Petroleum Society of the CIM, **94**, paper #73
- Galimov, E. M. (1988) Sources and mechanisms of formation of gaseous hydrocarbons in sedimentary rocks. *Origins of Methane in the Earth. Chem. Geol.* **71**, 77-95
- Hood, A., Gutjahr, C. C. M., and Heacock, R. L. (1975) Organic metamorphism and the generation of petroleum: AAPG Bull., **59**, 986-996
- James, A. T. (1983) Correlation of natural gas by use of carbon isotopic distribution between hydrocarbon components. AAPG Bull., **67**, 1176-1191

- James, A. T. (1990) Correlation of reservoir gases using the carbon isotopic compositions of wet gas components. *AAPG Bull.* **74**, 1441-1458
- James, A. T. and Burns, B. J. (1984) Microbial alteration of subsurface natural gas accumulations. *AAPG Bull.*, **68**, 957-960
- Leckie, D. A., Bhattacharya, J. P., Bloch, J., Gilboy, C. F., Norris, B. (1994) Cretaceous Colorado/Alberta Group of the Western Canadian Sedimentary Basin. In *Geological Atlas of the Western Canadian Sedimentary Basin*, G. D. Mossop and I. Shetsen (comps.), Canadian Society of Petroleum Geologists and Alberta Research Council, 335-352
- McRory, R.E. (1982) *Energy Heritage, Oil Sands and Heavy Oils of Alberta*, 94
- Orr, R.D., Johnston, J.R. and Manko, E.M. (1977) Lower Cretaceous geology and heavy oil potential of the Lloydminster area. *Bulletin of Canadian Petroleum Geology*, vol. 25, 1187-1221
- Rich, K. (1995) Determination of the source of migrating gas from oil and gas wells in the Lloydminster area using stable isotope analyses. M.Sc. Thesis, University of Alberta
- Rich, K., Muehlenbachs, K., *Soc. Petrol. Eng.* **30265** (1995)
- Schmitz, R., Carlson, P. B., Lorenz, G. D., Watson, M. D. and Erno, B. P. (1993) Husky Oil's gas migration research effort- an update. In: 10th Heavy oil and oil sands technical symposium, Canadian Heavy Oil Association
- Schoell, M. (1980) The hydrogen and carbon isotopic composition of methane from natural gases of various origins. *Geochim. Cosmochim. Acta.* **44**, 649-661
- Sackett, W. M. (1978) Carbon and hydrogen isotope effects during the thermocatalytic production of hydrocarbons in laboratory simulation experiments. *Geochim. Cosmochim. Acta*, **42**, 571-580
- Saskatchewan Research Council (1995) Migration of methane into groundwater from leaking production wells near Lloydminster. Canadian Association of Petroleum Producers, **1995-0001**
- Stahl, W. J. and Carey B. D. Jr. (1975) Source-rock identification by isotope analyses of natural gases from fields in the Val Verde and the Delaware Basins, West Texas. *Chem. Geol.* **16**, 257-267

CHAPTER FOUR

ISOTOPIC ANOMALIES IN NATURAL GAS ASSOCIATED WITH HIGH TEMPERATURE STEAM INJECTIONS AT FORT KENT, ALBERTA

4.1 FORT KENT ANOMALY

Some heavy reservoirs in northeastern Alberta have been steamed for decades to enhance oil recovery. Migrating gases obtained from above a steamed heavy oil reservoir at the Fort Kent field (figure 4.1) differ systematically in isotopic composition from other

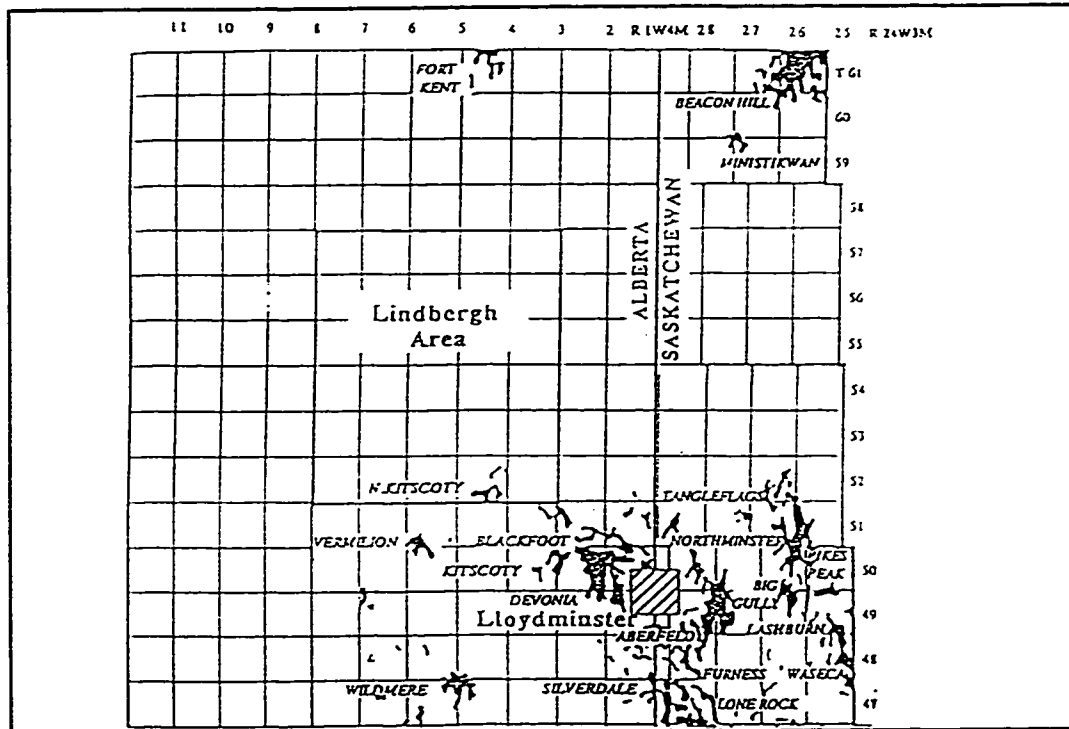


Figure 4.1 Location of the Fort Kent heavy oil field, Alberta.

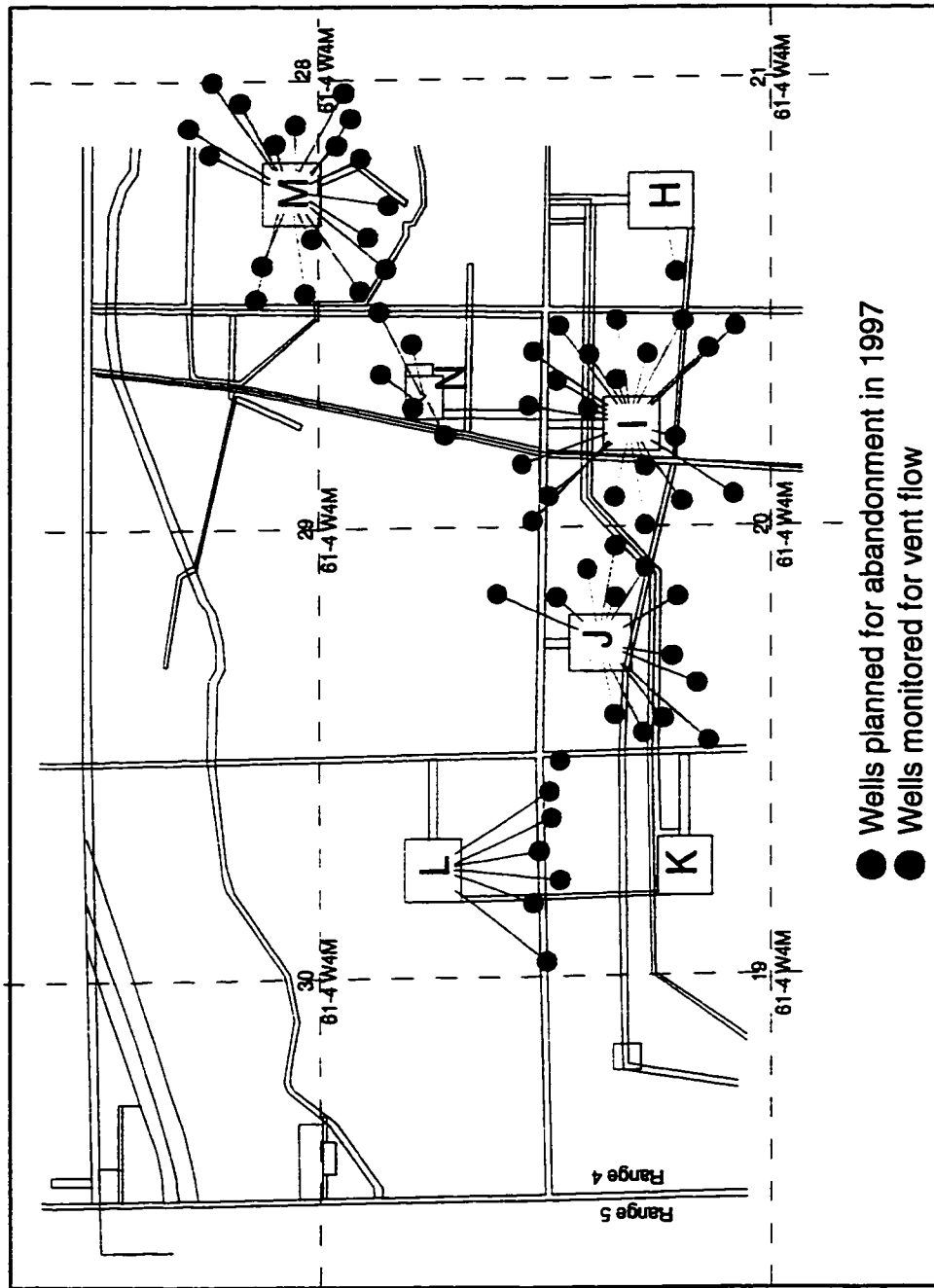


Figure 4.2 Plan view of the Fort Kent Thermal Project, showing wells that have been targeted for abandonment in 1997 (red). The green wells continue to be monitored for SCV flow, and soil gas migration.

nearby migrating gases. The $\delta^{13}\text{C}_{\text{C}_2+}$ values of the Fort Kent gases are enriched in ^{13}C , compared to migrating gases from adjacent heavy oil fields.

4.2 SITE CHARACTERIZATION

The Fort Kent Thermal Project was initiated by Worldwide Energy in August 1976. Suncor Inc. purchased the site in 1980, and continued to drill new wells until 1986, when a total of 139 wells had been installed at seven clusters (H, I, J, K, L, M, and N) (figure 4.2). Steam cycles stimulated oil recovery at these seven clusters for a period of approximately five years, from 1983 to 1988 (Tam and Yeung, 1989). Low oil prices forced all operations to be suspended in 1989. In 1996, Koch Exploration Canada purchased the site but was not able to produce from any of the wells. Subsequently, they initiated abandonment procedures on all active wells (figure 4.2). Details of any activity at the Fort Kent site between 1988 and 1998 were unavailable, but due to low oil prices, production was most likely suspended.

In 1996 Koch Exploration Canada identified a severe gas migration problem, with measurable SCV flows at 39 wells (mostly in the I, J and M clusters). Initially, cement plugs were placed near the Belly River formation (1996), but this was unsuccessful in stopping the migration. Failure to stop the migration was due to the combination of not knowing the origin of the migrating gases and poor cement bonding in the Belly River formation.

4.3 RESULTS

Isotopic analyses of gases from 30 wells are shown in table 4.1, and figure 4.3. Each of these wells is completed in the Mannville Group Grand Rapids formation, which

has an isotopic signature similar to those of the Mannville formations elsewhere in the heavy oil region ($\delta^{13}C_{C1} = -55\text{‰}$, $\delta^{13}C_{C2} = -26\text{‰}$, $\delta^{13}C_{C3} = -24\text{‰}$, $\delta^{13}C_{nC4} = -24\text{‰}$).

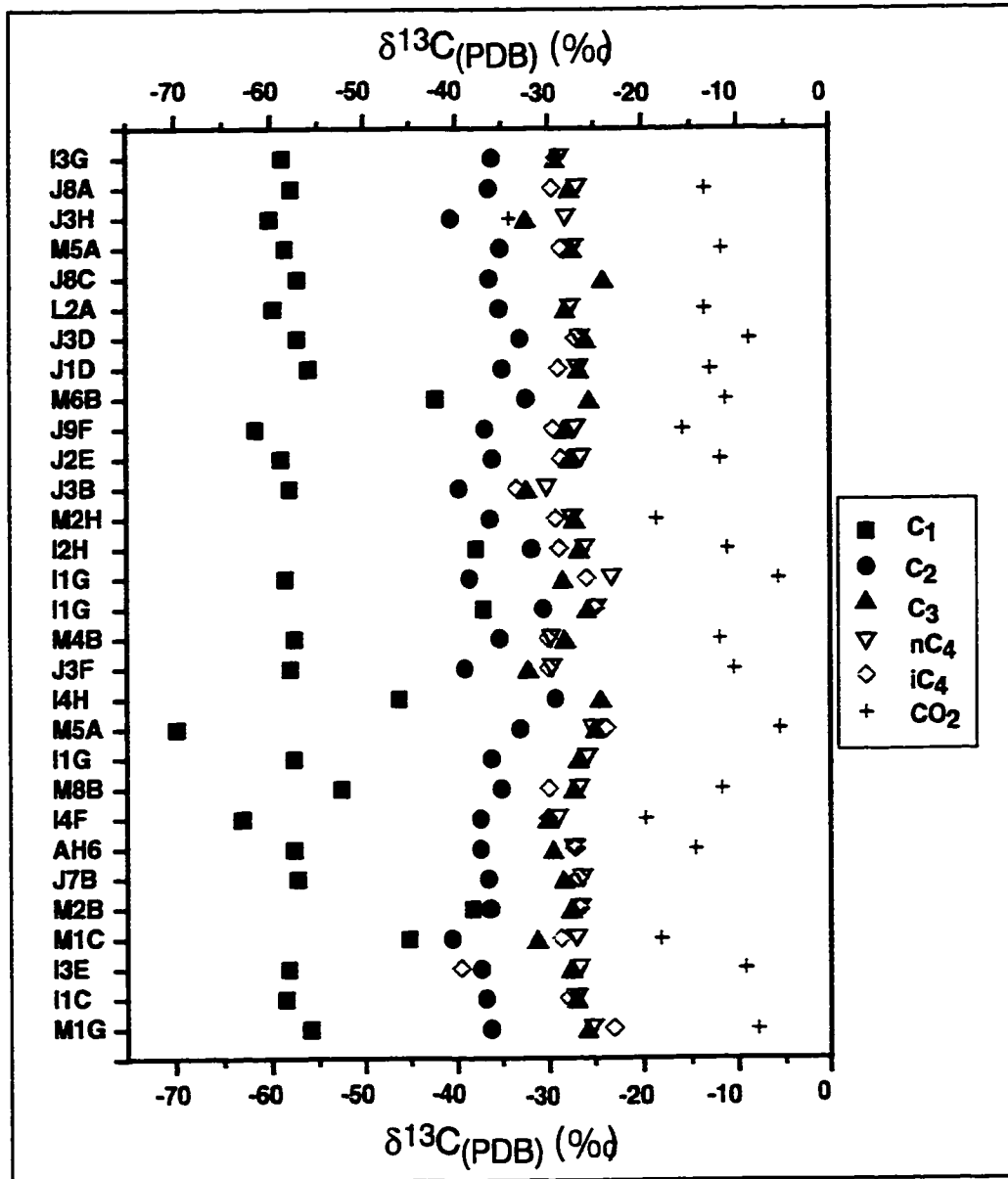


Figure 4.3 Isotope ratios of migrating gases from the Fort Kent field. The data are sorted according to increasing $C_3 - C_2$ isotopic separation.

Well ID	SEC	T	R	M	$\delta^{13}\text{C-C1}$	$\delta^{13}\text{C-C2}$	$\delta^{13}\text{C-C3}$	$\delta^{13}\text{C-iC4}$	$\delta^{13}\text{C-nC4}$	$\delta^{13}\text{C-CO2}$
J8C	20	61	4	4	-58.8	-36.0	-29.5	-28.4	-29.1	
M8B	28	61	4	4	-57.8	-36.4	-27.9	-26.5	-29.6	-13.5
M4B	28	61	4	4	-60.2	-40.6	-32.7	-27.7		-34.2
J3B	20	61	4	4	-58.5	-35.1	-27.8	-26.9	-28.6	-11.7
M1G	28	61	4	4	-57.2	-36.4	-24.4			
M6B	28	61	4	4	-59.8	-35.3	-28.4	-27.3		-13.5
J1D	20	61	4	4	-57.2	-33.1	-26.2	-26.2	-27.0	-8.8
J3F	20	61	4	4	-56.0	-35.0	-27.0	-26.4	-28.9	-12.9
M5A	28	61	4	4	-42.3	-32.4	-25.9			-11.3
M5A	28	61	4	4	-61.7	-36.9	-28.6	-26.7	-29.5	-15.8
I4H	29	61	4	4	-59.0	-36.1	-28.1	-26.1	-28.6	-11.9
J2E	20	61	4	4	-58.1	-39.7	-32.7	-29.9	-33.4	
I4F	20	61	4	4		-36.3	-27.5	-27.1	-29.2	-18.6
J3H	29	61	4	4	-37.8	-31.8	-27.0	-25.7	-28.8	-11.1
I3E	20	61	4	4	-58.6	-38.6	-28.8	-22.9	-25.9	-5.7
I3G	20	61	4	4	-37.1	-30.6	-26.2	-24.5	-25.0	
J3D	20	61	4	4	-57.6	-35.3	-28.5	-29.4	-30.1	-12.0
L2A	20	61	4	4	-58.0	-39.1	-32.6	-29.3	-30.0	-10.4
J8A	20	61	4	4	-46.3	-29.3	-24.8			
I1G	20	61	4	4	-69.9	-33.1	-25.3	-25.0	-23.9	-5.6
J7B	20	61	4	4	-57.7	-36.2	-27.1	-25.5		
M2H	28	61	4	4	-52.6	-35.1	-27.6	-26.4	-30.0	-11.8
J9F	20	61	4	4	-63.1	-37.4	-30.5	-28.6	-30.1	-19.8
I2H	20	61	4	4	-57.6	-37.4	-29.9	-26.9	-27.2	-14.6
I1G	20	61	4	4	-57.3	-36.6	-28.7	-26.0	-26.8	
I1G	20	61	4	4	-38.3	-36.3	-27.9	-26.3	-26.7	
AH6	28	61	4	4	-45.2	-40.6	-31.6	-26.7	-28.6	-18.2
M2B	28	61	4	4	-58.2	-37.3	-28.0	-26.3	-39.5	-9.3
M1C	28	61	4	4	-58.6	-36.8	-27.4	-26.7	-27.8	
I1C	20	61	4	4	-55.9	-36.3	-26.1	-25.0	-23.1	-8.0

Table 4.1 Isotopic ratios of migrating gases from the Fort Kent Thermal Project.

The $\delta^{13}\text{C}_{\text{C2}}$ and $\delta^{13}\text{C}_{\text{C3}}$ values of the Fort Kent migrating gases are isotopically different than the Grand Rapids formation gas, and following the logic of Chapter 3, they appear to be sourced in shallower horizons. Figure 4.4 is a comparison of the Fort Kent migrating

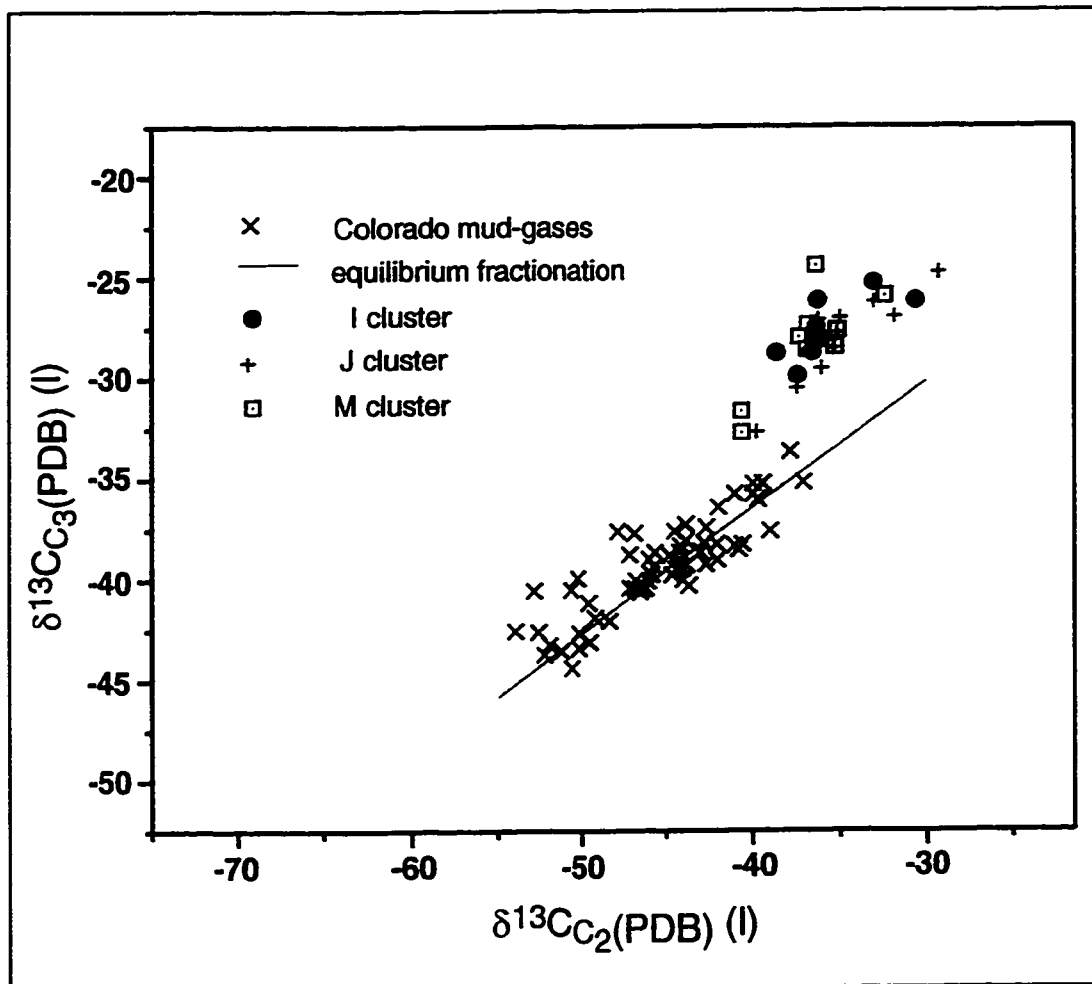


Figure 4.4 Relationship between isotope ratios of propane and ethane components of Colorado Group gases from oil fields near Lloydminster, and migrating gases from the Fort Kent Thermal Project. A theoretical C₃-C₂ fractionation line, assuming a -30‰ source is shown in red.

gases with the shallow gases from adjacent oil fields. Isotopically, the Fort Kent gases are clearly different from the shallow gases. A theoretical C₃/C₂ fractionation line (see figure 2.3, and Appendix E) has been superimposed over the shallow gas data, and this line provides a reasonable fit. The isotopic composition of the source material used in the calculation of this fractionation line is -30‰, typical of the marine derived type-II

kerogen of the WCSB. The isotope ratios of the steamed (Fort Kent) gases are enriched by about 10‰ in both $\delta^{13}\text{C}_{\text{C}_2}$ and $\delta^{13}\text{C}_{\text{C}_3}$ values relative to the shallow gases ($\delta^{13}\text{C}_{\text{C}_4}$ values are also slightly enriched, see table 4.1 and figure 3.3) and because of this enrichment, an acceptable fit with a theoretical fractionation line cannot be achieved (i.e. by varying the source composition). It appears that in the Fort Kent gases, the intense steaming has destroyed the quasi-equilibrium relationships that are characteristic of migrating gases throughout the rest of the WCSB heavy oil region.

The origin of these migrating gases is uncertain. The intense heat may have altered the isotope ratios of the existing shallow gas, or alternatively, the high temperatures may be facilitating *in-situ* gas generation around the wellbores. Subsurface temperatures greater than 100°C can be achieved during steamflooding, essentially ‘cooking’ the organic materials that surround the wellbores, liberating gaseous hydrocarbons. The isotopic enrichment of the Fort Kent gases suggests that if the migrating gases are being generated thermally, the isotopic composition of the source material is significantly enriched (-20‰) relative to kerogen (-30‰). Coal (or other terrestrial) deposits represent a potential source of isotopically enriched organic matter, and a number of small coal seams can indeed be found throughout the Mannville Group in the Fort Kent area. Although the majority of WCSB migrating gases do not originate in the Mannville Group formations, the poorly cemented casings at the Fort Kent site may provide extraordinary gas conduits for gas sourced in these deep horizons. Because the wells are inclined at approximately 45°, the casing can shift several centimetres off-centre, even with the use of casing centralizers (figure 4.5).

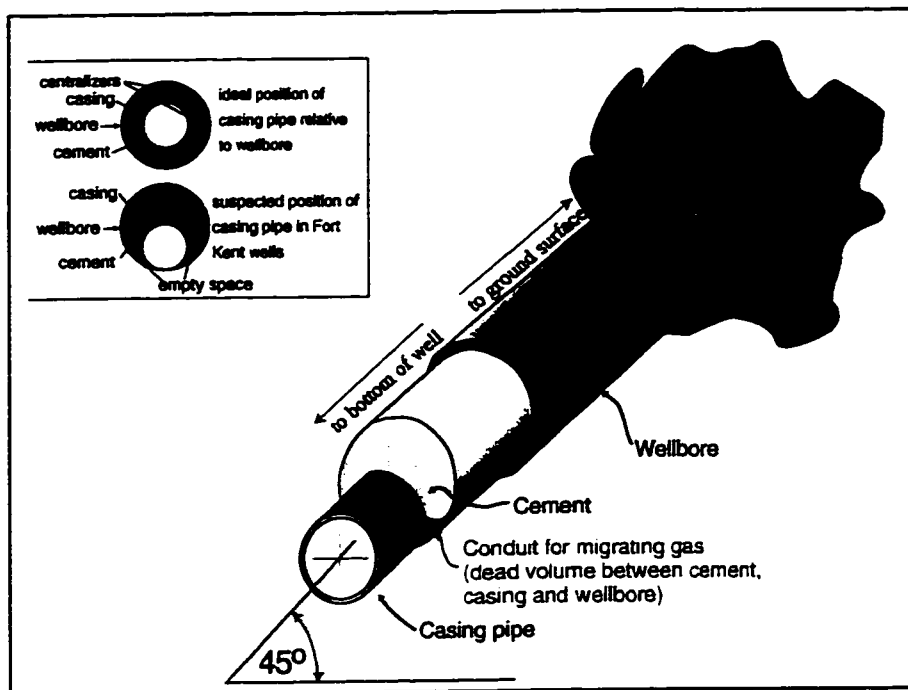


Figure 4.5 Schematic cross section of an inclined well at the Fort Kent site. In some cases, it was observed (pers. comm. Jim Quehl, Abandonrite Environmental Services) that the casing had shifted significantly, creating a large void between the wellbore and the cement. This void can act as a major conduit for migrating gases.

For natural gases generated thermally, the isotopic separation between propane and ethane (i.e. $\delta^{13}\text{C}_{\text{C}_3} - \delta^{13}\text{C}_{\text{C}_2}$) can be interpreted as a maturity indicator. The data in figure 4.3 have been sorted according to increasing thermal maturity ($\delta^{13}\text{C}_{\text{C}_3} - \delta^{13}\text{C}_{\text{C}_2}$ separation). Smaller separations (data located towards the top of figure 4.3) correspond to more mature gases, while larger separations reflect lower maturity gases (also see figures 3.8, 3.9). In figure 4.6, the relative thermal maturity (compared to the median maturity, or $\delta^{13}\text{C}_{\text{C}_3} - \delta^{13}\text{C}_{\text{C}_2}$ separation, well I1G) of the gases from each of the wells studied has been indicated by colouring the wells red (more mature than the median) or blue (less mature than the median). The wells from the Fort Kent suite were also sorted

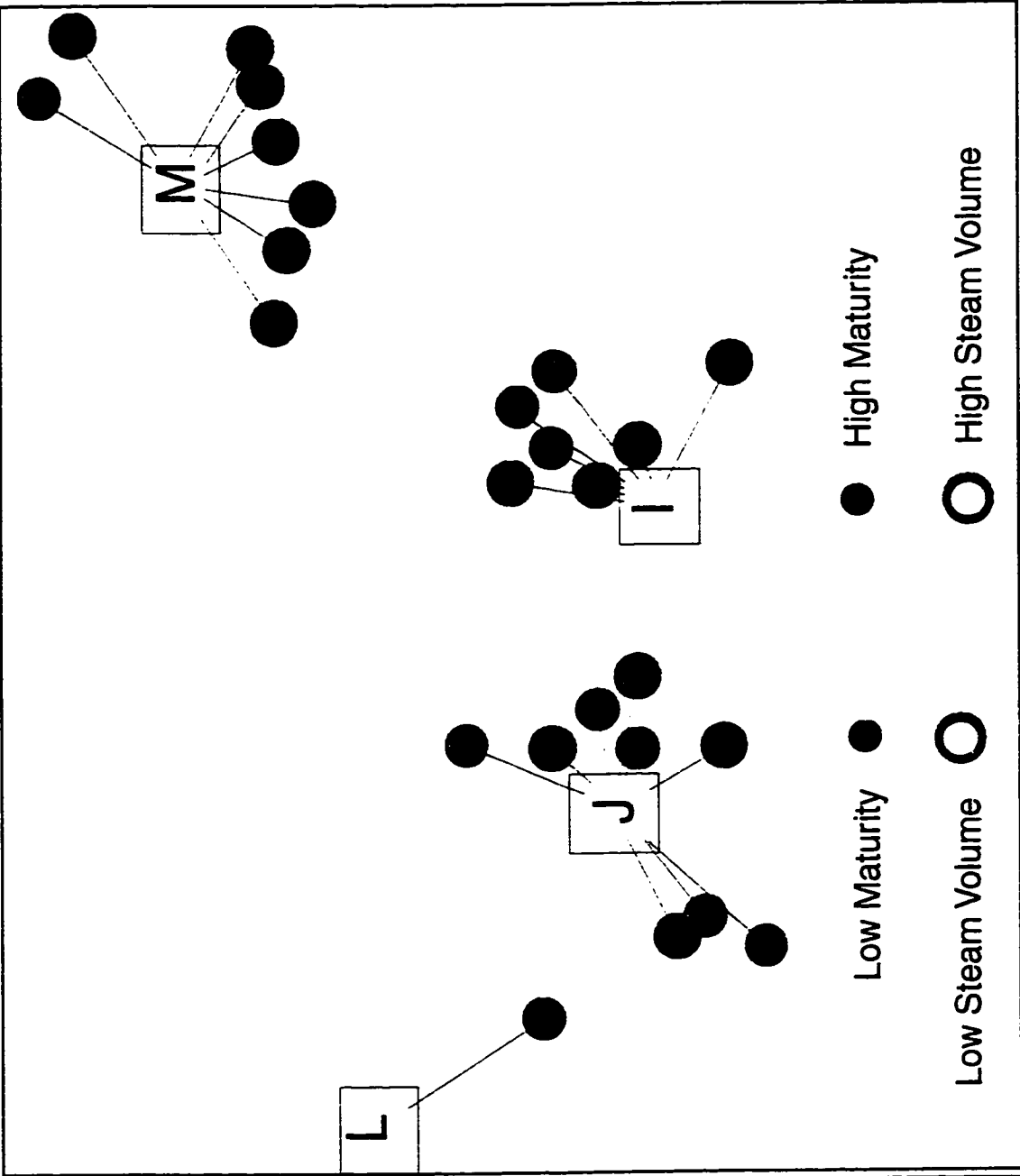


Figure 4.6 Plan view of the Fort Kent Thermal Project. Wells from which migrating gases were analysed have been colour coded to indicate the thermal maturity predicted from the C_3-C_2 isotopic separation (inner circle) and steam injection volume (outer ring). (Thermal maturity and steam injection volume are shown relative to the median values from the data in figure 4.3, i.e. red/orange circles/rings indicate higher maturity/steam volume, blue circles/rings indicate lower maturity/steam volume.)

according to steam injection volumes. Analogous to the procedure above, the wells with high and low steam injection volumes (relative to the well with the median injection volume) have been marked in figure 4.5 by orange and blue rings (respectively). Remarkably, in 19 cases, wells with predicted relative higher thermal maturities (from the isotopic separations) also had relatively higher steam injection volumes (red wells with orange rings), while wells with predicted lower maturities had experienced relatively lower steam injection volumes (blue wells with cyan rings). Five wells showed contradictory results (blue wells with orange rings, or red wells with blue rings).

4.4 IMPLICATIONS

Recognizing the possibility of multiple gas sources or generation mechanisms in the Fort Kent field has implications to the interpretations of the data presented in Chapters 2 and 3. Figure 4.4 shows the $\delta^{13}\text{C}_{\text{C}_3}$ versus $\delta^{13}\text{C}_{\text{C}_2}$ relationship between the shallow Colorado Group gases collected from several locations in the heavy oil region. The calculated fractionation line suggests that the Colorado Group gases were generated at temperatures ranging from 30°C to 70°C (also see figure 2.3). There is considerable scatter of the data about this theoretical fractionation line, however. Figure 4.7 demonstrates the degree of scatter that one would expect for gases generated from a

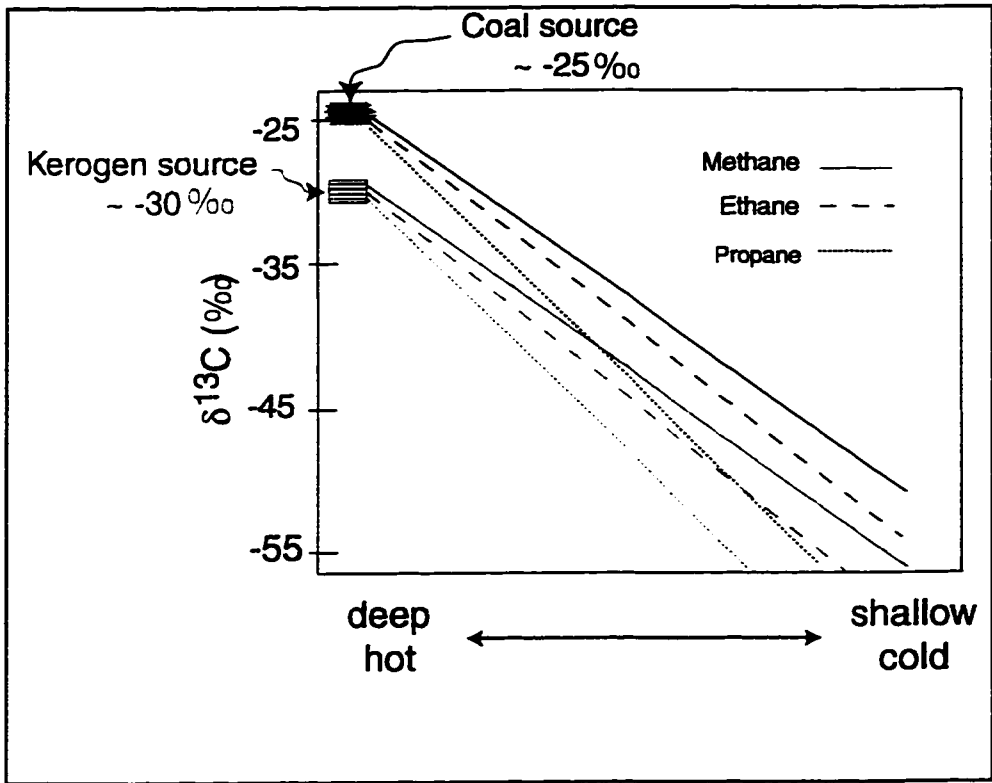


Figure 4.7 Variation in isotope ratios of C₁-C₃ components derived thermally from different source materials.

combination of coal and kerogen sources. Small variations in the isotopic composition of the shallow organic matter that is the source of gas could quite conceivably account for the scatter observed in the gas data in figure 4.4 (and similarly in figure 2.3).

4.5 CONCLUSIONS

The isotopic separations in the migrating gas at the Fort Kent site suggest that these gases are thermally more mature than the migrating gases from adjacent heavy oil fields. There is a positive correlation between high steam injection volumes and thermal maturity (interpreted from C_3/C_2 isotopic separations) in gases from the wells that have been studied to date, and the increased maturities may be a direct result of the steam injection operations at this site.

The fingerprinting techniques described in Chapters 2 and 3 have not been applied at the Fort Kent field, as the migrating gases at this site appear to deviate significantly from those in nearby fields that have not been steamed. Remediation efforts have focussed on achieving competent cement squeezes above the Second White Speckled Shale (SWS) formation, in the hopes that if the gases are sourced in deeper horizons they will not migrate past the cement plugs. Some success in stopping SCV flows has been reported, although soil migration has been observed at a number of wells (in some cases in wells where soil migration was not previously noted). One soil gas (J9F) collected before cementing at the SWS had isotopic ratios similar to Grand Rapids formation gas ($\delta^{13}C_{C1} = -55\text{‰}$, $\delta^{13}C_{C2} = -26\text{‰}$, $\delta^{13}C_{C3} = -24\text{‰}$, $\delta^{13}C_{nC4} = -24\text{‰}$), which suggests that gases from the Mannville formations may be contributing to the migration problem.

The anomalous isotope ratios of the Fort Kent gases highlight the need to combine geochemical data with well histories (e.g. steaming, firefloods, acid injection, etc.), and an accurate geologic characterization of the area (including potential variations in hydrocarbon sources) to determine the sources of migrating gases. Additional emphasis should be placed on designing new cements and/or refining cementing techniques for special applications such as inclined/horizontal, or steamed wells, where traditional techniques may be of limited success.

4.6 REFERENCES

Tam, E., and Yeung, K.C. (1989) Fort Kent Thermal Project Progress Report, Suncor Inc.

CHAPTER 5

CONCLUSIONS

5.1 CONCLUSIONS

The main objectives of this study were to develop and apply a new technique for identifying gas migration sources throughout the heavy oil region of Alberta and Saskatchewan. In achieving these objectives, the following conclusions have been reached:

1. $\delta^{13}\text{C}$ isotopic 'fingerprints' of light hydrocarbons (methane, ethane, propane, and butane) in mud-gases can be used to accurately identify the source depths of migrating gases from the Colorado Group shales. The fingerprinting technique developed in this study has been used to direct remediation efforts on a number of 'leaking' wells.
2. The Colorado Group shales contain very immature, incipient thermogenic gases displaying near equilibrium $^{13}\text{C}/^{12}\text{C}$ ratios in the ethane, propane and butane (C_{2+}) components. The isotopic separations between C_{2+} components can be used to determine the maturities of the Colorado gases, which generally increase with depth. The $\delta^{13}\text{C}$ values of Colorado gases indicate that the isotopic composition of organic source materials also varies throughout the Colorado Group. My calculations indicate that the average isotopic compositions of organic source material are -20‰ (for gases shallower than 200m) and -30‰ (for gases deeper than 200m). Mannville Group gases are associated with the heavy oil, and extensive microbial alteration has led to distinctive ^{13}C enrichment of the C_2 to C_4 components. The Colorado and Mannville

Group gases are of two different origins and genetic histories.

3. The regional isotopic database (initiated in Phase I of the C.A.P.P. Gas Migration Research Program) was extended to a number of fields outside of the Lloydminster area. The collective data from Phases I and II have been compiled in *ISOtrak*, a digital isotopic database created and maintained by Maxxam Analytics Inc. This database will be available for purchase from Maxxam Analytics Inc.

In summary, the isotopic fingerprinting technique is a valuable tool in determining the sources of migrating gases from heavy oil wells in Alberta and Saskatchewan. Isotopic fingerprints have elucidated the contrasting generation mechanisms that are responsible for Mannville and Colorado Group gases in the Western Canadian Sedimentary Basin.

5.2 FUTURE WORK

Considerable research potential still remains in isotopic studies of WCSB shallow gases. Future research should address the following concerns:

1. The number of mud-gas profiles was limited in this study, and should be increased in future studies. Migrating gas source depths must be estimated on a case by case basis; an isotopic fingerprint from the same field as the migrating gas is essential.
2. A number of wells that have used the isotopic fingerprinting technique for aiding in remediation programs will have to be resampled to determine the success or failure of the remediation. This resampling can begin as early as Fall 1998.
3. Carbon isotope compositions of Colorado and Mannville Group gases have provided

a wealth of information, but for completeness, hydrogen isotope analyses should be performed. $\delta^2\text{H}$ analyses of formation waters or mud-gases are two possible research avenues, although the latter requires a significant analytical upgrade to a continuous-flow mass spectrometer configured for hydrogen analyses.

4. Very little geologic characterization exists for the shallow horizons of the heavy oil regions of Alberta and Saskatchewan. In light of the realization that the shallow gases may be sourced from organic materials of varying isotopic composition and/or thermal maturity, a directed study of the physical properties of these shallow horizons should be conducted. Other indicators of source maturity should be used (i.e. vitrinite reflectance or coal rank) to determine quantitative relationships between the isotopic variations in the shallow natural gases and the source material properties.

APPENDIX A IAEA CALIBRATION

The IAEA NGS-3 standard gas was purchased from the National Institute of Standards and Technology. NGS-3 was chosen as a standard because its composition (table A.1) most resembles typical gases analyzed in this study. The accepted range for $\delta^{13}\text{C}_{\text{Cl}}$ of NGS-3 is -69.6‰ to -73.1‰, with respect to the VPDB standard (Hut, 1987).

NGS-3			
$\delta^{13}\text{C}_{\text{Cl}}$ (‰)		Approximate vol%	
-71.86		CH_4	98.825
-72.09		C_2H_6	0.042
-72.23		C_3H_8	0.004
-71.45		iC_4H_{10}	0.00
-71.43		nC_4H_{10}	0.01
-71.39		nC_5H_{12}	0.00
-71.63		nC_6H_{14}	0.00
-71.49		O_2	0.002
-71.26		N_2	1.118
		CO_2	0.009

Table A1 Bulk composition (as reported by IAEA) and $\delta^{13}\text{C}_{\text{Cl}}$ values (measured) of NGS-3 gas standard.

Tedlar[®] bags versus steel cylinders

	$\delta^{13}\text{C}_{\text{C1}}$	$\delta^{13}\text{C}_{\text{C2}}$	$\delta^{13}\text{C}_{\text{C3}}$	$\delta^{13}\text{C}_{\text{C4}}$	$\delta^{13}\text{C}_{\text{nC4}}$
Tedlar[®] bag	-48	-31.2	-27.7	-26.5	-26.1
	-47.8	-31.4	-27.4	-27.6	-26.6
	-47.8	-31.1	-27.6	-27.6	-26.5
Steel cylinder	-49	-31.7	-27.7	-27.7	-26.4
	-48.7	-31.4	-27.5	-28.6	-26.8
	-47.8	-31.7	-27.6	-27.7	-27.5

Table A2 Isotope ratios of identical natural gas, delivered to the laboratory in two different containers

The data above are from a single well that was sampled in duplicate, in steel cylinders. The first set of cylinders was received by Maxxam Labs, who transferred the gases into Tedlar[®] bags. Transferring the high pressure samples (above atmospheric) into the bags has resulted in a 0.5 ‰ ¹³C enrichment in the samples analysed in Tedlar[®] bags. The second set of cylinders was accidentally sent directly to the university laboratory. Fortunately, migrating gases are generally collected at atmospheric pressure, so this enrichment rarely needs to be considered (the sample in table A2 is from a deep conventional oil well located near the foothills).

REFERENCES

Hut, G. (1987) Report to the Director General of the International Atomic Energy Agency: Consultants' group meeting on stable isotope reference samples for geochemical and hydrological investigations

Appendix B Mud-gases

Table B.1-B.20 Isotope ratios of 'mud-gases'

Isotope ratios of 'mud-gases' that were collected during drilling of new wells. Drilling muds were captured in plastic bottles, and the gases retained within these muds were analysed for $^{13}\text{C}/^{12}\text{C}$ composition. These data are used to create isotopic depth profiles, as shown in Chapters 2 and 3. The tops of Colorado Group formations have been indicated (if known) to the right of the corresponding table.

B.1 Husky Mervin 1												
LSD	SEC	T	R	M	Depth from	$\delta^{13}\text{C-C1}$	$\delta^{13}\text{C-C2}$	$\delta^{13}\text{C-C3}$	$\delta^{13}\text{C-iC4}$	$\delta^{13}\text{C-nC4}$	$\delta^{13}\text{C-CO2}$	
A14	36	49	20	3	100m	-77.5	-63.4					-8.7
A14	36	49	20	3	150m	-73.7	-52.9	-40.6	-30.4			-8.9
A14	36	49	20	3	200m	-69.9	-49.2	-41.9	-33.3	-34.7		-7.6
A14	36	49	20	3	250m	-69.1	-47.1	-38.8	-33.1			-10.4
A14	36	49	20	3	300m	-59.5	-42.0	-39.0	-31.7	-37.3		-14.6
A14	36	49	20	3	350m	-68.7	-46.1	-40.1	-32.2	-35.5		-12.6
A14	36	49	20	3	400m	-68.0	-43.2	-33.4	-32.0	-33.2		-10.9
A14	36	49	20	3	450m	-66.6	-30.5	-18.8	-21.7	-18.8		-10.7
A14	36	49	20	3	500m	-64.1	-32.4	-23.4	-22.7	-19.5		-11.4
A14	36	49	20	3	545m	-65.3	-35.7	-23.8	-23.0	-20.2		-7.6

B.2 Husky Frog Lake 1													
LSD	SEC	T	R	M	Depth from	$\delta^{13}\text{C-C1}$	$\delta^{13}\text{C-C2}$	$\delta^{13}\text{C-C3}$	$\delta^{13}\text{C-iC4}$	$\delta^{13}\text{C-nC4}$	$\delta^{13}\text{C-CO2}$	Picks	Depth (m)
12B	7	57	3	4	100m						-14.7	SWS	265.0
12B	7	57	3	4	150m	-72.0	-51.1				-10.1	BFS	307.0
12B	7	57	3	4	200m	-63.9	-51.2	-43.5			-10.7	Viking	362.0
12B	7	57	3	4	255m	-65.7	-51.9	-43.3	-35.2	-37.2	-9.4		
12B	7	57	3	4	300m	-63.4	-50.1	-43.4	-33.8	-39.6	-7.7		
12B	7	57	3	4	350m	-60.8	-46.9	-37.7	-28.7	-24.5	-10.2		
12B	7	57	3	4	400m	-54.5	-26.9	-22.8					
12B	7	57	3	4	450m	-55.0	-29.0	-27.2	-26.2	-24.0	-8.0		
12B	7	57	3	4	500m	-52.8	-27.9	-28.3		-28.5	-12.2		
12B	7	57	3	4	545m	-56.5	-31.0	-24.4	-22.2	-24.1	-3.1		

B.3 Husky Frog Lake 2														
LSD	SEC	T	R	M	Depth from	$\delta^{13}\text{C-C1}$	$\delta^{13}\text{C-C2}$	$\delta^{13}\text{C-C3}$	$\delta^{13}\text{C-iC4}$	$\delta^{13}\text{C-nC4}$	$\delta^{13}\text{C-CO2}$	Picks	Depth (m)	
11B	7	57	3	4	100m						-3.3	SWS	259.0	
11B	7	57	3	4	150m	-71.1	-52.0					3.9	BFS	304.0
11B	7	57	3	4	200m	-69.7	-52.6	-42.6	-32.7	-38.8		-0.2	Viking	357.0
11B	7	57	3	4	250m	-63.1	-49.5	-43.1	-34.3	-40.3				
11B	7	57	3	4	300m	-63.3	-50.1	-42.7	-33.7	-39.0				
11B	7	57	3	4	350m	-59.5	-46.2	-37.0	-28.4	-36.1				
11B	7	57	3	4	400m	-56.7		-32.4		-33.3				
11B	7	57	3	4	450m	-53.3	-27.0	-24.0						
11B	7	57	3	4	500m	-54.0	-31.5	-28.8		-29.0				

B.4 Husky Frog Lake 3													
LSD	SEC	T	R	M	Depth from	$\delta^{13}\text{C-C1}$	$\delta^{13}\text{C-C2}$	$\delta^{13}\text{C-C3}$	$\delta^{13}\text{C-iC4}$	$\delta^{13}\text{C-nC4}$	$\delta^{13}\text{C-CO2}$		
14C	7	57	3	4	150m	-73.3	-51.6	-28.8			-0.1		
14C	7	57	3	4	200m	-69.2	-54.0	-42.6	-32.8	-37.4			
14C	7	57	3	4	250m	-58.8	-52.2	-43.7	-35.4	-38.8			
14C	7	57	3	4	300m	-63.6	-50.6	-44.4	-34.9	-43.0			
14C	7	57	3	4	350m	-59.8	-39.1	-40.5	-32.7	-38.4			
14C	7	57	3	4	400m	-56.8	-35.0	-32.8					
14C	7	57	3	4	450m	-55.6	-27.4	-23.1	-22.1	-26.7			
14C	7	57	3	4	500m	-53.0	-29.1	-25.7	-22.1	-29.0			
14C	7	57	3	4	550m	-54.0	-29.3	-24.6	-22.7	-25.9			

B.5 Husky Greenstreet													
LSD	SEC	T	R	M	Depth from	$\delta^{13}\text{C-C1}$	$\delta^{13}\text{C-C2}$	$\delta^{13}\text{C-C3}$	$\delta^{13}\text{C-iC4}$	$\delta^{13}\text{C-nC4}$	$\delta^{13}\text{C-CO2}$		
5A	31	51	26	3	250m	-34.9					-12.4		
5A	31	51	26	3	300m	-53.0	-47.4	-39.3	-33.3	-35.5			
5A	31	51	26	3	350m	-55.1	-39.6	-37.8	-33.8	-35.7			
5A	31	51	26	3	400m	-58.0	-44.6	-38.4	-33.0	-35.7			
5A	31	51	26	3	450m	-58.1	-34.2	-34.1	-32.7	-36.0			
5A	31	51	26	3	500m	-55.5	-30.5	-31.3	-29.8				
5A	31	51	26	3	550m	-56.3	-31.6	-31.7	-32.6	-34.2			

B.6 Husky C7-6													
LSD	SEC	T	R	M	Depth from	$\delta^{13}\text{C-C1}$	$\delta^{13}\text{C-C2}$	$\delta^{13}\text{C-C3}$	$\delta^{13}\text{C-iC4}$	$\delta^{13}\text{C-nC4}$	$\delta^{13}\text{C-CO2}$		
c7	6	48	21		200m	-54.1	-43.8		-27.5		-12.2		
c7	6	48	21		300m	-63.9	-44.2	-38.6	-34.5	-38.2			
c7	6	48	21		400m	-59.6	-39.9	-35.2	-28.0	-28.1			
c7	6	48	21		500m	-58.9	-30.7	-21.0	-22.1	-14.8			
c7	6	48	21		545m	-61.5	-31.7	-25.0	-23.3	-26.4			

B.7 Husky A3-14											
LSD	SEC	T	R	M	Depth from	$\delta^{13}\text{C-C1}$	$\delta^{13}\text{C-C2}$	$\delta^{13}\text{C-C3}$	$\delta^{13}\text{C-iC4}$	$\delta^{13}\text{C-nC4}$	$\delta^{13}\text{C-CO2}$
a3	14	45	26	3	100m						-19.8
a3	14	45	26	3	150m	-67.1	-38.1				-20.2
a3	14	45	26	3	200m	-66.4	-39.0				-18.8
a3	14	45	26	3	250m	-65.5	-40.2				-18.3
a3	14	45	26	3	300m	-65.6	-42.7		-29.2	-25.8	-19.9
a3	14	45	26	3	350m	-63.4	-41.5				-19.5
a3	14	45	26	3	400m	-63.9	-41.0	-38.3		-36.4	-18.2
a3	14	45	26	3	450m	-63.5	-39.9	-37.9	-31.2	-37.3	-19.7
a3	14	45	26	3	500m	-64.8	-34.8	-31.2	-28.7	-35.2	-18.0
a3	14	45	26	3	550m	-65.1	-34.8	-32.1	-35.2	-35.4	-17.2
a3	14	45	26	3	600m	-65.0	-34.7	-32.1	-29.4	-35.9	-18.0
a3	14	45	26	3	650m	-64.9	-34.2	-31.6	-31.5	-35.5	-18.0
a3	14	45	26	3	700m	-65.1	-32.7	-28.0	-31.0	-26.7	-18.1
a3	14	45	26	3	TD	-65.3	-32.1	-28.0			-18.7

B.8 Husky A9-3											
LSD	SEC	T	R	M	Depth from	$\delta^{13}\text{C-C1}$	$\delta^{13}\text{C-C2}$	$\delta^{13}\text{C-C3}$	$\delta^{13}\text{C-iC4}$	$\delta^{13}\text{C-nC4}$	$\delta^{13}\text{C-CO2}$
A9	3	50	27	3	50m	-54.8					-16.1
A9	3	50	27	3	100m	-59.0	-42.6	-28.2			-16.2
A9	3	50	27	3	150m						-17.0
A9	3	50	27	3	200m	-56.0	-43.8	-38.1	-28.5		-15.4
A9	3	50	27	3	250m	-56.3	-42.0	-38.2	-31.4		-16.3
A9	3	50	27	3	300m	-54.7	-41.9	-36.4	-22.8		-13.7
A9	3	50	27	3	350m	-52.0	-40.6	-38.3	-30.9	-33.3	-15.2
A9	3	50	27	3	400m	-44.4	-37.1	-35.2	-33.6	-26.0	-17.1
A9	3	50	27	3	450m	-54.5	-39.9	-35.8	-31.8		-17.7
A9	3	50	27	3	500m	-56.9	-31.7	-32.9	-28.2		-11.5
A9	3	50	27	3	550m	-53.6	-27.9	-22.3	-25.2	-24.9	-12.2
A9	3	50	27	3	600m	-53.7	-26.1	-17.4	-24.0	-21.0	-13.9
A9	3	50	27	3	650m	-50.9	-27.6	-31.8	-28.2	-24.5	-12.7
A9	3	50	27	3	700m	-55.9	-28.1	-20.8	-24.8	-27.2	-13.5

B.9 Husky Lashburn 1													
LSD	SEC	T	R	M	Depth from	$\delta^{13}\text{C-C1}$	$\delta^{13}\text{C-C2}$	$\delta^{13}\text{C-C3}$	$\delta^{13}\text{C-iC4}$	$\delta^{13}\text{C-nC4}$	$\delta^{13}\text{C-CO2}$	Picks	Depth (m)
A13	5	48	25	3	100m	-64.4	-44.8	-38.8	-31.0	-33.8	-8.5	SWS	327.0
A13	5	48	25	3	150m	-64.2	-46.3	-40.5	-38.6	-38.7	-10.1	BFS	362.5
A13	5	48	25	3	200m	-65.2	-49.6	-41.2	-33.6	-36.0	-13.3	Viking	426.0
A13	5	48	25	3	250m	-64.0	-44.6	-39.8	-34.3	-37.2	-12.0		
A13	5	48	25	3	300m	-61.3	-44.0	-39.4	-33.8	-39.3	-21.2		
A13	5	48	25	3	350m	-62.5	-43.0	-38.6	-34.3	-36.8	-20.6		
A13	5	48	25	3	400m	-62.4	-41.0	-35.7	-32.1	-36.3	-18.4		
A13	5	48	25	3	450m	-62.9	-32.2	-29.3	-28.4	-32.2	-19.8		
A13	5	48	25	3	500m	-62.9	-31.9	-30.9	-24.5	-43.6	-9.7		
A13	5	48	25	3	550m	-63.5	-30.2	-25.9	-22.4	-30.3	-12.7		
A13	5	48	25	3	600m	-63.7	-29.8	-25.6	-26.0		-17.5		

B.10 Husky Lashburn 2													
LSD	SEC	T	R	M	Depth from	$\delta^{13}\text{C-C1}$	$\delta^{13}\text{C-C2}$	$\delta^{13}\text{C-C3}$	$\delta^{13}\text{C-iC4}$	$\delta^{13}\text{C-nC4}$	$\delta^{13}\text{C-CO2}$	Picks	Depth (m)
A5	5	48	25	3	100m	-74.1					-7.5	SWS	326.0
A5	5	48	25	3	150m	-71.7	-54.7				-8.6	BFS	363.0
A5	5	48	25	3	200m	-66.3	-46.8	-40.5	-33.8	-35.6	-9.9	Viking	420.5
A5	5	48	25	3	250m	-64.1	-47.1	-40.4	-34.6	-36.9	-9.6		
A5	5	48	25	3	300m	-62.2	-44.0	-40.0	-33.9	-37.7	-8.4		
A5	5	48	25	3	350m	-62.7	-44.2	-39.4	-32.2	-36.6	-14.0		
A5	5	48	25	3	400m	-62.5	-42.6	-37.4	-33.1	-36.1	-11.2		
A5	5	48	25	3	450m	-62.5	-39.7	-36.0	-29.8	-34.2	-6.6		
A5	5	48	25	3	500m	-62.8	-37.3	-34.0	-27.7	-15.2	-7.5		
A5	5	48	25	3	550m	-64.1	-30.3	-25.9	-28.7		-13.2		
A5	5	48	25	3	600m	-63.0	-30.4	-26.3	-26.9	-31.5	-16.1		
A5	5	48	25	3	617m	-63.6	-30.6	-25.8	-26.0	-25.0	-13.7		

B.11 Husky Mervin 2													
LSD	SEC	T	R	M	Depth from	$\delta^{13}\text{C-C1}$	$\delta^{13}\text{C-C2}$	$\delta^{13}\text{C-C3}$	$\delta^{13}\text{C-iC4}$	$\delta^{13}\text{C-nC4}$	$\delta^{13}\text{C-CO2}$		
A10	35	49	21	3	100m	-77.5					-7.0		
A10	35	49	21	3	150m	-71.4	-50.6	-40.5	-32.6	-34.8	-4.6		
A10	35	49	21	3	200m	-70.7	-50.2	-39.9	-32.6	-35.6	-7.3		
A10	35	49	21	3	250m	-69.5	-47.1	-40.4	-32.8	-36.7	-20.0		
A10	35	49	21	3	300m	-70.5	-45.9	-39.8	-32.6	-37.0	-17.3		
A10	35	49	21	3	350m	-69.6	-45.7	-39.4	-32.1	-36.7	-20.5		
A10	35	49	21	3	400m	-67.9	-33.9	-26.8	-26.7	-29.9	-13.4		
A10	35	49	21	3	450m	-68.0	-25.4	-20.8	-24.4	-24.7	-13.3		
A10	35	49	21	3	500m	-68.1	-26.0	-20.0	-24.8	-22.4	-13.7		
A10	35	49	21	3	550m	-64.8	-28.2	-19.5	-19.3	-23.5	-15.3		
A10	35	49	21	3	568m	-66.1	-29.2	-24.1	-25.8	-22.2	-15.9		

B.12 Husky Rivercourse											
LSD	SEC	T	R	M	Depth from	$\delta^{13}\text{C-C1}$	$\delta^{13}\text{C-C2}$	$\delta^{13}\text{C-C3}$	$\delta^{13}\text{C-iC4}$	$\delta^{13}\text{C-nC4}$	$\delta^{13}\text{C-CO2}$
9C	27	47	1	4	100m	-71.8					-12.8
9C	27	47	1	4	150m	-67.9	-47.4				-11.7
9C	27	47	1	4	200m	-64.1	-46.1	-36.2		-30.3	-12.8
9C	27	47	1	4	250m	-62.8	-44.5	-37.6	-33.0	-33.8	-20.7
9C	27	47	1	4	300m	-62.5	-43.8	-39.3	-33.3	-37.1	-8.0
9C	27	47	1	4	350m	-61.7	-42.7	-39.2	-29.5	-29.8	-8.5
9C	27	47	1	4	400m	-59.8	-40.8	-38.5	-31.6	-31.4	-23.3
9C	27	47	1	4	450m	-58.4	-37.8	-33.6	-28.1	-26.3	-24.9
9C	27	47	1	4	500m	-60.3	-32.8	-27.9	-27.0	-27.6	-11.6
9C	27	47	1	4	550m	-61.4	-32.6	-29.1	-26.1	-34.7	-8.1
9C	27	47	1	4	600m	-61.0	-30.7	-28.4	-28.2	-22.8	-11.2
9C	27	47	1	4	650m	-61.6	-29.9	-23.0	-26.8	-28.3	-13.9
9C	27	47	1	4	680m	-59.8	-30.6	-27.0	-28.4	-29.2	-12.6

B.13 Husky Tangleflags													
LSD	SEC	T	R	M	Depth from	$\delta^{13}\text{C-C1}$	$\delta^{13}\text{C-C2}$	$\delta^{13}\text{C-C3}$	$\delta^{13}\text{C-iC4}$	$\delta^{13}\text{C-nC4}$	$\delta^{13}\text{C-CO2}$	Picks	Depth (m)
A9	19	50	25	3	100m	-64.6					-11.0	SWS	338.5
A9	19	50	25	3	150m	-62.9	-46.0	-39.0	-34.0	-37.1	-10.9	BFS	385.5
A9	19	50	25	3	200m	-65.7	-46.5	-40.6	-33.9	-42.7	-10.5		
A9	19	50	25	3	250m	-65.1	-46.8	-40.1	-33.8	-37.5	-8.1		
A9	19	50	25	3	300m	-64.2	-46.2	-40.4	-34.2	-36.9	-8.1		
A9	19	50	25	3	350m	-62.8	-44.4	-39.5	-32.4	-37.2	-8.6		
A9	19	50	25	3	400m	-63.2	-42.7	-38.2	-33.2	-35.3	-14.2		
A9	19	50	25	3	450m	-61.3	-39.0	-37.6	-31.5	-35.1	-8.3		
A9	19	50	25	3	500m	-58.8	-28.9	-28.0	-26.6	-25.4	-15.7		
A9	19	50	25	3	550m	-57.7	-28.5	-25.7	-27.9	-28.3	-8.3		
A9	19	50	25	3	600m	-59.6	-29.5	-25.3	-30.0	-34.0	-12.1		

B.14 Husky Baxter Lake													
LSD	SEC	T	R	M	Depth from	$\delta^{13}\text{C-C1}$	$\delta^{13}\text{C-C2}$	$\delta^{13}\text{C-C3}$	$\delta^{13}\text{C-iC4}$	$\delta^{13}\text{C-nC4}$	$\delta^{13}\text{C-CO2}$	Picks	Depth (m)
D2	1	47	6	4	150 m						-14.4	SWS	494.0
D2	1	47	6	4	200 m	-69.3	-54.9	-30.3			-13.2	BFS	543.0
D2	1	47	6	4	250 m	-65.5	-50.0	-39.9	-32.4	-36.4	-16.7	Viking	599.0
D2	1	47	6	4	300 m	-64.6	-51.1	-39.7	-32.8	-36.0	-7.9		
D2	1	47	6	4	350 m	-62.1	-51.3	-35.7	-32.7	-34.3	-16.3		
D2	1	47	6	4	400 m	-31.6	-37.5	-39.5	-34.0	-37.1	-20.6		
D2	1	47	6	4	450 m	-3.1		-39.4	-33.6	-37.3	-20.1		
D2	1	47	6	4	500 m	-53.1	-39.1	-38.6	-32.9	-36.6	-17.5		
D2	1	47	6	4	550 m	-46.0	-34.5	-35.8	-32.8	-36.2	-17.5		
D2	1	47	6	4	600 m	-59.5	-31.7	-27.5	-27.3	-26.3	-12.0		
D2	1	47	6	4	650 m	-60.6	-35.1	-29.8	-28.0	-27.9	-13.9		
D2	1	47	6	4	700 m	-59.3	-29.9	-23.1	-26.6		-13.1		

B.15 Koch Cold Lake												
LSD	SEC	T	R	M	Depth from	$\delta^{13}\text{C-C1}$	$\delta^{13}\text{C-C2}$	$\delta^{13}\text{C-C3}$	$\delta^{13}\text{C-iC4}$	$\delta^{13}\text{C-nC4}$	$\delta^{13}\text{C-CO2}$	
5.0	11	65	6	4	100m						-4.3	
5.0	11	65	6	4	150m						-8.0	
5.0	11	65	6	4	200m	-79.3	-45.9				-4.3	
5.0	11	65	6	4	250m	-69.3	-44.1	-38.3	-29.8		-12.2	
5.0	11	65	6	4	300m	-63.0	-39.4	-35.2	-29.9	-33.9	-18.4	
5.0	11	65	6	4	350m	-57.3	-31.5	-29.6			-10.0	
5.0	11	65	6	4	400m	-53.5	-24.9	-21.0	-22.4	-22.3	-5.2	
5.0	11	65	6	4	445m	-53.8	-26.4		-25.2	-21.3	-4.8	

B.16 PCP Brooks												
LSD	SEC	T	R	M	Depth from	$\delta^{13}\text{C-C1}$	$\delta^{13}\text{C-C2}$	$\delta^{13}\text{C-C3}$	$\delta^{13}\text{C-iC4}$	$\delta^{13}\text{C-nC4}$	$\delta^{13}\text{C-CO2}$	
6.0	22	19	17	4	150m	-62.0						
6.0	22	19	17	4	200m	-63.3					-3.2	
6.0	22	19	17	4	465m	-61.8	-48.5	-34.8			-17.5	
6.0	22	19	17	4	558m	-59.7	-49.0	-36.6			-17.9	
6.0	22	19	17	4	841m	-60.0	-43.9	-37.3				
6.0	22	19	17	4	876m	-59.7					-15.1	

B.17 Murphy Elk Point												
LSD	SEC	T	R	M	Depth from	$\delta^{13}\text{C-C1}$	$\delta^{13}\text{C-C2}$	$\delta^{13}\text{C-C3}$	$\delta^{13}\text{C-iC4}$	$\delta^{13}\text{C-nC4}$	$\delta^{13}\text{C-CO2}$	
6.0	32	57	5	4	200m	-61.0	-47.8	-37.6	-28.9	-30.9	-10.7	
6.0	32	57	5	4	250m	-61.0	-48.3	-42.1	-34.2	-37.4	-13.1	
6.0	32	57	5	4	300m	-38.8	-39.4	-38.4	-28.9	-32.4	-16.8	
6.0	32	57	5	4	350m	-55.6	-43.7	-40.3	-33.5	-36.9	-7.2	
6.0	32	57	5	4	400m	-51.0	-32.3	-30.0	-27.7	-30.3	-21.6	
6.0	32	57	5	4	450m	-50.9	-32.2	-28.4	-28.8		-18.8	
6.0	32	57	5	4	500m	-50.3	-28.8	-30.8	-24.0	-27.0	-16.8	
6.0	32	57	5	4	554m	-51.4	-37.4	-30.6	-25.9	-28.2	-16.9	

B.18 Koch Lindbergh												
LSD	SEC	T	R	M	Depth from	$\delta^{13}\text{C-C1}$	$\delta^{13}\text{C-C2}$	$\delta^{13}\text{C-C3}$	$\delta^{13}\text{C-iC4}$	$\delta^{13}\text{C-nC4}$	$\delta^{13}\text{C-CO2}$	
3.0	31	56	5	4	150m	-66.0					-14.0	
3.0	31	56	5	4	200m	-57.0	-47.0	-43.0	-33.0	-37.5	-13.8	
3.0	31	56	5	4	250m	-59.0	-45.0	-39.0	-31.0	-35.0	-13.6	
3.0	31	56	5	4	300m	-56.0	-46.0	-39.5	-32.0	-38.2	-14.0	
3.0	31	56	5	4	350m	-55.0	-42.0	-39.0	-34.0	-38.0	-12.0	
3.0	31	56	5	4	400m							
3.0	31	56	5	4	450m	-51.0	-23.0	-20.0	-22.0	-28.0	-12.0	

B.19 Wascana Edam											
LSD	SEC	T	R	M	Depth from	$\delta^{13}\text{C-C1}$	$\delta^{13}\text{C-C2}$	$\delta^{13}\text{C-C3}$	$\delta^{13}\text{C-iC4}$	$\delta^{13}\text{C-nC4}$	$\delta^{13}\text{C-CO2}$
A5	20	48	20	3	200m	-56.3					-11.5
A5	20	48	20	3	250m	-63.7	-45.9				-7.5
A5	20	48	20	3	300m	-50.5					-7.3
A5	20	48	20	3	350m	-43.5					-7.7
A5	20	48	20	3	400m	-65.2	-37.5				-8.7
A5	20	48	20	3	450m	-67.0	-38.5				-23.2
A5	20	48	20	3	500m	-49.4	-24.8	-16.9			-26.2

B.20 Norcen Hairy Hills											
LSD	SEC	T	R	M	Depth from	$\delta^{13}\text{C-C1}$	$\delta^{13}\text{C-C2}$	$\delta^{13}\text{C-C3}$	$\delta^{13}\text{C-iC4}$	$\delta^{13}\text{C-nC4}$	$\delta^{13}\text{C-CO2}$
2.0	2	56	15	4	200m						-0.8
2.0	2	56	15	4	250m	-52.8	-42.8	-37.2	-28.1	-30.4	-1.6
2.0	2	56	15	4	300m		-21.5	-34.1	-31.7	-35.4	
2.0	2	56	15	4	350m	-39.6	-35.5	-36.7	-31.1	-34.4	4.4
2.0	2	56	15	4	400m	-55.1	-38.4	-38.6	-31.0	-33.3	4.9
2.0	2	56	15	4	450m	-51.4	-30.9	-32.1	-29.8	-32.0	0.1
2.0	2	56	15	4	500m						
2.0	2	56	15	4	550m	-45.6	-23.9	-24.8			-5.3
2.0	2	56	15	4	600m						
2.0	2	56	15	4	650m	-56.2	-24.4	-23.1	-21.5	-25.8	-9.1

Appendix C

Mannville Production Gases

Table C1. Isotopic ratios of Mannville production gases
 These gases were collected from wells that did not display gas migration problems,
 and are intended to expand the areal coverage of the isotopic database.

Q	LSD	SE	T	R	Company	Formation	Sample ID	Collection	Sample Co	$\delta^{13}\text{C}$ -C1	$\delta^{13}\text{C}$ -C2	$\delta^{13}\text{C}$ -C3	$\delta^{13}\text{C}$ -C4	$\delta^{13}\text{C}$ -C4	$\delta^{13}\text{C}$ -C4	$\delta^{13}\text{C}$ -CO	$\delta^{13}\text{C}$ -CO2			
B	1	20	38	1	4	Murphy	McLaren	96-16344-3	formation g	-56.9	0.9671	-28.7	0.0063	-25.6	0.0005	-26.2	-28.1	5.9	0.0017	
B	15	13	39	1	4	Murphy	Lloyd	96-16344-4	formation g	-61.4	0.9684	-30.6	0.0128	-18.3	0.0011	-23.4	0.0019	-23.8	0.0004	
A	5	28	49	1	4	Murphy	GP	96-15394-03	formation g	-62.0	0.9406	-27.6	0.0079	-17.9	0.0002	-23.4	0.0003	-21.5	0.0001	
A	14	5	50	1	4	Murphy	Spaiky	97-16785-02	formation g	-58.5	0.9638	-25.9	0.0083	-13.4	0.0002	-24.8	0.0006	-22.8	0.0003	
A	100/1	29	67	2	4	Amoco/PCP	Colony	97-17235-5	wellhead	-52.7								0.7	5.8	
	12	4	67	3	4	Amoco/PCP	Colony	97-17235-6	wellhead	-52.9								11.8		
100/1	9	68	3	4	Amoco/PCP	Clearwater	97-17235-4	97/09/19	wellhead	-56.2								2.2		
102/1	9	68	3	4	Amoco/PCP	McLaren	97-17235-9	97/09/19	wellhead	-58.2								4.6		
100/1	9	68	3	4	Amoco/PCP	Colony	97-17235-7	97/09/19	wellhead ca	-53.5								16.0		
	4	28	15	11	4	PCP	SWS		production	-65.1								-28.9		
	7	16	21	15	4	PCP	Milk River		production	-67.9								-30.8		
C1	16	20	61	4	4	Koch			production	-55.2								-30.8		
D3	20	61	4	4	Koch				production	-55.2								-30.8		
D3	20	61	4	4	Koch				production	-55.2								-30.8		
11	10	20	61	4	4	Koch	Colony	16557-2	formation g	-69.9	0.9791	-33.1	0.0016	-25.3	0.0006	-25.0	-23.9	-26.7	5.6	0.0005
11	10	20	61	4	4	Koch	SWS	16557-4	formation g	-68.3	0.9935	-36.3	0.0037	-27.9	0.0004	-26.3	-26.7	-26.7	8.0	0.0001
K	23	48	5	4	Murphy	Lloyd			formation g	-59.3								-23.2		
	4	28	15	11	4	PCP	SWS	97-15083-0	formation g	-65.1	0.9551	-48.3	0.0031	-37.1	0.0005	-28.9	0.0001	-31.8	0.0001	
	4	30	55	5	4	Elgin	McLaren		formation g	-51.7								-26.3		
	11	5	75	6	4	Amoco	Clearwater	16401-3	wellhead	-67.6								-26.3		
	13	33	55	13	4	Norcen	Spaiky	97-15927-7	formation g	-54.2	0.9578	-24.5	0.0285	-21.9	0.0012	-24.4	0.0005	-23.4	0.0000	
	6	16	34	11	4	Norcen	SWS	97-15884-1	formation g	-55.4	0.9097	-28.6	0.0341	-26.1	0.0215	-26.0	0.0046	-15.0	0.0036	
	10	32	35	11	4	Norcen	Belly River	97-15884-2	formation g	-57.1	0.9947	-33.0	0.0021	-34.1	0.0002	-28.4	-28.2	-8.6	0.0029	
	10	29	52	14	5	Norcen	Bear Quai	97-15927-6	formation g	-60.5	0.9850	-40.7	0.0008	-32.6	0.0019	-25.5	0.0007	-24.6	0.0004	
	16	31	55	14	4	Norcen	Colony	97-15927-9	formation g	-52.5	0.9628	-23.6	0.0024	-23.8	0.0024	-25.8	0.0007	-24.6	0.0004	
	7	16	21	15	4	PCP	Milk River	97-15083-0	formation g	-67.9	0.9657	-30.9	0.0029	-38.0	0.0003	-30.8	0.0001	-29.9	0.0036	
	16	16	21	15	4	PCP	Medicine Hat		formation g	-70.3								-22.9		
	13	33	55	13	4	Norcen	Spaiky	97-15927-7	formation g	-54.0	0.9630	-26.9	0.0146	-26.6	0.0024	-26.4	0.0006	-27.2	0.0004	
	13	33	55	13	4	Norcen	Viking	97-15927-8	formation g	-60.1	0.9757	-36.5	0.0032	-30.7	0.0003	-27.2	0.0001	-28.3	0.0034	
A	5	18	48	22	3	Murphy	Wascana		formation g	-66.7								-18.3		
A	10	2	48	24	3	Murphy	McLaren		formation g	-72.6	0.9707	-32.5	0.0064	-22.1	0.0026	-21.4	0.0002	-24.3	0.0063	
C	11	4	40	26	3	Murphy	Cummings/Dina	96/12/12	formation g	-65.4								-25.4		
A	3	27	39	27	3	Murphy	Spaiky		formation g	-65.8								-23.7		
C	4	4	49	27	3	Murphy	Spaiky	97-16785-01	formation g	-62.1	0.9088	-27.5	0.0110	-17.9	0.0001	-22.6	0.0001	-22.4	0.0000	
D	3	4	49	27	3	Murphy	GP		formation g	-57.8	0.9461	-25.5	0.0155	-15.2	0.0025	-25.3	0.0064	-22.4	0.0023	
C	16	4	49	27	3	Murphy	Spaiky		formation g	-56.5								-23.3		
C	16	19	16	28	3	Murphy	McLaren	16344-2	formation g	-58.2	0.9828	-27.8	0.0021	-22.6				6.3	0.0025	
C	3	35	39	28	3	Murphy	Spaiky		formation g	-58.9	0.9138	-29.0	0.0100	-12.2	0.0014	-25.7	0.0269	-21.0	0.0067	
C	11	4	40	28	3	Murphy	Cummings/Dina	96/12/12	formation g	-63.4								-24.8		
A	7	1	49	28	3	Murphy	Spaiky	97-16785-03	POP valve	-58.1								-27.7		
A	10	24	10	29	3	Amoco	Viking		formation g	-59.7								-27.7		
						Humby	Camrose		formation g	-59.7								-23.2		

Note- X = bulk composition fraction

Appendix D Migrating Gases

Table D1. Isotopic ratios of migrating gases.
Migrating gases were collected from surface casing vents, or as soil gases. Bulk composition data is included, if known

Q	LSID	SEC	T	R	M	Company	Sample ID	Collection	Sample Comment	$\delta^{13}\text{C-C1}$	X C1	$\delta^{13}\text{C-C2}$	X C2	$\delta^{13}\text{C-C3}$	X C3	$\delta^{13}\text{C-C4}$	X C4	$\delta^{13}\text{C-nC4}$	XnC4	$\delta^{13}\text{C-CO2}$	XCO2
	10	35	51	14	4	Amoco	97-16724-1	97/8/1		-33.8	0.9144	-30.0	0.0274	-29.6	0.0097	-29.0	0.0020	-30.5	0.0021	-30.5	0.0007
	9	3	21	19	3	Norcen	97-17354-1	97/09/26	Battery Separator/prod	-68.9	0.9368	-58.5	0.0022	-44.4	0.0002	-31.8	0.0001	-31.8	0.0001	-37.6	0.0399
	10	19	47	4	4	Koch		96/08/09	casing, after blow down	-36.3	0.8128	-27.7	0.0424	-20.5	0.0281	-25.1	0.0420	-22.7	0.0349	-22.7	0.0399
A	16	8	55	6	4	Elm	15808-02		casing, before blow down	-63.1		-48.4		-40.9		-29.4		-34.7		-35.6	
	16	8	55	6	4	Elm	15808-01		casing, before blow down	-37.7		-46.8		-40.2		-29.3		-25.7		-34.7	
	13H3	29	61	4	4	Koch	97-16647-06	97/07/25	flat bag SCV	-37.8		-31.8		-27.0		-24.8		-23.7		-28.8	
	18A13	20	61	4	4	Koch	97-16647-05	97/07/25	flat bag SCV	-46.3		-29.3		-24.8							-11.1
	16	8	55	6	4	Elm	97-16647-04	97/07/25	flat bag SCV	-42.3		-32.4		-25.9							-11.3
	MSA5	28	61	4	4	Koch	97-16647-04	97/02/28	migrating	-39.7		-34.3		-28.5		-20.9				-20.3	
A	8	24	47	5	4	Elm			migrating	-67.0	0.9802	-45.7	0.0024	-38.5	0.0002	-30.3		-33.2		-31.1	0.0034
	7	36	55	14	5	Norcen	97-15927-3	97/05/23	migrating	-61.3	0.9687	-36.1	0.0052	-31.6	0.0006	-29.6	0.0001	-30.0	0.0001	-31.1	0.0034
	6	3	51	16	4	Norcen	97-15927-1	97/05/23	migrating	-40.1		-38.6		-33.4						-14.3	
	6	11	62	3	4	Husky	97-14973-02	97/02/27	migrn outside of casing	-61.0	0.9982	-38.6	0.0016	-22.3		-30.4				-35.7	
	14	9	34	11	4	Norcen	97-15709-02	97/04/26	outside casing	-62.7	0.9844	-43.5	0.0024	-33.8		-27.4				-18.0	0.0341
C	6	11	62	3	4	Husky	97-18007-1	97/11/24	outside casing	-64.3		-38.6		-33.8		-27.4				-30.1	0.0031
	3	17	48	19	3	Anderson	97-17889-2	97/05/09	outside casing bubbles	-63.1	0.9896	-37.4	0.0038	-30.5	0.0004	-28.6		-24.6	0.0136	-22.1	0.0125
A	3	17	48	19	3	Anderson	97-17889-1	97/11/14	Prod Jack Gas	-53.1	0.9184	-28.1	0.0223	-20.8	0.0113	-24.6	0.0136	-23.0	0.0038	-18.0	0.0044
	5	21	47	4	4	Husky		96/08/24	Production Casing	-59.4	0.9149	-28.0	0.0365	-28.9		-23.3		-24.1		-22.8	0.0366
	3	16	47	4	4	Koch		96/08/09	Production Casing	-53.8	0.9878	-27.0	0.0022	-21.2		-26.1		-23.3		-23.3	0.0004
	6	22	61	8	4	Koch	97-17890-1	97/11/14	Production Casing	-53.1		-27.0		-21.2		-26.1		-23.3		-23.3	0.0004
	9	25	47	5	4	Koch	1466	96/08/07	Production Casing	-60.1		-28.9		-21.9		-25.9		-22.8		-21.1	
	11	25	47	5	4	Koch	bag B7	96/08/07	Production Casing	-54.0	0.7353	-25.2	0.0345	-20.2	0.0481	-25.8	0.0849	-21.9	0.0619	-21.9	0.0354
	11	25	47	5	4	Koch	bag B9	96/08/09	Production Casing	-54.4	0.7486	-25.1	0.0321	-19.8	0.0450	-25.6	0.0808	-21.7	0.0600	-21.7	0.0335
	11	25	47	5	4	Koch	bag B14	96/08/09	Production Casing	-55.2	0.9902	-30.1	0.0036	-23.3	0.0029	-23.8	0.0007	-22.8	0.0009	-22.8	0.0013
	65	12	31	60	4	Koch	97-15806-04	97/05/09	Production Casing	-55.6	0.8286	-28.7	0.0339	-21.2	0.0248	-26.6	0.0473	-22.8	0.0366	-22.8	0.0288
C	13	19	47	4	4	Koch	bag 15344-2	96/08/07	Production Casing	-55.9		-36.3		-26.1		-25.0		-23.1		-23.1	0.0288
	11C16	20	61	4	4	Koch			Production Casing	-58.6	0.9686	-38.6	0.0033	-28.8	0.0005	-22.9	0.0001	-25.9	0.0001	-25.9	0.0001
	13E16	20	61	4	4	Koch	16647-17		Production Casing	-37.1		-30.6		-26.2		-24.5		-25.0		-25.0	0.0001
	13G16	20	61	4	4	Koch			Production Casing	-37.1		-30.6		-26.2		-24.5		-25.0		-25.0	0.0001
A	3	17	48	19	3	Anderson	97-17889-1	97/11/14	Production Casing	-65.8		-39.2		-33.6		-29.4		-27.2		-25.4	0.0001
	6	29	72	7	6	PCP	Wemby bag1	96/08/23	Production Casing	-55.9		-40.9		-23.3		-22.8		-20.3		-20.3	0.0001
	6	29	72	7	6	PCP	Wemby bag2	96/08/23	Production Casing	-58.4		-40.9		-23.3		-22.8		-20.3		-20.3	0.0001
	6	7	51	24	3	Husky		96/08/24	Production Casing	-64.2		-38.7		-32.7		-28.0		-28.0		-33.1	0.0001

	NASAS	28	61	4	4	Koch	97-16647-04		SCV		-61.7	0.9721	-36.9	0.0030	-28.6	0.0003	-26.7	-29.5	-15.8	0.0001
	NIGTS	28	61	4	4	Koch	97-16647-21		SCV		-59.8	0.8955	-35.3	0.0023	-28.4	0.0007	-27.4	-28.2	-13.5	0.0001
C		11	29	46	6	4	Huuky	98-21586-04	971/222	SCV	-45.3	0.9777	-35.1	0.0049	-29.9	0.0007	-27.4	-28.2	-17.0	0.0001
B		6	5	48	6	4	Huuky	98-21545-02	971/218	SCV	-69.9	0.9638	-46.0	0.0033	-39.9	0.0003	-32.5	-34.8	-16.7	0.0001
D		10	4	50	6	4	Anderson	16498-1		SCV	-65.1		-48.7		-40.2		-32.1	-34.8		
B		6	5	6	4	Ellen	18808-03		SCV	-64.4		-48.2		-40.9		-32.1	-34.8			
B		6	11	52	7	4	Huuky	98-21545-01	971/218	SCV	-69.5	0.9669	-43.8	0.0037	-39.0	0.0003	-31.9	-36.6	-7.2	0.0008
		6	14	15	12	4	PCP	16458-1		SCV	-62.7	0.9414	-52.0	0.0011	-35.3				-12.5	0.0008
		7	21	15	15	4	PCP			SCV	-61.0		-45.8		-35.3				-12.5	0.0001
100V		7	21	15	15	4	PCP	97-16191-01	9706/12	SCV	-63.3	0.9776	-48.0	0.0026	-38.2	0.0002	-30.4	-32.5		0.0001
1022		12	26	17	14	4	PCP	97-13568-01	975/1	SCV	-66.2	0.9960	-52.2	0.0028	-35.3				-12.0	0.0012
		10	35	51	14	4	Amoco	97-16724-2	9709/05	SCV	-58.5		-38.5		-35.3		-31.2	-34.0	-7.8	
		10	23	55	14	5	Noreen	97-15927-5	9705/23	SCV	-69.9	0.9796	-49.3	0.0019	-40.4	0.0001	-31.8	-33.7	-13.1	0.0034
		9	28	55	14	5	Noreen	97-15927-4	9705/23	SCV	-64.3	0.9769	-46.6	0.0023	-38.6	0.0002	-29.6	-33.7	-13.1	0.0033
		7	36	55	14	5	Noreen	97-15927-2	9705/23	SCV	-67.8	0.9754	-46.0	0.0025	-39.6	0.0002	-28.4	-26.6		
	CAL12	26	17	14	4	PCP			973/1	SCV	-65.4								-14.5	0.0103
	CAL12	26	17	14	4	PCP	97-15835-04		973/13	SCV	-65.3	0.9862	-52.5	0.0034					-45.1	
100V		13	18	18	15	4	PCP	97-16156-8	9706/11	SCV	-61.9		-48.0	0.0022	-36.0	0.0002			-12.2	0.0001
100V		13	18	18	15	4	PCP	97-16193-2		SCV	-61.3	0.9886	-48.0	0.0022	-36.0	0.0002			-12.2	0.0001
100V		11	20	18	15	4	PCP	97-16156-2		SCV	-64.1	0.9779	-46.5	0.0021	-30.7	0.0001			-12.9	0.0001
100V		11	20	18	15	4	PCP	97-16156-3		SCV	-60.3	0.9704	-47.4	0.0021	-30.4	0.0001			-12.9	0.0001
100V		11	9	19	13	4	PCP	97-16156-5		SCV	-71.6	0.9790	-50.9	0.0014	-31.4	0.0001			-12.3	0.0002
100V		11	9	19	13	4	PCP	97-16156-6		SCV	-64.0	0.9129	-49.6	0.0012	-35.0	0.0003			-12.3	0.0012
		12	10	19	16	4	PCP	97-16077-1	9706/04	SCV	-61.3	0.9722	-47.9	0.0024	-33.4	0.0001			-12.8	0.0003
		12	19	23	25	4	PCP	97-15799-01	9705/09	SCV	-52.5	0.9686	-43.9	0.0031	-31.8	0.0001			-18.0	0.0001
		12	21	24	21	4	PCP	97-15799-02		SCV	-56.1	0.9811	-44.7	0.0028	-31.8	0.0001			-18.0	0.0001
100V		16	22	24	21	4	PCP	97-16229-2	9706/17	SCV	-60.1	0.9926	-46.0	0.0036	-28.8	0.0004	-27.8	-25.3	0.0001	
		11	19	28	22	4	PCP	97-15799-03		SCV	-53.5	0.9929	-42.0	0.0038	-29.5	0.0003			-11.9	0.0029
		1	25	36	18	4	PCP	97-17120-1		SCV	-57.7		-41.9		-30.9		-28.8		-10.0	
D		6	36	37	17	4	PCP	97-16156-4	9706/11	SCV	-58.6	0.9838	-45.2	0.0029	-36.9	0.0007	-28.6	-33.6	-33.0	0.0007
		10	31	44	11	4	PCP	97-15910-1	9705/23	SCV	-57.3	0.9614	-47.1	0.0031	-37.4	0.0003	-30.0	-30.7	-13.7	0.0037
		3	7	45	11	4	PCP	97-15910-2	9705/23	SCV	-59.9	0.9626	-48.1	0.0028	-38.9	0.0002	-29.9	-35.9	-11.6	0.0033
		10	7	48	8	4	PCP	97-15910-3	9705/23	SCV	-70.8	0.9784	-47.2	0.0030	-40.5	0.0003	-30.4	-35.0	-11.6	0.0003
100V	3A	7	55	5	4	PCP	97-15910-4		9705/23	SCV	-61.8	0.9618	-48.1	0.0032	-40.1	0.0003	-29.4	-35.0	-13.3	0.0033
A		14	36	48	23	3	Huuky	98-21586-03	971/222	SCV	-60.7	0.9415	-34.8	0.0058	-29.1	0.0010	-27.7	-28.7		0.0001
A		9	12	51	24	3	Huuky	98-21586-02	971/222	SCV	-66.2	0.9478	-52.5	0.0016	-40.5	0.0002	-32.6	-34.8		
A		10	11	47	26	3	Murphy	98-21531-02	971/217	SCV	-70.2	0.9653	-50.5	0.0018	-40.8	0.0001	-32.5	-36.2		
	MHB5	28	61	4	4	Koch	97-16647-19		9608/29	SCV	-63.8		-39.3		-33.9		-24.6	-22.4	-10.0	0.0001
		2	29	61	4	Koch	97-16557-10			SCV	-60.2	0.9761	-36.4	0.0032	-27.9	0.0004	-26.5	-29.6	-13.5	0.0001
						Huuky	#10			SCV	-53.4	0.9187	-40.9	0.0037	-36.6	0.0003	-31.5	-32.7	-16.2	0.0001
						Huuky	98-22140			SCV	-50.9		-19.6		-18.0		-22.2	-21.0		0.0000
B		5	3	56	6	4	PCP	98-22749-03	9803/31	SCV	-60.5		-43.0		-37.3				-23.6	
		9	3	56	6	4	PCP	98-22749-03	96/11/1	SCV	-60.5		-43.0		-37.3				-23.6	
						Huuky	Kinderley 1		96/11/1	SCV	-72.7		-56.0		-42.9		-29.6			
						Huuky	Kinderley 2		96/11/1	SCV	-68.6		-55.5		-42.9		-28.6		-36.2	

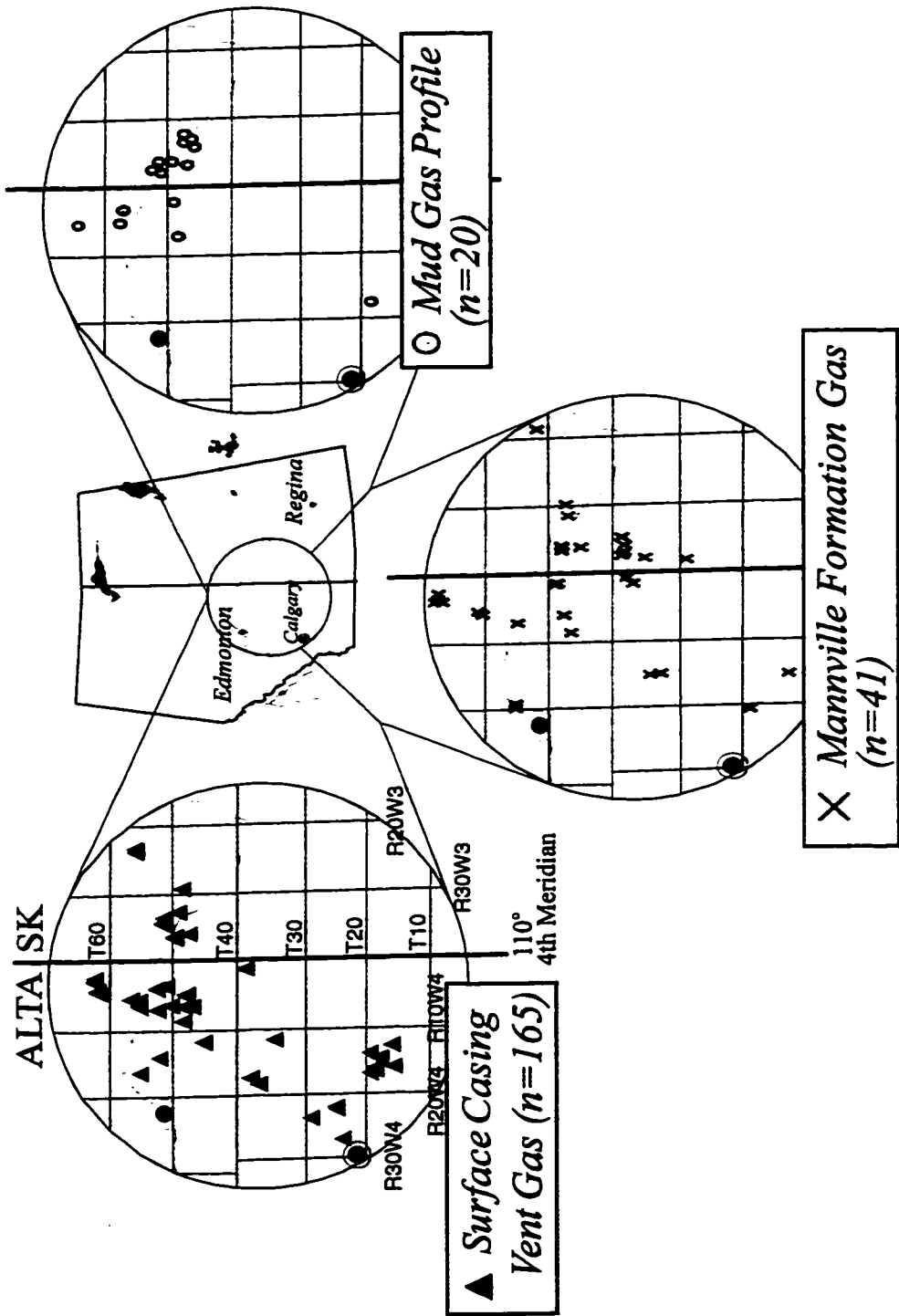
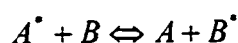


Figure D.1 Locations of samples in Appendices B, C, and D. Due to the scale of the diagrams, many of the samples are hidden by others nearby (i.e. less data points are visible on the diagrams).

APPENDIX E CALCULATION OF FRACTIONATION CURVES

THEORY

The isotopic separations discussed in Chapters 2 and 3 are based on James' (1983) quasi-equilibrium model. In this model, the isotopic compositions of light hydrocarbons are assumed to approach the equilibrium compositions. If we assume that the isotopic compositions of the light hydrocarbons are indeed due to equilibrium processes, we can define an equilibrium constant for the isotopic exchange that occurs between the various gases (Urey, 1947),



where the * denotes an isotopically heavy atom in the molecule. The equilibrium constant, K , can be written in terms of the total molecular partition functions, Q :

$$K = \frac{Q_A Q_{B^*}}{Q_{A^*} Q_B}$$

The total partition functions can be decomposed into vibrational, rotational, translational, electrical, and nuclear contributions:

$$Q = q_{vib} q_{rot} q_{trans} q_{elec} q_{nuc}$$

For isotopic exchange reactions between the molecules of interest $q_{elec}=1$ and q_{nuc} is the same for each molecule (i.e. it will divide out). The equilibrium constant can then be reduced to

$$K = \frac{\left(\frac{q^\bullet}{q}\right)_B \text{rot} \left(\frac{q^\bullet}{q}\right)_B \text{trans} \left(\frac{q^\bullet}{q}\right)_B \text{vib}}{\left(\frac{q^\bullet}{q}\right)_A \text{rot} \left(\frac{q^\bullet}{q}\right)_A \text{trans} \left(\frac{q^\bullet}{q}\right)_A \text{vib}}$$

where

$$\left(\frac{q^\bullet}{q}\right)_{\text{rot}} = \frac{\sigma^\bullet I^\bullet}{\sigma I} . \sigma \text{ is the molecular symmetry number. } I \text{ is the moment of inertia}$$

$$\left(\frac{q^\bullet}{q}\right)_{\text{trans}} = \left(\frac{m^\bullet}{m}\right)^{\frac{1}{2}} . m \text{ is the molecular mass}$$

$$\left(\frac{q^\bullet}{q}\right)_{\text{vib}} = \prod_j \frac{\frac{h\nu_j}{kT} \exp\left(-\frac{h\nu_j}{2kT}\right)}{1 - \exp\left(-\frac{h\nu_j}{kT}\right)}$$

ν_j is the frequency of the j th normal mode of vibration.

k is the Boltzmann constant. T is temperature

Combining the above three expressions, the equilibrium constant for the isotopic exchange reaction becomes

$$K = \prod_{j=1}^{3m-6} \left(\frac{\nu_j}{\nu_j^\bullet}\right)_A \prod_{k=1}^{3n-6} \left(\frac{\nu_k^\bullet}{\nu_k}\right)_B \exp\left\{\frac{1}{2kT}(\nu_{k_B}^\bullet + \nu_{j_A} - \nu_{k_B} - \nu_{j_A}^\bullet)\right\} \quad (\text{equation E.1})$$

where m and n are the number of atoms in molecules A and B.

Therefore, given the normal mode frequencies (ν, ν^\bullet) it is straightforward to calculate the equilibrium constant at any temperature. (The Teller-Redlich product rule has been applied, and symmetry numbers have been ignored following Bigeleisen and Mayer (1947)).

The actual vibrational frequencies of light hydrocarbons (needed to compute equation D.1) can be determined in a number of ways. James (1983) calculated ν and ν^* from force field matrices (Galimov and Ivlev, 1974), while Richet *et al.* (1977) determined them experimentally. For comparison, I chose a third method utilizing the ab initio molecular orbital theory capabilities of a commercial software package (Gaussian 94) (Hehre *et al.*, 1986). This program builds the molecules 'from scratch' by determining the geometric configuration that minimizes the molecular energy. Once the configuration is determined, the vibrational frequencies are calculated.

Knowledge of the value of K for a particular exchange reaction allows one to calculate the isotopic fractionation of a heavy atom between two molecules, A and B at any temperature,

$$\Delta_{A-B} = \delta_A - \delta_B = 1000 \ln K(T)$$

PROGRAM INPUT- GAUSSIAN 94

There are two routines that must be run in G94 to calculate vibrational frequencies- GeomOpt and FreqTest. GeomOpt determines the optimal molecular configuration given initial estimates and the FreqTest uses the results from GeomOpt to calculate vibrational frequencies (alternatively, the geometric configuration can be defined if it is known). One possible input file for the geometrical optimization ethane is:

```
%chk=ethtestgopt.chk
# HF/6-31G* opt
```

Ethane Geometry Optimization

```
0 1
C
C 1 RCC
H 1 RCH 2 ACCH
H 1 RCH 2 ACCH 3 ACCH2
H 1 RCH 2 ACCH 3 -ACCH2
H 2 RCH 1 ACCH 3 ACCH3
H 2 RCH 1 ACCH 6 ACCH2
H 2 RCH 1 ACCH 6 -ACCH2
```

Variables:

```
RCH 1.5
RCC 1.1
ACCH 111.2
ACCH2 120.0
ACCH3 180.0
```

The input file ethtestisot.inp defines the atomic masses of each atom (before vibrational frequencies are calculated)

```
%chk=ethtestisot.chk
# freq=(ReadFC,ReadIsotopes) geom=check
```

Ethane HF/6-31G* Isotope Frequencies and Thermochemistry

```
0 1
300 1.0 1.0
12
13
1
1
1
1
1
1
1
```

To call the appropriate subroutines, the following commands are required:

```
#!/bin/csh
```

```
runG94 ethtestgopt >& messages
/bin/cp ethtestgopt.chk ethtestfreq.chk
runG94 ethtestfreq >& messages
/bin/cp ethtestfreq.chk ethtestisot.chk
runG94 ethtestisot >& messages
```

The output file ethtestisot.out will contain a variety of thermochemical data, including vibrational frequencies which can be used to compute K (equation E.1).

RESULTS

The calculated partition functions for methane, ethane and butane are shown in table E.1.

Component	Calculated $^{13}\text{C}/^{12}\text{C}$ partition function (Q^*/Q)									
	300°C		400°C		500°C		600°C		700°C	
		James (1983)		James (1983)		James (1983)		James (1983)		James (1983)
C ₁	1.1302	1.1136	1.0885	1.1076	1.0648	1.0554	1.0496	1.0421	1.0393	1.0331
C ₂	1.1515	1.1317	1.0999	1.0861	1.0714	1.0610	1.0536	1.0455	1.0418	1.0353
nC ₄	1.1528	1.1419	1.1003	1.0915	1.0713	1.0641	1.0535	1.0475	1.0416	1.0366

Table E.1 Calculated partition functions from this study, and James (1983) for methane (C₁), ethane (C₂) and normal butane (nC₄).

Values for propane were not determined due to time constraints. The partition functions calculated using the ab initio approach appear to be slightly higher than those of James (1983). James' values agree with Richet *et al.* (1977), which suggests that my values are likely in error. This is not surprising because the orbital basis set used for the ab initio routines was quite simple (HF 6-31G*). In order to better represent the molecular interactions in alkane structures, a more complex basis set should be chosen (perhaps HF 6-31G** (d, f)).

TEMPERATURE DEPENDENT FRACTIONATION CURVES

The theoretical C₃/C₂ fractionation curves that are discussed in Chapters 2-4 were calculated from the partition functions reported in James (1983). The partition functions calculated from the ab initio approach were not used because time constraints did not allow calculations for C₃ to be made. To calculate Δ_{C₃-C₂}, we make use of the relationship between the equilibrium constant K, and the isotopic fractionation factor, α:

$$\alpha = K^{1/n} \text{ so that}$$

$$\Delta_{C_3-C_2} = \delta_{C_3} - \delta_{C_2} = 1000 \ln \alpha(T)$$

The fractionation factors are simply determined from the ratios of the partition functions of propane and ethane, which gives the following simple temperature dependent isotopic relationship between δ¹³C_{C₃} and δ¹³C_{C₂},

$$\delta_{C_3}(T) = \delta_{C_2}(T) + 1000 \ln \alpha_{C_3-C_2}(T)$$

Combining this expression with an analogous one for fractionation between C₂ and C₃₀ (kerogen), and inserting the appropriate values,

$$\delta_{C_2}(T) = \delta_{C_{30}}(T) - 1000 \ln \alpha_{C_{30}-C_2}(T) = -30 + 0.5034 - 1.5359 \times \frac{1E6}{T^2}$$

$$\delta_{C_3}(T) = -30 + 0.5034 - 1.5359 \times \frac{1E6}{T^2} + 1000 \ln \alpha_{C_3-C_2}(T)$$

$$\delta_{C_3}(T) = -30 + 0.5034 - \left(1.5359 \times \frac{1E6}{T^2} \right) - 0.3512 + \left(0.5724 \times \frac{1E6}{T^2} \right). \quad (\text{equation E.2})$$

Equation E.2 defines the temperature dependent fractionation curve for the equilibrium isotopic exchange between propane and ethane. Values of $\delta^{13}\text{C}_{30}$ can be chosen depending on the desired source material. For the WCSB, type-II kerogen with values from -25‰ to -30‰ are appropriate.

REFERENCES

- Bigeleisen, J., and Mayer, G. (1947) Calculation of equilibrium constants for isotopic exchange reactions. *Jour. Chem. Phys.*, **15**, 261-267
- Galimov, E. M., and Ivlev A. A. (1974) Thermodynamic isotope effects in organic compounds; I. Carbon isotope effects in straight-chain alkanes: *Russian Jour. Phys. Chemistry*, **47**, 1564-1566
- Hehre, W. J., Pople, J. A., Radom, L., Schleyer, P. v.R. (1986) Ab initio molecular orbital theory
- James, A. T. (1983) Correlation of natural gas by use of carbon isotopic distribution between hydrocarbon components. *AAPG Bull.*, **67**, 1176-1191
- Richet, P., Bottinga, Y., Javoy, M. (1977) A review of hydrogen, carbon, nitrogen, oxygen, sulphur and chlorine stable isotope fractionation among gaseous molecules. *Earth and Planetary Sci., Ann. Rev.*, **5**, 65-110
- Urey, H. C. (1947) The thermodynamic properties of isotopic substances. *Jour. Chem. Soc.*, 562-581

APPENDIX F

INDEX OF ABSTRACTS

CSPG-SEPM Joint Convention, Calgary, Alberta
June 1997

Contrasting Carbon Isotope Fingerprints of Migrating and Solution Gas in Heavy Oil Fields of Northeastern Alberta

Rowe, D., Muehlenbachs, K., Greenwood, G. (Chemex Labs), Jensen, E. (Amoco Canada)

Thousands of wells have been drilled in northeastern Alberta and adjacent Saskatchewan, Canada, in order to develop heavy oil reservoirs in the Lower Cretaceous Mannville sands. In a large fraction of these, migration of gas to surface has been observed (up to 200 m³/day) via well casings and adjacent soil, and is a cause for concern for government and industry alike. We tested the utility of $\delta^{13}\text{C}$ for fingerprinting gases in this region to facilitate remediation.

The solution gases in the heavy oil are comprised of biogenic methane, with trace C₂₊ components that are residues from biodegradation. The various Mannville sand units do not show unique fingerprints (typical $\delta^{13}\text{C}$ values C₁= -66; C₂=-26; C₃=-19; iC₄=-25; nC₄=-23). Gases from the overlying Upper Colorado shale units are isotopically distinct. The $\delta^{13}\text{C}$ of the methanes in the shales have values equivalent to those in the sands, but the $\delta^{13}\text{C}$ of the C₂₊ components are unambiguously different. Surprisingly, and contrary to our previous reports, the gases from the Upper Cretaceous shales have $\delta^{13}\text{C}$ values indicative of thermogenesis ($\delta^{13}\text{C}_{\text{C}_1}$ from -73 to -64; C₂ from -56 to -37; C₃ from -43 to -31; iC₄ from -30 to -28; nC₄ from -36 to -32). The ¹³C partitioning observed in the shale gases reflect pseudo-equilibrium, indicative of very low maturation, whereas in the Mannville sands, the solution gases show isotopic reversals between C₃ and C₄, iC₄ and nC₄.

In our study, most of the gases migrating in and near the wells show the isotopic signal of the shallower Upper Cretaceous shales and not the Mannville sands in which the wells were completed. Graphically the migrating gases can be differentiated by plotting the isotopic partitioning between iC₄ and C₃ versus $\delta^{13}\text{C}$ of C₄.

The 4th Canadian Continuous-Flow Isotope Ratio Mass Spectrometry Workshop,
Waterloo, Ontario
August 1997

A successful application of GC-C IRMS: isotopic fingerprinting of trace hydrocarbons in migrating gas for environmental remediation of Western Canada's leaking heavy oil wells.

D. Rowe, K. Muehlenbachs

Thousands of wells have been drilled in northeastern Alberta and adjacent Saskatchewan in order to develop heavy oil reservoirs. In a large number of these wells, undesirable migration of gas to surface has been observed (up to 200 m³/day) via well casings and surrounding soil, and is a cause for concern to government and industry alike. Environmental regulations require remediation efforts to stop this migration, but current methods are plagued by dismal success rates. Isotopic fingerprints of migrating gases can be used to identify their source depths, greatly improving remediation success.

Continuous flow technology has significantly improved our ability to detect and accurately measure the isotopic ratios of trace gases found in shallow formations of Alberta and Saskatchewan's heavy oil fields. Gases exsolved from drilling muds collected at well sites typically contain light hydrocarbons (methane, ethane, propane, butane) and carbon dioxide, with abundances ranging from 0.01 to 95%. Even the most dilute gas components can be quickly and easily analysed with the continuous flow system. Hydrocarbons are converted directly to CO₂ in a Finnigan MAT gas chromatography-combustion unit, which connected to a Finnigan MAT 252 isotope ratio mass spectrometer used for isotopic analyses (GC-C IRMS). Since the addition of the combustion interface 1 year ago, several hundred gas samples have been successfully run without any mechanical failures or degradation of columns or furnaces.

Geological Society of America Fall Meeting, Salt Lake City, Utah
October, 1997

Carbon Isotope Fingerprints of Solution and Migrating Gases in Heavy Oil Fields of Northeastern Alberta

Rowe, D., Muehlenbachs, K., Lorenz, G., (Husky Oil Operations)

Thousands of wells have been drilled in northeastern AB and adjacent SK, in order to develop heavy oil reservoirs in the Cretaceous Mannville sands. In a large fraction of these, migration of gas to surface has been observed (up to 200 m³/day) via well casings and surrounding soil, and is a cause for concern to government and industry alike. We tested the utility of $\delta^{13}\text{C}$ for fingerprinting gases using CF/C/IRMS in this region to facilitate future remediation. Mud samples from new wells being drilled were collected at 50m intervals from surface down to completion depth, and the exsolved gases were analysed for ^{13}C composition.

The gases in the heavy oil are comprised of biogenic methane, with trace C_{2+} components that are residues from biodegradation. The various Mannville sand units do not show unique fingerprints. Gases from the overlying Colorado shale units are isotopically distinct. The $\delta^{13}\text{C}$ values of the methanes in the shales have values equivalent to those in the sands, but the $\delta^{13}\text{C}$ of the C_{2+} components are unambiguously different. Surprisingly, the gases from the Cretaceous shales have $\delta^{13}\text{C}$ values indicative of thermogenesis. $\delta^{13}\text{C}$ partitioning observed in the shale gases reflect a very low maturation, whereas in the Mannville sands, the (deeper) oil gases show reversals between C_3 and $i\text{C}_4$, $i\text{C}_4$ and $n\text{C}_4$. Most of the gases migrating in and near the wells show the isotopic signal of the shallower Cretaceous shales and not the Mannville sands in which the wells were completed.

American Chemical Society National Meeting, Dallas, Texas
March, 1998

IN SITU GENERATION OF GAS IN SHALES OVERLYING STEAMED HEAVY OIL RESERVOIRS

D.M. Rowe, K. Muehlenbachs, S. Talman

Some reservoirs of NE Alberta have been steamed for decades to produce heavy oil. The oil reservoirs are L. Cretaceous sands and are overlain by organic rich, immature shales. The isotopic composition of hydrocarbon gases in the shales obtained from mud gases is indicative of depth of origin, and is useful in designing remediation strategies for problem wells. Gases

obtained from shales above steamed reservoirs differ systematically in isotopic composition from virgin mud gases sampled in the same region and depth. For a given delta 13C value of C2, the fractionation between C3 and C2 is 3 to 4 ppt greater in gas from the heated shales. We

suggest that C1 and higher homologues are generated in the shale by the hot well bores during steaming. This 'new' gas is now migrating to surface.

CSPG-CSEG-CWLS Joint Convention, Calgary, Alberta
June, 1998

Economic benefits of carbon isotope fingerprint-logs used to determine source depths of migrating gas in the heavy oil fields of Alberta and Saskatchewan

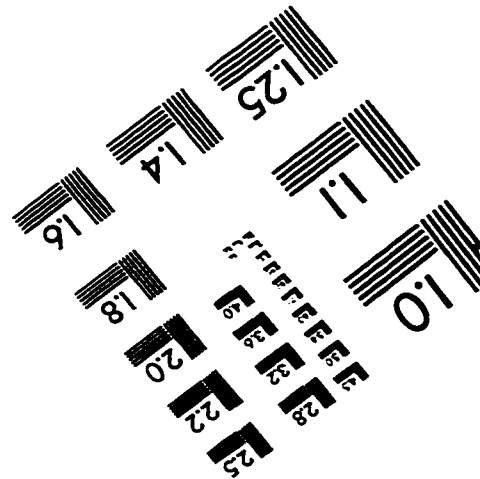
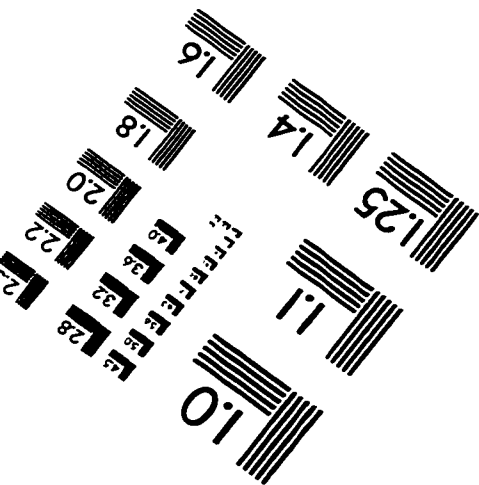
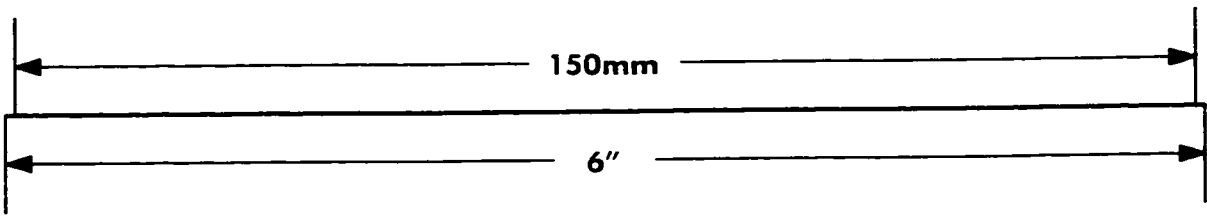
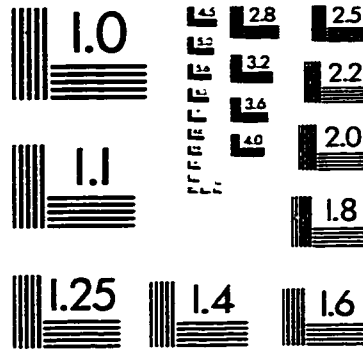
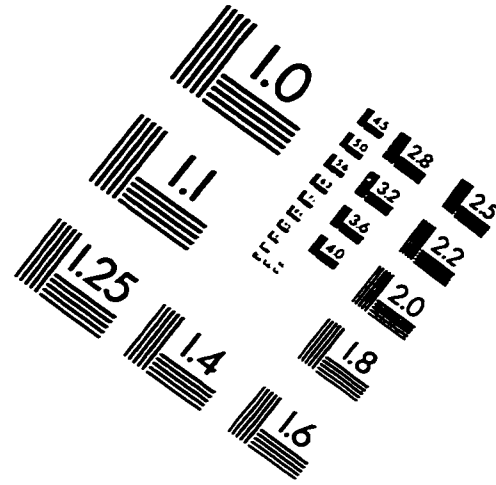
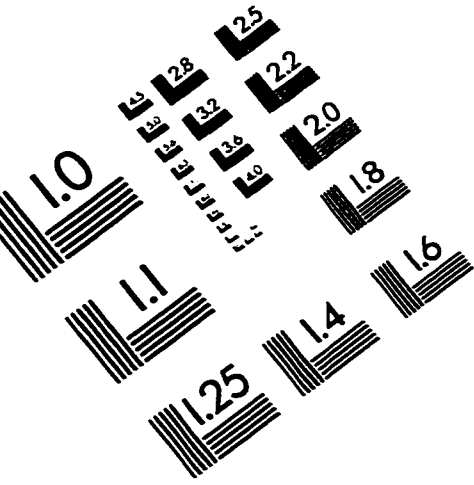
D. ROWE, K. MUEHLENBACHS, E. JENSEN (AMOCO CANADA PETROLEUM COMPANY LTD.)*

Natural gas migration to surface is an environmental and financial liability in many heavy oil and conventional oil fields in Alberta and Saskatchewan, especially in those fields that have very close well spacings. Many thousands of wells are known to have undesired gas emissions. In the past, remediation efforts have been unsuccessful due to the inability of traditional geophysical and/or logging techniques to accurately identify the source of gas migration.

Our study has shown that in most cases the problem gas does not originate from the heavy oil reservoirs, but from the shallower overlying shales. The two gas sources can be identified isotopically because the gases have different origins in the two reservoirs. The gases associated with heavy oils originated as thermal cracking products, but have since been degraded and isotopically fractionated by bacteria that altered the oil after emplacement. The shale gases are a mixture of bacterial methane and traces of ethane, propane and butane produced by incipient thermal cracking.

Isotopic profiles of gases extracted from drilling muds show the different signatures of gases generated in the shales and those originating in the heavy oil formations. Using these fingerprints or 'isotope logs', the source depth of migrating gas in nearby problem wells can be accurately determined. This information aids in assessing potential environmental risk and guides engineering efforts at remediation in a more cost efficient manner.

IMAGE EVALUATION TEST TARGET (QA-3)



APPLIED IMAGE . Inc
1653 East Main Street
Rochester, NY 14609 USA
Phone: 716/482-0300
Fax: 716/288-5989

© 1993, Applied Image, Inc., All Rights Reserved